Conformational Disorder and the Degree of Conjugation in Conjugated Polymers

Phillip Wood

31 January 2002

A thesis submitted to the School of Physics and Astronomy, at the University of St Andrews, for the degree of Doctor of Philosophy.

Abstract

Conformational Disorder and the Degree of Conjugation in Conjugated Polymers

This thesis presents an investigation into conformational disorder and the effect of the extent of electron delocalisation on the photophysics of conjugated polymers. Conjugated polymers are semiconducting materials that are easy to process and show great potential for display and photovoltaic applications. Using a novel technique of fitting the absorption spectrum of the polymer to the absorptions of shorter conjugated segments, the distribution of conjugated segments of a family of conjugated polymers was obtained. The distribution of conjugation lengths is found to peak at the shortest segment length. As the polymer solutions are cooled their absorption moves to lower photon energies and the distribution of conjugated segments within them shifts to longer segments. The results of these fits are compared with the theoretical predictions of Yaliraki and Silbey.[1] There is good qualitative agreement between the model and the experimental results.

The effect of the extent of conjugation on the photophysics of poly[2-methoxy,5-(2'-ethyl-hexyloxy)-1,4-phenylenevinylene] (MEH-PPV) has also been investigated. As the degree of conjugation is reduced the photoluminescence quantum yield increases. The mechanism of the migration of the excited state is found to alter upon the introduction of single bonds to limit the extent of conjugation. The partially conjugated samples show spectroscopic evidence of static disorder, the fully conjugated polymer shows much stronger electronic coupling along the polymer chain.

[1] S. N. Yaliraki and R. J. Silbey. *Journal of Chemical Physics*, **104**, 1245 (1996).

Contents

Declarations

I, Phillip Wood, hereby certify that this thesis has been written by me and that it is a record of work carried out by myself and has not been submitted in any previous application for any degree.

Phillip Wood 31 January 2002

I was admitted as a research student and a candidate for the degree of Doctor of Philosophy at the University of Durham in October 1998. I transfered to the University of St Andrews in September 2000.

Phillip Wood 31 January 2002

I herby certify that the candidate has fulfilled the conditions for the resolution and regulations appropriate for the degree of Doctor of Philosophy in the University of St Andrews and that the candidate is qualified to submit this thesis in application for that degree.

Ifor Samuel 31 January 2002

Copyright Declaration

In submitting this thesis to the University of St Andrews I understand that I am giving permission for it to be made available for use in accordance with the regulations of the University Library for the time being in force, subject to any copyright vested in the work not being affected thereby. I also understand that the title and abstract will be published, and that a copy of the work may be made and supplied to any bona fide library or research worker.

Phillip Wood 31 January 2002

Acknowledgements

There are many people who have helped me during the last three years. I would like to thank my parents and sister for their support and encouragement. I am very grateful to Ifor for his supervision, help and guidance. Thank you to everyone in the mechanical and electronics workshops in Durham and St Andrews for all your help. I would also like to thank the members of my research group especially Graham and LO for their optics and spectroscopy knowledge. Stephen's chemical knowledge has been invaluable and I am grateful to John, Jon and Justin for their help and humour. Thank you Anna for reading so much of this thesis and for your friendship. Thank you also to my officemates for discussions and conversation in the six offices I have occupied in the last three years.

I would like to thank Arvydas, Villy and Mette for all their help and everyone else in Lund for the friendly welcome on my visits there. I am still amazed how slow ultrafast spectroscopy experiments are to perform! I am grateful to Ron and Garry for their help and making data available to me. Thank you to the chemists who have made all the samples I have looked at.

Finally without the financial support of EPSRC I would not have been able to do any of this work. I am also grateful to the EU TMR fund for funding my trips to Lund.

List of Figures

List of Tables

Chapter 1

Introduction

Conjugated molecules pervade the whole of life, from insects in the air, through plants and animals on the land, to fish in the deep ocean. Conjugated molecules are responsible for key processes in vision and photosynthesis. In the deep ocean, reactions involving conjugated molecules provide the only light. Conjugated molecules give colour to our food and provide vitamins essential to life. Conjugated polymers are a fascinating class of materials, which are longer versions of their naturally occuring counterparts. Like their biological cousins they are poised to make an impact on our everyday life. The promise of flexible, large area flat screen displays and solar cells has attracted much interest and there have been several technological developments in recent years. However, despite the relative success of technological developments, there is still much to be learnt about the basic physics of these materials. If they are to fulfill their full potential then a thorough understanding of how the basic photophysics relates to their structure is essential for the systematic development of better materials. The work presented in this thesis explores the factors affecting the degree of conjugation, or electron delocalisation, in these materials and how this impacts upon their photophysical properties.

Conventional plastics are insulators. They are ubiquitous in everyday life from simple carrier bags to videotapes and the housings of the latest

DVD players. The advent of modern electronic equipment such as DVD players has been made possible by the development of inorganic semiconductors which have, in the last 50 years, revolutionised the world we live in. Conjugated polymers combine the easy processing properties of conventional plastics with novel semiconducting properties. Combining these two properties opens the possibility of a whole host of new applications, from light emitting wallpaper that can be changed to suit your mood to clothing with a built-in television or internet terminal. Conjugated polymers were first developed in the 1970's when Heeger, Mac Diarmid and Shirakawa [1–3] first demonstrated that plastics could be made to conduct. The award of the Nobel prize for chemistry to Heeger, Mac Diarmid and Shirakawa recognises the importance of conjugated polymers and their work in developing them. The discovery of electroluminescence in 1989 by Burroughes et al. [4] opened up a whole new area of research and potential applications. Since then there have been many developments, with the efficiency of displays increasing to the point where they are beginning to be commercialised. Optically pumped lasers [5, 6] and solar cells [7, 8] based on conjugated polymers are also under active development.

In order to improve devices based upon these materials it is important to understand them at a molecular level. The extent of conjugation in a conjugated polymer determines its electrical and optical properties [9]. It is governed by the conformation of the molecule and its synthesis. Polymers are naturally disordered materials. A given sample will generally contain a range of chain lengths and different local environments. As the chains twist and fold, the electrons within them may become more localised, changing the optical and electronic properties of the molecule. Much of the theoretical work in the literature neglects these effects; a small number of theoretical studies have discussed the effects of conformational disorder on conjugated polymers and the factors affecting it [10–18]. There has, however, been relatively little experimental work investigating how the conformational properties of conjugated polymer chains change with temperature, or comparing the theoretical

predictions of the models to the behaviour of real systems [16, 19].

The work in this thesis aims to address the question of how the degree of conjugation and conformational disorder affect the photophysical properties of a conjugated polymer, and is structured as follows. Chapter 2 introduces some theory and background information relevant to conjugated molecules and conjugated polymers in particular. The spectroscopic impact of conformational disorder is introduced. Chapter 3 goes on to explain the experimental techniques used in the subsequent chapters. Spectroscopic measurements are introduced and their utility is explained. They allow a great deal of information to be obtained about conjugated polymers (or any material that interacts with light) in a very elegant manner.

In chapter 4 a new method is presented which is used to extract the distribution of conjugated segments from the absorption spectra of novel conjugated polymers with a well defined chain length [20, 21]. These distributions are then compared with the theoretical predictions of the model of Yaliraki and Silbey [15]. The conformation of the polymer as a function of temperature is explored and compared to the predictions of the model.

The degree of conjugation within the polymer will effect the nature of its excited (luminescent) state. The nature of the excited state in conjugated polymers has been the subject of much debate in the literature [22–25]. Taking advantage of recent developments in polymer synthesis, chapter 5 presents a systematic study of the excited state in a family of poly[2-methoxy,5-(2'-ethyl-hexyloxy)-1,4-phenylenevinylene] (MEH-PPV) samples where the degree of conjugation has been carefully controlled [26]. The careful control of the conjugation means that these samples present a unique opportunity for carefully studying the effect of the degree of conjugation on polymer photophysics. By combining steady state and time resolved polarised spectroscopy it is shown that the nature of the excited state in the fully conjugated polymer is different from the excited state in the partially conjugated polymers. The results are interpreted as two different migration mechanisms in these polymers. Finally chapter 6 draws together the conclusions of this work.

References

[1] A. J. Heeger. *Reviews of Modern Physics*, **73**, 681, (2001).

[2] A. G. MacDiarmid. *Reviews of Modern Physics*, **73**, 701, (2001).

[3] H Shirakawa. *Reviews of Modern Physics*, **73**, 713, (2001).

[4] J. H. Burroughes, D. D. C. Bradley, A. R. Brown, R. N. Marks, K. Mackay, R. H. Friend, P. L. Burn, and A. B. Holmes. *Nature*, **347**, 539, (1990).

[5] M. D. Mc Gehee and A. J. Heeger. *Advanced Materials*, **12**, 1655, (2000).

[6] N. Tessler. *Advanced Materials*, **11**, 363, (1999).

[7] O. Inganäs, L. S. Roman, F. L. Zhang, D. M. Johansson, M. R. Andersson, and J. C. Hummelen. *Synthetic Metals*, **121**, 1525, (2001).

[8] C. J. Brabec, N. S. Sariciftci, and J. C. Hummelen. *Advanced Functional Materials*, **11**, 15, (2001).

[9] D. Hu, J. Yu, K. Wong, B. Bagchi, P. J. Rossky, and P. F. Barbara. *Nature*. **405**, 1030, (2000).

[10] Z. G. Soos and K. S. Schweizer. *Chemical Physics Letters*, **139**, 196, (1987).

[11] K. S. Schweizer. *Journal of Chemical Physics*, **85**, 4181, (1986).

[12] M. L. Shand, R. R. Chance, M. Postollec. and M. Schott. *Physical Review B*, **25**, 4431, (1982).

[13] G. Rossi. R. R. Chance, and R. J. Silbey. *Journal of Chemical Physics*, **90**, 7594, (1989).

[14] G. J. Exharos, W. M. Risen, and R. H. Baughman. *Journal of the American Chemical Society*, **98**, 396, (1976).

[15] S. N. Yaliraki and R. J. Silbey. *Joural of Chemical Physics*, **104**, 1245, (1996).

[16] B. E. Kohler and J. C. Woehl. *Journal of Chemical Physics*, **103**, 6253, (1995).

[17] R. R. Chance. *Macromolecules*, **13**, 396, (1980).

[18] R. H. Baughman and R. R. Chance. *Journal of Polymer Science, Polymer Physics Edition*, **14**, 2037, (1976).

[19] B. E. Kohler and I. D. W. Samuel. *Journal of Chemical Physics*, **103**, 6248, (1995).

[20] H. H. Fox, M. O. Wolf, R. Odell, B. L. Lin. R. R. Schrock, and M. S. Wrighton. *Journal of the American Chemical Society*, **116**, 2827, (1994).

[21] F. J. Schattenmann, R. R. Schrock, and W. M. Davis. *Journal of the American Chemical Society*, **118**, 3295, (1996).

[22] T. Q. Nguyen, V. Doan, and B. J. Schwartz. *Journal of Chemical Physics*. **110**, 4068, (1999).

[23] U. Rauscher, H. Bässler, D. D. C. Bradley, and M. Hennecke. *Physical Review B*. **42**, 9830, (1990).

[24] M. Yan, L. J. Rothberg, E. W. Kwock, and T. M. Miller. *Physical Review Letters*, **75**, 1992, (1995).

[25] I. D. W. Samuel G. R. Hayes and R. T. Phillips. *Physical Review B*, **52**, R11569, (1995).

[26] G. R. Webster. *Advanced polymers for light emitting diodes*. PhD thesis, University of Oxford, (2000).

Chapter 2

The Theory of Conjugated Polymers

2.1 Introduction

In this chapter the most relevant physical theories pertaining to conjugated polymers are reviewed. The general properties of this class of materials have been outlined in the previous chapter. This chapter presents a more detailed account of the theory used in this work. First of all an explanation of what a conjugated molecule is and how its electronic structure relates to its optical properties is given, then issues specific to conjugated polymers are reviewed.

2.2 Bonding in conjugated molecules

Conjugated polymers are organic materials and the main building block is the carbon atom. The term conjugated describes the way the carbon atoms bond to each other. In conjugated molecules carbon atoms form a chain and are joined by alternating single and double bonds. A simple conjugated molecule is 1,3-butadiene in figure 2.1(a). It consists of a backbone of four carbon atoms linked by alternating single and double bonds. In order to understand how the double bonds are formed, it is useful to consider a simpler

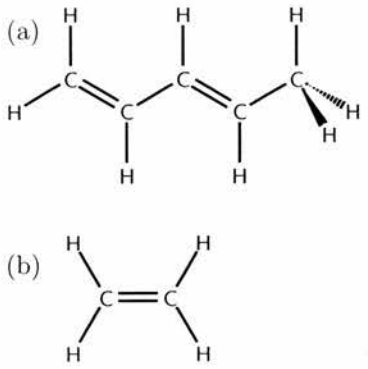

Figure 2.1: *The chemical structures of (a) 1,3-butadiene and (b) ethene.*

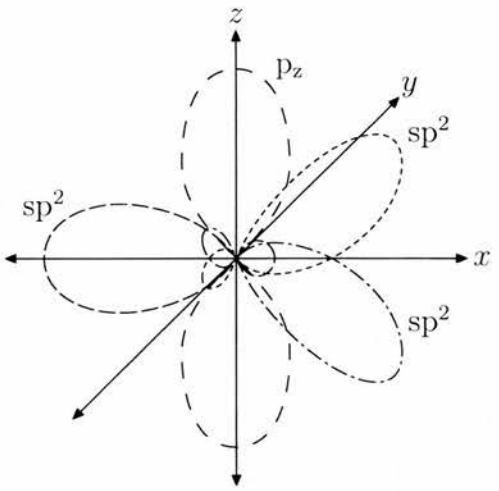

Figure 2.2: *The p_z and the three sp^2 orbitals of a carbon atom.*

example, ethene, shown in figure 2.1(b). It consists of two carbon atoms connected by a double bond and four hydrogen atoms. Carbon has the electronic configuration $1s^2 2s^2 2p^2$, however, in order to bond to another atom it is energetically favourable for the 2s and one or more of the 2p orbitals to hybridise to form new orbitals. To form a double bond the 2s orbital hybridises with two of the 2p orbitals (p_x and p_y) so that three new sp^2 hybrid orbitals are formed. The sp^2 orbitals lie in the xy plane at 120° to each other. The sp^2 orbitals along with the remaining p_z orbital are shown in figure 2.2.

These three sp^2 orbitals and the remaining p_z orbital then form the bonding orbitals of the carbon atom. Two sp^2 orbitals on two neighbouring carbon atoms overlap to form a single σ bond. The p_z orbitals on these atoms also overlap to form a π bond as shown in figure 2.3. The π bond makes the molecule very rigid, as in order for the two carbon atoms to rotate relative to each other, the π bond would have to be broken. The electrons in the π bond are more weakly bound than those in the sigma bond. In a conjugated molecule such as 1,3-butadiene the π bonds extend over the whole

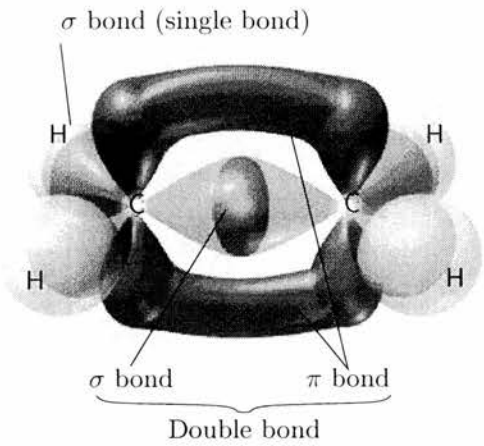

Figure 2.3: *σ and π bonds form from the overlap of the sp^2 and p_z orbitals on two neighbouring carbon atoms [1].*

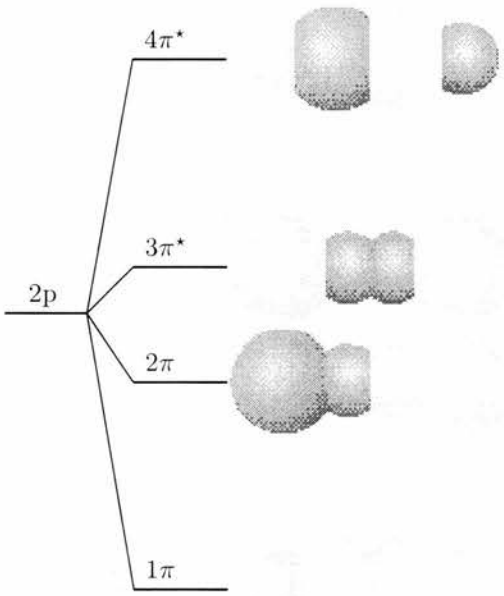

Figure 2.4: *The π orbitals in 1,3-butadiene [2].*

molecule. Figure 2.4 shows the π orbitals and their energies relative to a p orbital calculated using Hückel theory for 1,3-butadiene [3].

As there are four electrons in the π bonds, the lower two orbitals (1π and 2π) are fully occupied in the ground state. These two orbitals are predominately bonding in character. The 2π is referred to as the highest occupied molecular orbital (HOMO) and the $3\pi^\star$ is referred to as the lowest unoccupied molecular orbital (LUMO). It is clear from the figure that the total energy of the four electrons in these orbitals is less than the energy of four electrons in isolated p orbitals. This figure also shows the sign of the wave functions of the four orbitals, the 1π and $3\pi^\star$ orbitals have even parity (the sign of their wave function is unchanged under inversion) and the 2π and $4\pi^\star$ have odd parity (the sign of their wave function is changed under inversion). The parities of the wave functions are important for the absorption

and emission of light by the molecule. In a conjugated polymer the number of conjugated double bonds is very large and consequently the number of π orbitals is also very large. The bonding and anti-bonding orbitals form two pseudo continua of energy levels separated by an energy gap. This leads to a band-like picture of the electronic structure of the polymer, where the top of the valence band is given by the energy of the highest occupied molecular orbital (HOMO) and the bottom of the valance band is given by the energy of the lowest unoccupied molecular orbital (LUMO). However, band like models can only give a limited description of the optical and electronic properties of conjugated polymers. Molecular exciton models have proved more appropriate for explaining many experimental results, such as site selective fluorescence [4], as electron correlations are very strong in conjugated polymers and these are neglected in band like models.

2.3 Absorption and emission of light

The energies of the π electrons in conjugated materials correspond to optical energies. In nature conjugated molecules are used in photosynthesis to harvest light energy, bioluminescence to produce light energy and they also give colour to fruits and vegetables. Chlorophyll captures light in plants for photosynthesis, carrots get their orange colour from β-carotene and tomatoes get their red colour from lycopene. Conjugated polymers share similar optical properties to these naturally occuring molecules and so optical spectroscopy is a powerful tool for probing and understanding the properties of these materials.

2.3.1 Absorption of light

When a molecule is exposed to electromagnetic radiation the field interacts with the electric dipole moment of the molecule. The oscillating field will induce oscillations in the charge density of the molecule. The charge density behaves like a damped oscillator and there is only a significant interaction

if the frequency of the field matches the resonant frequency of the molecule. The resonant frequency of the molecule is determined by its electronic structure. If there is a significant interaction then, classically, the field transfers some energy to the molecule and quantum mechanically an electron in the molecule may be excited into a higher energy state and a photon from the field absorbed. Spectroscopically the strength of the interaction at a frequency ν is measured by the molar absorption or extinction coefficient $\epsilon(\nu)$. This is expressed in the Beer Lambert law [5]. The intensity of light I with frequency ν propagating a distance z through a medium of concentration c and extinction coefficient $\epsilon(\nu)$ is related to the initial intensity I_0 by

$$I(z, \nu) = I_0 10^{-\epsilon(\nu)cz} \tag{2.1}$$

The extinction coefficient may be related to the electronic structure of the molecule by considering the electronic energy levels within it. The lower half of figure 2.5 shows an absorption and a fluorescence spectrum for a conjugated molecule. The top half of this figure shows the molecular potential plotted as a function of the molecular coordinates of the molecule. The dotted lines in the potentials represent the square of the wave function for each energy level. The number of nodes in the wave function increases as the energy increases. As the potential is not infinite the wave functions penetrate the barrier slightly. The left-hand side of this figure represents the absorption of a photon. The spacing of the energy levels within the potentials is greater than $k_B T_{room}$ so that only the lowest vibronic level of the ground state (S_0) is populated at room temperature. The ground state and excited state potentials are offset from each other. This is because the nuclear configuration coordinates of the ground and excited states are offset. The transition between the ground state and the excited state is depicted as a straight line because the electronic transition takes 10^{-15} s and the nuclei in the molecule take about 10^{-12} s to rearrange. This is a statement of the Franck Condon principle [6]. When a photon is absorbed it excites an electron from the ground state (S_0) into a vibronic sub-level of the excited state (S_1). The sub-level that is excited depends on the energy of the photon. The

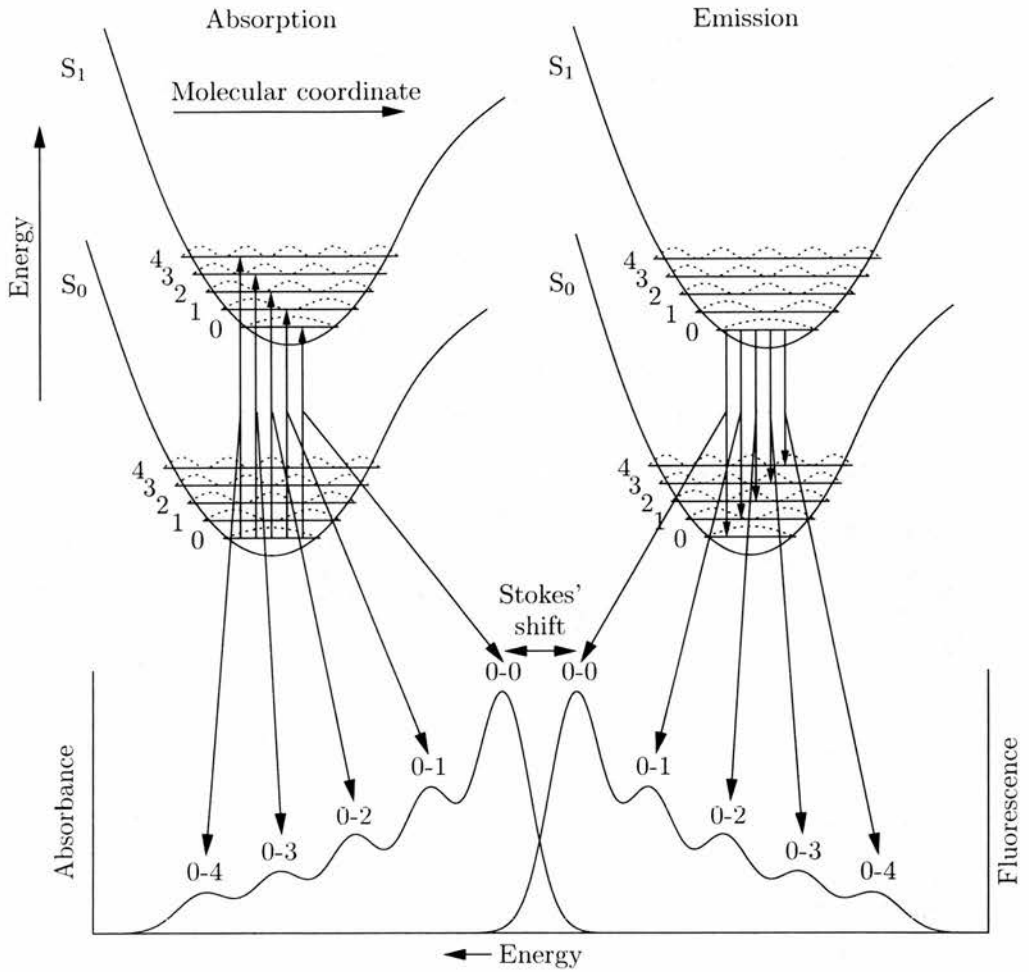

Figure 2.5: *Jablonski diagram showing the absorption and emission of light. Based on figure I.C.10 in [7].*

probability of excitation from the ground state to a given vibronic sub-level of the excited state is proportional to the overlap of the ground state wave function and the excited state wave function for that vibronic sub-level. This leads to an envelope of vibronic bands in the absorption spectrum known as the Franck Condon envelope [6].

2.3.2 Emission of light

After an electron is excited the charge density within the molecule will be different from the ground state and the molecule will rearrange itself to minimise its energy for this new electron density. The surrounding solvent may also rearrange itself as a result of the change in charge density and molecular configuration. As a result the excited state potential will change shape as seen on the right hand side of figure 2.5. This results in a shift between the 0-0 transitions in absorption and fluorescence. The electron will decay to the lowest vibronic level within the excited state via a non-radiative process such as phonon emission. From here it may return to the ground state by radiating a photon or by a non-radiative mechanism. Radiative decay is represented by the vertical lines in this figure. The electron may initially decay to any of the ground state vibronic levels. This determines the energy of the photon emitted and gives the fluorescence spectrum plotted in the lower half of this figure. From this level the electron then decays to the lowest vibronic level of the ground state by internal conversion.

Not all electrons that are excited by the absorption of a photon will result in the emission of a photon as non radiative decay from the excited state is possible. The proportion of excitations that decay via a radiative decay is called the photoluminescence quantum yield (PLQY) of a material. It is defined as

$$\Phi = \frac{\text{number of photons absorbed}}{\text{number of photons emitted}} \tag{2.2}$$

For some conjugated polymers the PLQY can approach 50%. This is much larger than some polyenes where the quantum yield is negligible.

2.3.3 Selection rules and polarisation

The preceding discussion assumed that the only factor affecting the probability of the absorption or emission of a photon is the Franck Condon factor for that transition. In fact the probability for a transition is governed by Fermi's golden rule, and the Franck Condon factor is one element in this

equation. There are a number of elements to take into consideration and these are summarised in a set of selection rules which must also be obeyed for a transition to be formally allowed. Transitions which are not formally allowed may take place but they are much weaker than formally allowed transitions. One of the most important selection rules is the Laporte selection rule [8] which states that the only allowed electric dipole transitions are those involving a change of parity. In figure 2.4 the 2π orbital has odd parity and the $3\pi^\star$ orbital has even parity and so an electric dipole transition is allowed. However an electric dipole transition is not allowed between orbitals 2π and $4\pi^\star$ so even if a photon of the correct energy is incident on the molecule it has a very low probability of being absorbed. In some molecules the lowest excited state is of the same parity as the ground state, this means that they do not decay radiatively. In these molecules a photon may be absorbed and an electron promoted to the second excited state but then this electron will tend to decay to the first excited state which is not optically coupled to the ground state and hence there is no fluorescence from the molecule. This is why some polyenes have such low quantum yields [9].

Another factor which affects the intensity of the absorption is the relative orientations of the polarisation of the electromagnetic field and the transition dipole moment of the molecule. If the polarisation of the field is perpendicular to the transition dipole moment of the molecule then the two will not couple together and there will be no interaction. If the relative angle between the field and the transition dipole is θ then the strength of the interaction will be proportional to $\cos^2\theta$. The emitted light will be polarised in the direction of the transition dipole moment of the molecule, so if the transition dipole moment changes direction between absorption and emission, the absorbed and emitted photons will be polarised in different directions. If the molecule is not straight and the excitation travels along the molecule before it decays, then the transition dipole moments where the photon was absorbed and where the new photon is emitted will be different as well. This is a useful tool to probe excitation migration along the polymer chain. The

anisotropy is used to measure the change in direction of the polarisation between absorption and emission. It is defined as

$$r = \frac{I_{\parallel} - I_{\perp}}{I_{\parallel} + 2I_{\perp}} \tag{2.3}$$

where $I_{\parallel}$ is the intensity of the emission when the excitation is polarised parallel to the polarisation of the emission and $I_{\perp}$ is the intensity of the emission when the excitation is polarised perpendicularly to the polarisation of the emission The angle between the two dipoles (φ) is related to the anisotropy by the Perrin equation [10]

$$r = \frac{1}{5}(3\cos^2\varphi - 1) \tag{2.4}$$

Polarised spectroscopy is used in chapter 5 to track the excitation moving along the polymer chain. In order to monitor the luminescence without polarisation anisotropy effects experiment were performed with the excitation and emission polarisers oriented at the magic angle (54.7^o) to each other. At this angle the effect of polarisation is not observed. This is because for an ensemble of molecules the average polarisation dynamics are monitored and these depend of the value of $3\cos^2\theta - 1$ where θ is the angle between the excitation and emission polarisers. With $\theta = 54.7^o$ $3\cos^2\theta - 1 = 0$ and so polarisation effects are eliminated.

2.4 Absorption and fluorescence of a conjugated polymer

The previous section discussed the general theory of absorption and emission spectroscopy of a conjugated molecule. This section addresses the issues related specifically to the absorption and emission of light in conjugated polymers. The absorption and emission of short conjugated molecules are normally mirror images of each other, the spectra show vibronic structure and there is a modest Stokes' shift between the peak of the absorption and

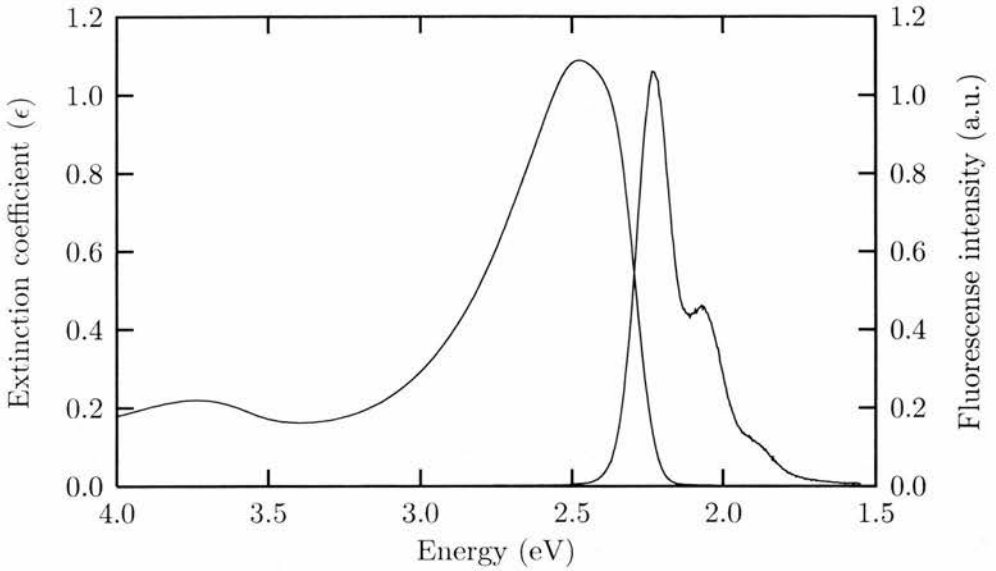

Figure 2.6: *The absorption and fluorescence of MEH-PPV in solution.*

emission as shown in figure 2.5. Figure 2.6 shows the absorption and photoluminescence of a typical conjugated polymer in solution. The absorption is much broader than the photoluminescence and both the absorption and photoluminescence are fairly structureless. There is also a large shift from the maximum of the absorption to the maximum of the fluorescence. These observations may be explained by considering disorder of the polymer chains [4, 11–14]. Conformational disorder twists and folds the polymer chains, causing breaks in conjugation along the length of the polymer chain. Because of this, the polymer contains many shorter conjugated segments or subunits. The absorption of the polymer reflects the inhomogeneously broadened absorption of the subunits [11]. This gives the broad featureless absorption spectrum in figure 2.6 which is typical of conjugated polymers. At first sight one might expect the photoluminescence of the polymer to be broadened in the same way as the absorption, but this is clearly not the case in figure 2.6. The observed photoluminescence spectrum (and the time resolved anisotropy) can be explained in terms of excitation migration along

the chain [11, 12, 15, 16]. Excitations are created on one segment and then migrate along the chain to segments of longer length and lower energy. As the excitations move to progressively longer segments on the chain they will be trapped as the neighbouring segments will have higher energies [13, 14]. As they are trapped on longer segments they will decay from these segments leading to a fluorescence spectrum that is predominately the fluorescence of just the longer segments within the chain. This explains the fluorescence spectrum typical of conjugated polymers in figure 2.6 and also the results of site selective fluorescence [4, 13, 14] and time resolved [15, 16] experiments.

When temperature is reduced the vibronic structure of the polymer absorption and emission spectra increase as they become more ordered because the thermal energy available to twist the polymer chain is reduced [17, 18]. The work in this thesis focuses on investigating the effects of conformational disorder and the extent of conjugation on the optical properties of conjugated polymers by using temperature and chemical control of the degree of conjugation. A method is developed to extract the distribution of subunits on the polymer chain from the absorption spectrum.

References

[1] Figure taken from http://kekule.chem.csus.edu.

[2] P. W. Atkins. *Molecular Quantum Mechanics*, Chapter 10, Page 275. Oxford University Press, Second edition, (1983).

[3] P. W. Atkins. *Physical Chemistry*, Chapter 14, Page 499. Oxford University Press, Fifth edition, (1994).

[4] H. Bässler, C. Brandl, M. Deussen, E.O. Göbel, R. Kertsing, H. Kurz, V. Lemmer, R.F. Mahrt, and A. Ochse. *Pure and Applied Chemistry*, **67**, 377, (1995).

[5] P. W. Atkins. *Physical Chemistry*, Chapter 16, Page 545. Oxford University Press, Fifth edition, (1994).

[6] J. B. Birks. *Photophysics of Aromatic Molecules*, Chapter 3, Page 52. Wiley and Sons, (1969).

[7] M. Pope and C. E. Swenberg. *Electronic Processes in Organic Crystals and Polymers*, Chapter I, Page 25. Oxford University Press, Second edition, (1999).

[8] P. W. Atkins. *Molecular Quantum Mechanics*, Chapter 9, Page 213. Oxford University Press, Second edition, (1983).

[9] B. S. Hudson, B. E. Kohler, and K. Schulten. *Excited States*, **6**, 1, (1982).

[10] J. Perrin. *Journal de Physique et le Radium*, **7**, 390, (1926).

[11] B. Mollay, U. Lemmer, R. Kersting, R. F. Mahrt, H. Kurz, H. F. Kauffmann, and H. Bässler. *Physical Review B*, **50**, 10769, (1994).

[12] M. C. J. M. Vissenberg and M. J. M. de Jong. *Physical Review Letters*, **77**, 4820, (1996).

[13] H. Bässler and B. Schweitzer. *Accounts of Chemical Research*, **32**, 173, (1999).

[14] S. Heun, R. F. Mahrt, A. Greiner, U. LEmmer, H. Bässler, D. A. Halliday, D. D. C. Bradley. P. L. Burn, and A. B. Holmes. *Journal of Physics: Condensed Matter*, **5**, 247, (1993).

[15] G. R. Hayes, I. D. W. Samuel, and R. T. Philips. *Physical Review B*, **52**, R11569, (195).

[16] M. M-L. Grage, T. Pullerits, A. Ruseckas, M. Theander, O. Inganäs, and V. Sundström. *Chemical Physics Letters*, **339**, 96, (2001).

[17] G. Dufresne, J. Bouchard, M. Belletête, G. Durocher, and M. Leclerc. *Macromolecules*, **33**, 8253, (2000).

[18] P. Wood, I. D. W. Samuel, G. R. Webster. and P. L. Burn. *Synthetic Metals*, **119**, 571. (2001).

Chapter 3

Experimental Techniques

3.1 Introduction

Optical spectroscopy is a powerful tool for probing the excited electronic states of conjugated polymers. In this chapter the experimental techniques of the spectroscopies employed in this work are outlined. First, steady state measurements of absorption and photoluminescence are introduced. Then the measurement of anisotropy is explained and the experimental setup for the time resolved measurements is presented. Time resolved measurements of the luminescence and transient absorption are particularly powerful for investigating excitation migration which is important for studying conformational disorder.

3.2 Absorption measurements

The theory of absorption of light was introduced in section 2.3. The absorption of a sample is defined as [1]

$$A = -\log_{10}(T) \tag{3.1}$$

where T is the transmission of the sample. The absorption is related to the decadaic molar extinction coefficient (ϵ) in equation 2.1 by

$$A = \epsilon c l \tag{3.2}$$

where c is the concentration and l is the path length of the sample.

The absorption measurements in this work were made on two different absorption spectrometers, a Perkin Elmer Lambda 19 and a Varian Cary 300. They both used a double beam configuration to eliminate the effects of solvent and cuvette absorption. Before any spectra were recorded a baseline scan was performed with a cuvette of solvent in each arm. This enabled the instrument to set its zero absorption level, compensating for any differences in the absorption of the two optical paths in the instrument. Then absorption measurements were taken with a cuvette of solvent in the reference arm and the solution to be measured in the sample arm. By taking the ratio of the intensities between the two arms the instrument calculates the absorption of just the solute without any background from the absorption of the solvent. When the cryostat was used in the absorption spectrometer a baseline was taken with both arms empty and spectra were taken with the cryostat in the sample arm. Separate measurements of the absorption of the solvent as a function of temperature were also performed and then subtracted from the spectra of the samples to correct them.

3.3 Photoluminescence measurements

Photoluminescence is a useful technique to probe the excited state of a material. All photoluminescence measurements were performed using a Jobin Yvon Fluoromax 2 spectrometer. This instrument uses a monochromated xenon lamp to excite the sample. The emission is collected perpendicular to the excitation, monochromated and detected by a photomultiplier tube operating in single photon counting mode. The instrument keeps a constant bandpass in wavelength for both the excitation and emission monochromators when it scans. This means that care must be taken when converting

the spectra from wavelength to units of energy [2]. In a photoluminescence spectrum, $S(\lambda)$, the total number of photons N between wavelengths λ_1 and λ_2 will be given by

$$N = \int_{\lambda_1}^{\lambda_2} S(\lambda) d\lambda \tag{3.3}$$

This integral may be written in terms of energy

$$N = \int_{hc/\lambda_2}^{hc/\lambda_1} S\left(\frac{hc}{E}\right) \frac{hc}{E^2} dE \tag{3.4}$$

$$= \int_{hc/\lambda_2}^{hc/\lambda_1} \mathcal{S}(E)\, dE \tag{3.5}$$

For the integrals in equations 3.3 and 3.5 to be equal the integrands must be identical. That is

$$S(\lambda) \frac{hc}{E^2} = \mathcal{S}(E) \tag{3.6}$$

Therefore when converting an emission spectrum from wavelength to energy it is necessary to multiply each value by hc/E^2. In order to avoid distortions in the measured spectra due to self absorption all solutions were prepared with a peak absorbance of $A < 0.1$.

3.4 Photoluminescence excitation spectroscopy

Photoluminescence excitation (PLE) spectroscopy is a powerful tool for probing the excited state of a material as it can distinguish between several emissive species within a sample. In a PLE experiment the intensity of the photoluminescence at a fixed photon energy is recorded as a function of excitation photon energy. For a single species the PLE spectrum can be related to the absorption spectrum. The number of photons emitted (N_{em}) at a given emission photon energy E_{em} is related to the number of photons absorbed (N_{ab}) at the excitation photon energy E_{ex} by the PLQY for this combination of excitation and emission photon energies $\Phi(E_{ex}, E_{em})$

$$N_{em} = \Phi(E_{ex}, E_{em}) N_{ab} \tag{3.7}$$

Neglecting reflection and scattering, the number of photons absorbed is related to the transmission (T) by

$$\begin{aligned} N_{ab} &\propto 1 - T \\ &\propto 1 - 10^{-A} \end{aligned} \tag{3.8}$$

where A is the absorbance of the sample defined in equation 3.1. Therefore the PLE signal is related to the absorption by

$$\begin{aligned} N(E_{em}) &\propto \Phi(E_{ex}, E_{em})(1 - T) \\ &\propto \Phi(E_{ex}, E_{em})(1 - 10^{-A}) \end{aligned} \tag{3.9}$$

Assuming the PLQY is independent of the excitation and emission photon energies then the PLE signal is proportional to $1 - T$. If a sample contains a mixture of two species which emit at different photon energies then PLE spectra at these two photon energies will show the absorption of these two species. A conventional absorption measurement outlined in section 3.2 will just be the combination of the absorptions of the two species. In this way PLE can be useful to distinguish between several emissive species in a sample. This is used in chapter 5 to investigate the extent of energy transfer within a partially conjugated polymer.

3.5 Steady state anisotropy

The concept of anisotropy was introduced in section 2.3. Steady state anisotropy measurements are used in chapter 5 to investigate the effect of the extent of conjugation on the excited state of a conjugated polymer. Steady state anisotropy measurements of the photoluminescence and photoluminescence excitation were performed in the fluorimeter. Polarisers were introduced into the excitation and detection paths. Spectra were recorded for horizontally and vertically polarised excitation and emission. In principle it might be expected that only two spectra need to be recorded, vertical excitation with

vertical and horizontal emission polarisations. However, as the detection system uses a monochromator it will have different sensitivities to horizontally and vertically polarised light. In order to determine these sensitivities the vertical and horizontal emission for horizontal excitation were used. The signal recorded when both the excitation and emission polarisers are vertical is denoted I_{VV} and the signal recorded when the excitation polariser is vertical and the emission polariser is horizontal is denoted I_{VH}. These signals are related to the parallel ($I_{\parallel}$) and perpendicular ($I_{\perp}$) emission spectra by [3]

$$I_{VV} = S_V I_{\parallel} \tag{3.10}$$

$$I_{VH} = S_H I_{\perp} \tag{3.11}$$

where S_V and S_H denote the sensitivity for the detector to vertically and horizontally polarised light respectively. The signals for horizontally polarised excitation are given by

$$I_{HV} = S_V I_{\perp} \tag{3.12}$$

$$I_{HH} = S_H I_{\perp} \tag{3.13}$$

Taking the ratio of equations 3.12 and 3.13 gives the ratio of the sensitivities of the detector to horizontally and vertically polarised light

$$\frac{S_V}{S_H} = \frac{I_{HV}}{I_{HH}} \tag{3.14}$$

Combining equations 3.10, 3.11 and 3.14 gives the degree of the polarisation (P_r) of the emission.

$$P_r = \frac{I_{\parallel}}{I_{\perp}} = \frac{S_H}{S_V}\frac{I_{VV}}{I_{VH}} = \frac{I_{HH}}{I_{HV}}\frac{I_{VV}}{I_{VH}} \tag{3.15}$$

Rearranging equation 2.3 the anisotropy is given by

$$r = \frac{P_r - 1}{P_r + 2} \tag{3.16}$$

The uncertainty on the value of the anisotropy was calculated using error analysis. As the instrument is a photon counting device the uncertainties on the individual spectra were assumed to form a Poisson distribution. For

this distribution the uncertainty on a given value x is $\sqrt{x}$ [4]. The fractional uncertainty on the polarisation is

$$\frac{\Delta P_r}{P_r} = \sqrt{\frac{1}{I_{VV}} + \frac{1}{I_{VH}} + \frac{1}{I_{HV}} + \frac{1}{I_{HH}}} \tag{3.17}$$

and the fractional uncertainty on the anisotropy is

$$\frac{\Delta r}{r} = \sqrt{\left(\frac{\Delta P_r}{P_r - 1}\right)^2 + \left(\frac{\Delta P_r}{P_r + 2}\right)^2} \tag{3.18}$$

It can be seen from equation 3.14 that when the anisotropy of the photoluminescence excitation is measured the ratio S_V/S_H should be constant as the detection photon energy is constant. This was found to be the case where the signal was reasonably strong. However where the photoluminescence excitation signal was small there was a greater uncertainty in this ratio. To reduce the uncertainty the ratio was determined as the average value over the range of excitation photon energies that gave a consistent value.

The anisotropy r is related to the angle between the absorption and emission dipoles φ by equation 2.4. Rearranging this equation the angle between the dipoles is related to the anisotropy by

$$\varphi = \cos^{-1}\left(\sqrt{\frac{5r+1}{3}}\right) \tag{3.19}$$

The uncertainty $\Delta\varphi$ in φ is related to the uncertainty in anisotropy Δr by

$$\Delta\varphi = \left|\frac{d\varphi}{dr}\right| \Delta r \tag{3.20}$$

The differential of inverse cosine is

$$\frac{\partial}{\partial x}\cos^{-1} u = \frac{-1}{\sqrt{1-u^2}}\frac{\partial u}{\partial x} \tag{3.21}$$

combining the equations above, the uncertainty in the angle between the absorption and emission dipoles is

$$\Delta\varphi = \left|\frac{5}{2\sqrt{3(2-5r)(5r+1)}}\right| \Delta r \tag{3.22}$$

3.6 Determining the PLQY

The photoluminescence quantum yield of a material was defined in equation 2.2 as the ratio of the number of photons emitted to the number of photons absorbed. This can also be written in terms of the radiative and non-radiative rate constants k_r and k_{nr} respectively

$$\Phi = \frac{k_r}{k_r + k_{nr}} = \frac{\tau}{\tau_r} \tag{3.23}$$

where τ is the lifetime measured by time resolved luminescence and τ_r is the natural radiative lifetime. By combining the PLQY with measurements of the time resolved luminescence it is possible to calculate the radiative and non-radiative decay rates. All samples were degassed before the quantum yield was measured as the PLQY can be decreased by oxygen quenching and also by photo-oxidation of the sample [5].

For solutions the easiest method to determine the PLQY of a material is to measure it relative to a standard of known quantum yield. Several standards have been studied [6], the standard used in this work is quinine sulphate dissolved in 0.5 M sulphuric acid. The PLQY of this has been determined to be 0.546 when excited at 365 nm [7, 8]. The quantum yield Φ_x of a solution of a sample is given by

$$\Phi_x = \Phi_r \frac{[1 - T_r(\lambda_r)]I(\lambda_r)n_x^2 \int F_x(\lambda)\, d\lambda}{[1 - T_x(\lambda_x)]I(\lambda_x)n_r^2 \int F_r(\lambda)\, d\lambda} \tag{3.24}$$

where Φ_r is the quantum yield of the reference material, λ_r and λ_x are the excitation photon energies used to obtain the photoluminescence spectra F_r and F_x of the reference and unknown respectively. T_r and T_x are the transmission of the reference and unknown sample respectively. $I(\lambda_r)$ and $I(\lambda_x)$ are the intensities of the excitation for the reference and unknown sample solution respectively. n_r and n_x are the refractive indices of the solvent used for the solutions of the reference and unknown respectively.

In order to ensure an accurate measurement it is important to ensure that the solutions have a peak absorption of $A < 0.1$ to minimise self absorption

and that the transmission at the excitation wavelength is similar for the reference and sample. It is also important to use the same slit widths for the emission and excitation monochromators in the spectrometer for the acquisitions of both spectra. The refractive indices are included as the refractive index of the solvent affects the area over which light is collected by the emission detection system [9]. The higher the refractive index of the solvent the more light will refract when it travels from the solvent into the cuvette and the smaller the fraction of the emission that will be collected by the detector.

3.7 Streak camera measurement of the time resolved luminescence

Measurements of the time resolved luminescence of a material can give useful information on the lifetime of the excited state and how this varies with photon energy. As explained in the previous section, when combined with the PLQY of a material, this allows the radiative and non-radiative decay rates to be calculated from equation 3.23. To measure the time dependence of the luminescence a streak camera was used. The experimental setup is shown in figure 3.1. All samples were degassed to prevent sample oxidation and quenching by oxygen. The sample was excited using approximately 100 fs pulses of the second harmonic of a titanium sapphire laser. The luminescence

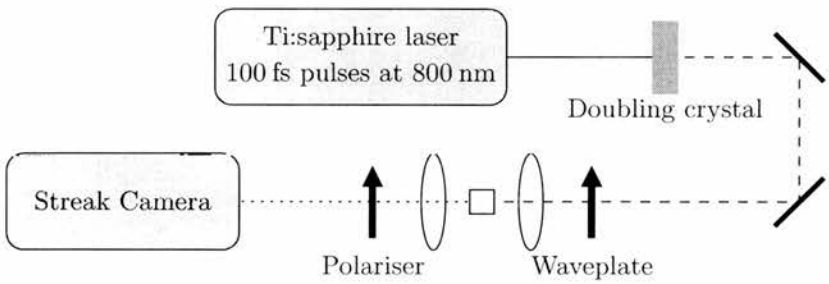

Figure 3.1: *The experimental setup for measurements taken using the streak camera.*

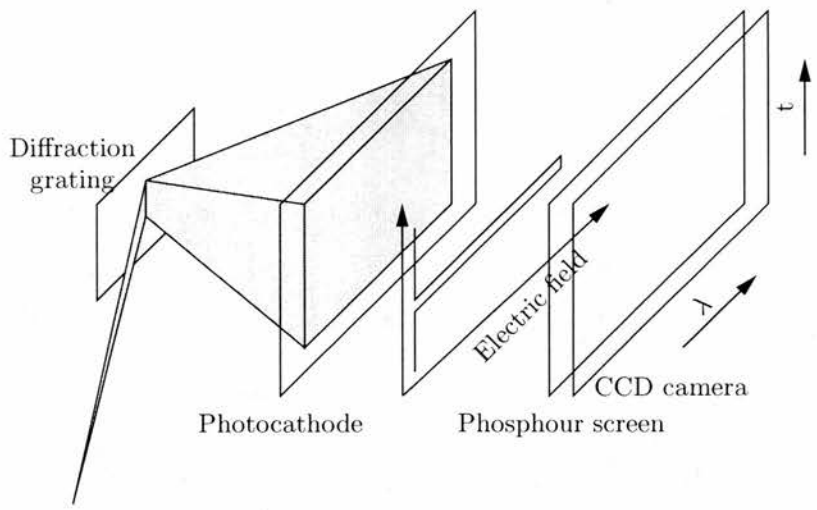

Figure 3.2: *The operation of a streak camera.*

was collected and focused onto the entrance slit of the streak camera spectrograph. The relative polarisation of the excitation and detected emission was varied using a waveplate in the excitation beam path.

The operation of the streak camera is illustrated in figure 3.2. The incident light is dispersed by a spectrograph. This light is then incident on a photocathode and is converted to electrons. These electrons are then accelerated by an electric field which scans down the streak tube. The electrons then hit a phosphor screen and the photons emitted are detected by a CCD camera. The time resolution comes from the sweeping of the electric field in the streak tube. As the voltage is swept down the plate, electrons at the photocathode are accelerated to the anode at different times. This results in a two dimensional image of intensity as a function of both wavelength and time. The streak camera instrument response was determined by measuring a scattered excitation pulse and was $1 - 2$ ps. Decays were measured at the magic angle to eliminate any polarisation effects. Anisotropy measurements were also performed by recording the luminescence signal with the excitation parallel and perpendicular to the detection polarisation. As the excitation power was the same for parallel and perpendicular excitations and the de-

tection polarisation was constant the anisotropy could be calculated directly from the parallel and perpendicular spectra using equation 2.3

3.8 Transient absorption

In contrast to the other methods presented in this chapter, transient absorption probes both emissive and non-emissive excited states. This means that it is particularly powerful, as the lifetimes and anisotropies of all the excitations generated by the absorption of a photon can be monitored. This also means that it can be a complicated technique to interpret as there can be several possible explanations for a given observation. Transient absorption has the best time resolution of all the techniques outlined in this chapter. The setup for the transient absorption measurements is shown in figure 3.3. 80 fs pulses of 800 nm radiation at a repetition rate of 5 kHz from a regeneratively amplified titanium sapphire laser where used to pump an optical

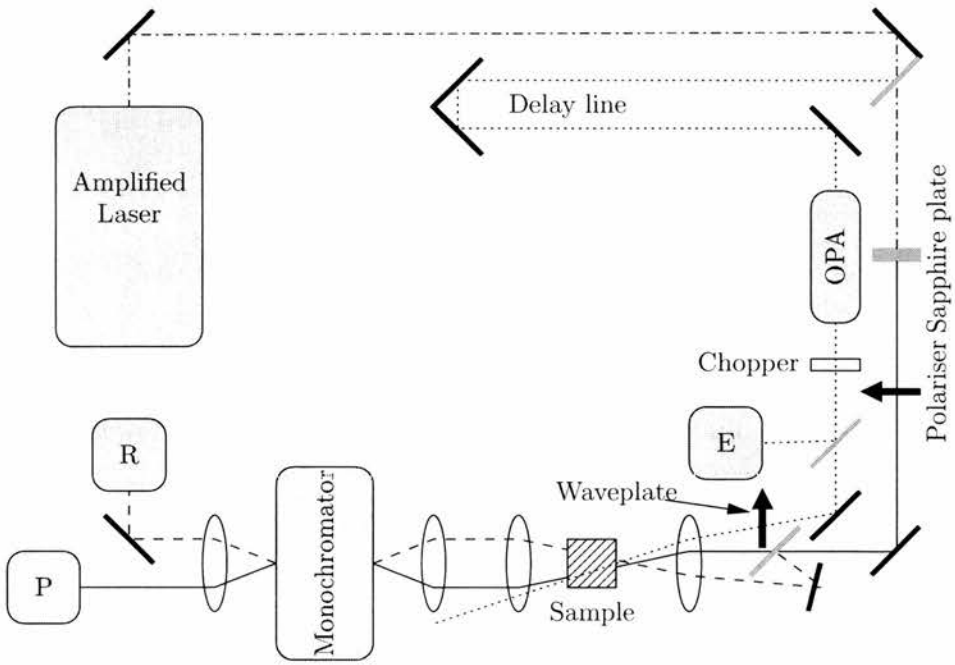

Figure 3.3: *The experimental set up for transient absorption measurements.*

parametric amplifier (OPA) to generate a tuneable excitation source for the sample. The output of the OPA was chopped so that the sample was excited by every other pulse from the laser. The output of the amplified laser was also used to generate a continuum in a sapphire plate which was used as the probe beam. The pump and probe beams were focused onto the sample and care was taken to ensure that they overlapped. A second probe pulse passed through an unexcited region of the sample to act as a reference. The excitation probe beams were detected using silicon photodiodes (E, P and R in figure 3.3). The relative polarisation of the pump and probe beams was controlled using a waveplate in the excitation beam. Decays were measured at the magic angle unless the anisotropy was being measured. As with the streak camera the anisotropy was calculated directly from the parallel and perpendicular decays.

References

[1] P. W. Atkins. *Physical Chemistry*, Chapter 16, Page 545. Oxford University Press, Fifth edition, (1994).

[2] J. R. Lakowicz. *Principles of Fluorescence Spectroscopy*, Chapter 2, Page 52. Kluwer Academic, Second edition, (1999).

[3] J. R. Lakowicz. *Principles of Fluorescence Spectroscopy*, Chapter 10, Page 291. Kluwer Academic, Second edition, (1999).

[4] J. R. Taylor. *An Introduction to Error Analysis*, Chapter 11, Page 207. Oxford University Press, (1982).

[5] M. Atreya, S. Li, T. Kang, K. G. Neoh, Z. H. Ma, K. L. Tan, and W. Huang. *Polymer Degradation and Stability*, **65**, 287, (1999).

[6] J. N. Demas and G. A. Crosby. *Journal of Physical Chemistry*, **75**, 991–1024, (1971).

[7] A. N. Fletcher. *Journal of Physical Chemistry*, **72**, 2742, (1968).

[8] J. E. Gill. *Photochemistry and Photobiology*, **9**, 313, (1969).

[9] T. Förster. *Fluoreszenz Organisher Verbindungen.* Vandnhoeck-Ruprecht, Germany, (1951).

Chapter 4

Conformational Disorder in Conjugated Polymers

4.1 Introduction

Polymers have enormous scope for conformational disorder. This has a strong influence on the electronic and optical properties of conjugated polymers, as the degree of delocalisation is strongly dependent on the conformation of the polymer chain. It is therefore important to understand the processes involved in conformational disorder, in order to fully understand the photophysics of these materials. Theoretical studies of the electronic states of polyenes [1–4] have concentrated on the room temperature properties of symmetric, short polyenes such as octatetraene. However, an understanding of the behaviour of polymer solutions and films is important for both fundamental science and for designing new materials for technological applications. The transition energy for the electric origin [(0-0) vibronic band] of the symmetry allowed ($1^1A_g \rightarrow 1^1B_u$) absorption of short polyenes can be expressed by $E = A + B/N$, where A and B are constants and N is the number of conjugated double bonds in the polyene [5]. This simple equation provides an excellent account of the peaks of spectra of model polyenes and carotenoids ($N < 15$). However, the absorption of long conjugated polymers tends to

lie at higher energies than predicted by this equation. Polymer absorption spectra tend to have unresolved shapes. In contrast, shorter conjugated molecules e.g., most carotenoids, exhibit vibronic structure, even in room temperature solutions [6]. This suggests that the polymers are disordered, with the polymer chain breaking into shorter conjugated segments. The spectra of conjugated polymers can be explained by breaks into shorter segments of different conjugation lengths. The absorptions of these segments overlap, leading to broad, unresolved spectra.

Extrapolation of the empirical $A + B/N$ equation for the $S_0 \rightarrow S_2$ transition energy to $N = \infty$ indicates that an infinitely long polyene should absorb (E_{0-0}) at about 1.8 eV ($\lambda \sim 700$ nm) [5]. It was quickly appreciated that the absorption spectra of the majority of polyacetylene and polydiacetylene solutions fell well short of this limit, indicating conjugated segments that are substantially shorter than the chain lengths of these polymers. Baughman and Chance [7], Exharos, Risen and Baughman [8], Shand et al. [9], and Rossi, Chance and Silbey [10] developed simple models that invoked a distribution of conjugated segments of different lengths within the polymer. These models explain the relatively broad, blue-shifted absorptions as being due to distributions of conjugated segments of different lengths, where the length of a conjugated segment is defined as the distance (N double bonds) over which the planarity of the polyene backbone is maintained without interruption. This model also explains the dispersion of the vibrational frequencies of C-C and C=C symmetric stretches observed in resonance Raman photoselection experiments [8]. Spectra obtained by exciting in different regions of the broad polymer absorption give rise to different vibrational frequencies. the frequency of the C=C symmetric stretch also shows an $A + B/N$ dependence, reaching a long chain limit of 180 meV [9]. As originally pointed out by Shand et al. [9], this should allow the distribution of conjugated segments to be extracted from the distribution of vibrational frequencies.

More recently, Kohler and Samuel [11] revisited the effect of conformational disorder on the electronic properties of conjugated polymers by fitting

absorption spectra of various long-chain polymers to a superposition of spectra of polyenes with known length. [12, 13]. These fits gave distributions that were dominated by the shortest polyene segments length. These conclusions were reinforced by a simple model [14] in which each single bond has the same energy barrier to twisting out of the plane of conjugation. Statistical and entropic considerations then rationalise the apparent domination of the shortest segment lengths. Yaliraki and Silbey [15] later extended the earlier work of Rossi et al. [10] to apply a more sophisticated theoretical approach, starting with a microscopic Hamiltonian that contained appropriate steric terms for the torsional motions that disrupt the conjugation. The resulting probability distributions for the lengths of conjugated segments show that short segments are the most probable.

The primary purpose of the work presented in this chapter is to investigate the temperature dependence of the conformation of conjugated polymers in solution and the validity of current conformational disorder models, especially that of Yaliraki and Silbey [15]. In general such models explain the room temperature behaviour of conjugated polymers. However, the temperature dependence of the model is a strong test of its validity. The work in this chapter also explores the connection between the optical properties of conjugated polymers and the relatively well understood electronic spectra of short polyenes. The temperature dependence of the absorption spectra of soluble polyene oligomers of known chain length ($\sim 100 - 3500$ double bonds), synthesised by Schattenmann et al. [16] and Fox et al. [12] using living polymerisation techniques has been studied. By using conjugated oligomers of well-defined length the effects that arise from samples containing large variations in chain length are reduced. Unlike carotenoids and other simple polyenes, the absorption spectra of the polymers experience significant red shifts when their solutions are cooled. The analysis of these temperature shifts provides further support for conformational disorder in the polymers.

Estimates of conjugation length distributions were obtained by fitting the polymer absorption spectra to superpositions of spectra of conjugated

polyene segments using a least squares method. This extends the approach of Kohler and Samuel [11] which assumed that the distribution of conjugated segments could be approximated by a sum of Gaussians centered at the shortest conjugation length ($N = 2$). The approach used here does not impose any functional form on the distribution of conjugated segments. This yields "experimental" distributions that can be compared to the distributions predicted by the model of Yaliraki and Silbey [15]. The experimental determination of the distribution of conjugation lengths as a function of temperature provides a demanding test of the conformational disorder model. The Yaliraki and Silbey model shows qualitative agreement with the experimental distributions but there are some quantitative differences in the temperature dependence of the polymer absorption spectra.

4.2 Experimental

Figure 4.1 shows the structures of the polymers used in this study, their masses and approximate number of double bonds per chain are given in table 4.1. **A** and **B** both have terminal phenyl rings conjugated to the rest of the polymer. **C** has only one ring conjugated to the rest of the chain. The synthesis of samples **A** and **B** has been described by Schattenmann and Schrock [16, 17], sample **C** was synthesised by Kai Hultzsch following the method outlined by Fox and Schrock [12]. **A** and **B** appear in table 3

Sample	M_n	M_w	γ	$\bar{n}$
A	16400	19800	1.21	137
B	104000	168000	1.62	880
C	390000	410000	1.05	3300

Table 4.1: *The number average (M_n) and weight average (M_w) molecular masses, polydispersity (γ), and approximate number of double bonds per chain ($\bar{n}$) of the polymers studied in this chapter.*

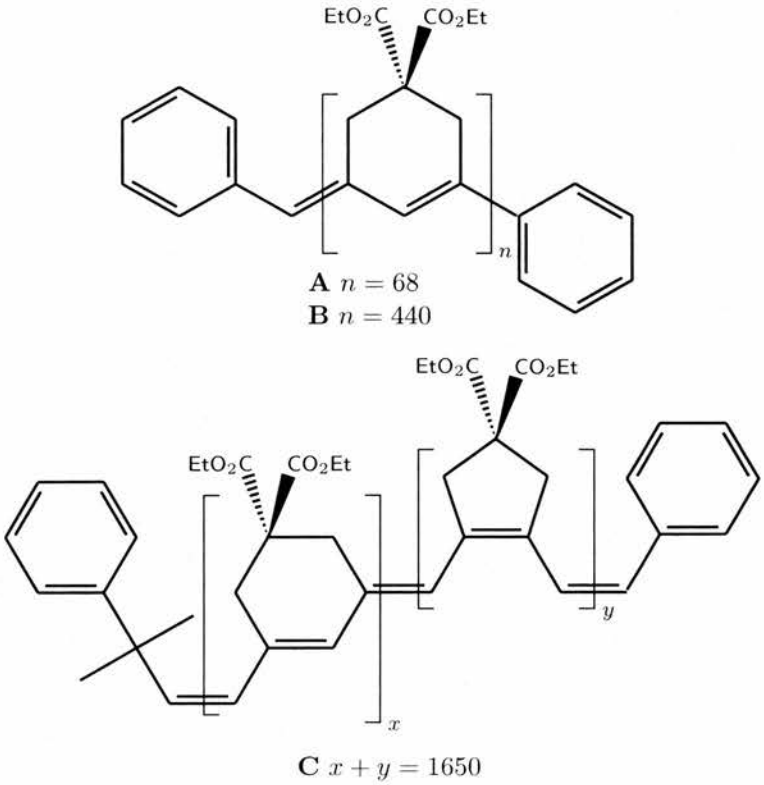

Figure 4.1: *The structure of the polymers used in this study.* ***C*** *contains a random mixture and five and six membered rings.*

of reference [18], **A** is the "3mer" and **B** is the "65mer" in this table. **A** and **B** contain only 6-membered rings, whereas **C** and the samples used by Kohler and Samuel contain random mixtures of 5 and 6-membered rings. Molecular masses and chain lengths of **A** and **B** were estimated by GPC using polystyrene standards and matrix assisted laser desorption ionisation time of flight (MALDI TOF) [18] mass spectrometry. The molecular masses determined from MALDI TOF were approximately half those obtained by GPC. As the conjugated polymers used in this study are more rigid than the polystyrene standards used in the GPC measurements, they appear heavier than they actually are when compared to the standards. The molecular mass of **C** was determined by GPC and light scattering. These polyenes

are much more stable than other simple polyenes such as octatetraene; this is thought to be due to the rings in the molecule making it more resistant to oxidation of the double bonds. Absorption spectra were obtained in 2-methyl tetrahydrofuran (2-MeTHF), a solvent that forms a glass at 135 K, permitting absorption measurements on the polymers over a wide range of temperatures by Ron Christensen and Arij Faksh. Absorption spectra were monitored in approximately 50 K intervals between 80 K and 300 K, and the spectra were corrected for the absorption of 2-MeTHF. The absorption spectrum of each sample was repeated to ensure there was no sample degradation on the time-scale of the experiment. In addition, spectra taken on different days were also compared and found to be identical.

4.3 Determination of the distribution of conjugated segment length within a polymer

Kohler and Samuel [11] found that it was possible to fit the absorption spectrum of a polymer to the superposition of the absorption spectra of conjugated segments. That is, given a reference library of all-trans linear conjugated segments,it is possible to decompose the absorption spectrum of a polymer into a distribution of conjugated segment absorption spectra. This is important because it makes it possible to extract the distribution of chain lengths within a polymer from its absorption spectrum. In this way the absorption spectrum can be used to obtain information of the extent of electron delocalisation within the polymer. The main problem faced in doing this is to generate the reference library of oligomer spectra. This problem is addressed later in this section.

The absorption of a polymer $A(E)$ may be modelled as the linear superposition of the absorption of a set of model conjugated segments $\mathcal{A}_N(E)$ where N is the number of double bonds in the segment.

$$A(E) = \sum_{i=1}^{P} a_i \mathcal{A}_i(E) \tag{4.1}$$

a_i are the unknown coefficients in the linear superposition. The values of these coefficients are determined by the method of least squares by minimising

$$\chi^2 = \sum_{j=1}^{Q} \left(A(E_j) - \sum_{i=1}^{P} a_i \mathcal{A}_i(E_j) \right)^2 \tag{4.2}$$

As a_i is an abundance it must satisfy

$$a_i \geq 0 \tag{4.3}$$

In order to minimise χ^2 subject to this constraint the method of non-negative least squares (NNLS) was employed. A computer program was written to do this using an algorithm from Lawson and Hanson [19]. The program generates a library of absorption spectra and then uses the NNLS algorithm to calculate the set of a_i's, the absorption spectrum from this set of a_i's is then calculated using the library of absorption spectra. The effect of the number and spacing of the lengths of the conjugated segments used in the fits has been investigated. In order to investigate the spacing of the lengths of the segments in the library the following form for the superposition in equation 4.1 was used

$$A(E) = \sum_{i=1}^{P} a_{f(i)} \mathcal{A}_{f(i)}(E) \tag{4.4}$$

in this equation the length of the chain is related to the summation index i by an arbitrary function f. The simple case where the segments are spaced by integers is given by $f(i) = i$ and then equation 4.4 becomes equation 4.1.

4.3.1 Library of absorption spectra

Expressing the polymer absorption as the superposition of the absorptions of conjugated segments [equation 4.1] requires a complete reference library of the absorption spectra of conjugated segments with N double bonds [$\mathcal{A}_N(E)$]. Three elements are required to generate such a library [11]: (*i*) How the energy of the absorption band varies with segment length (N); (*ii*) How the

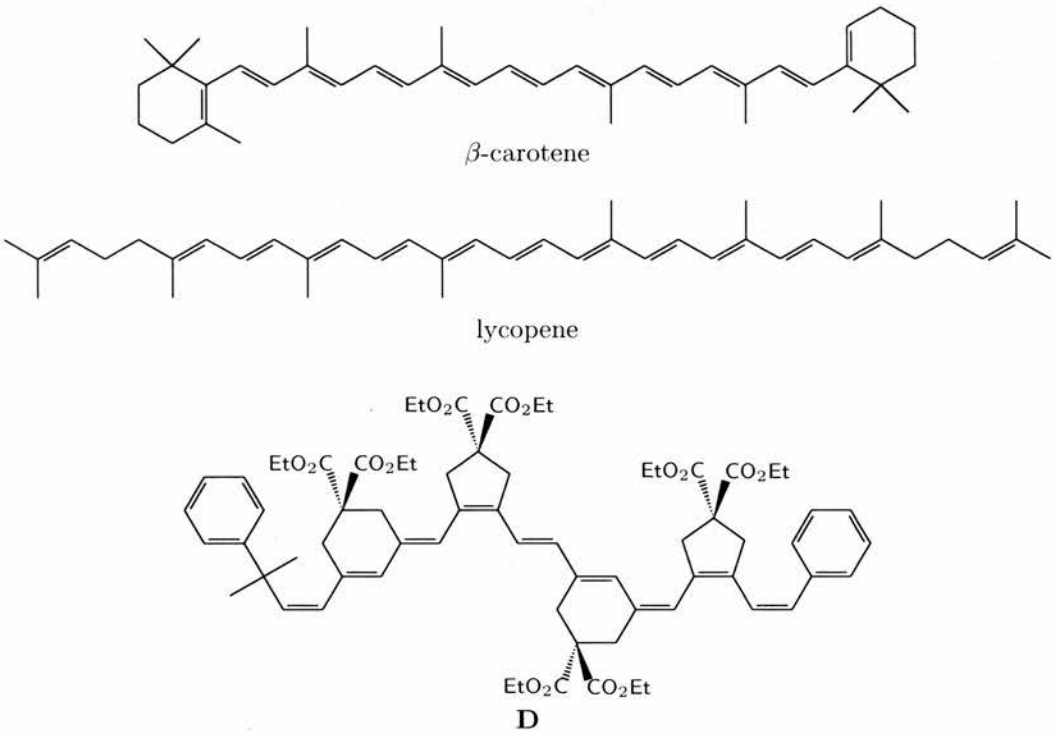

Figure 4.2: *The structure of the oligomers used as templates for the absorption library.*

shape of the absorption spectrum (relative Franck Condon factors) changes with segment length (N); (*iii*) How the intensity of the absorption (i.e. the oscillator strength of the $S_0 \rightarrow S_2$ transition) scales with segment length (N).

It is assumed that the Franck-Condon envelopes (relative vibronic intensities and line-widths) for the $S_0 \rightarrow S_2$ transition in the oligomer are appropriate for shorter and longer conjugated segments. This simplifying assumption probably underestimates the relative intensities of the $S_0 \rightarrow S_2$ (0-0) bands in longer conjugated systems. To generate a library of absorption spectra the absorption profiles of a number of oligomers have been used. The structures of these are shown in figure 4.2. *β*-carotene and lycopene are naturally occuring biological molecules and give carrots and tomatoes their

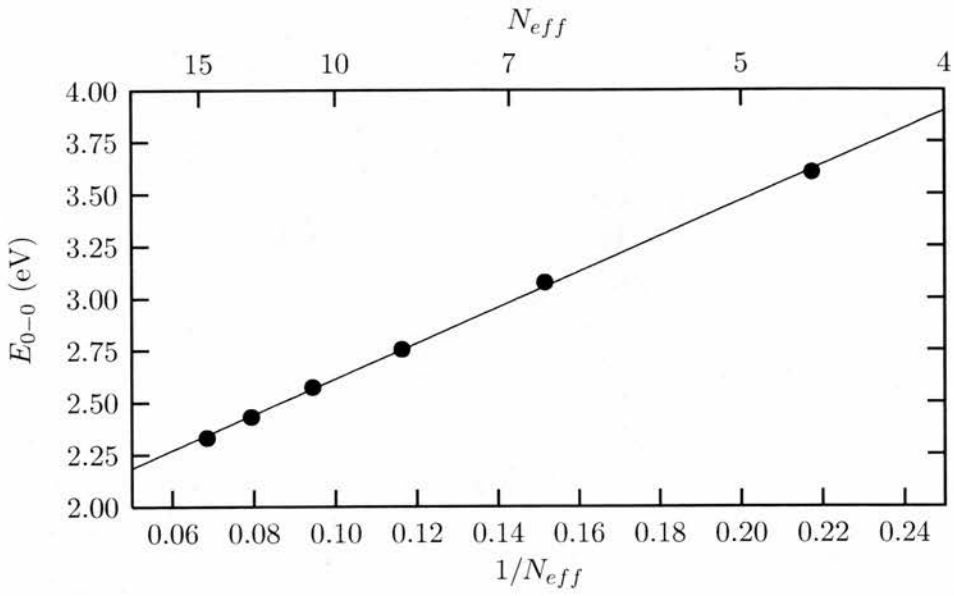

Figure 4.3: *E_{0-0} as a function of segment length for a series of oligomers with the same structure as* ***D****.*

characteristic colours. The third oligomer in this figure (molecule **D**) is an oligomer of the polymer **C** which was synthesised by Kai Hultzsch and then separated by HPLC by Ron Christensen and Arij Faksh. The structure presented here is one of several possible structural and geometric isomers, all of which are present in the sample used.

There are several expressions in the literature which relate the energy of absorption of a segment to its length. Kohler has proposed the Hückel spectrum simulator (HSS) model [20]. Knoll and Schrock [5] have shown that the transition energies for the electronic origins [(0-0) bands] for $S_0 \rightarrow S_2$ polyene spectra [$E_{0-0}(N)$] follow a simple empirical relationship: $E_{0-0}(N) = A + B/N$ where $A = 1.785\,\text{eV}$ and $B = 9.390\,\text{eV}$ Although these parameters only strictly apply to di-tert-butyl polyenes in room temperature n-pentane, they allow an estimate of the position of the electronic origin for any polyene. For example, $E_{0-0} = 2.641\,\text{eV}$ ($\lambda_{0-0} = 470\,\text{nm}$) for $N = 11$ which is in reasonable agreement with the absorption spectrum of β-carotene ($E_{0-0} =$

2.57 eV, $\lambda_{0-0} = 483$ nm in room temperature n-pentane). The best estimate for the absorption position of the polymers studied here is given by a $1/N$ extrapolation of the position of E_{0-0} for a series of six oligomers with the same structure as **D** in figure 4.2, with between three and thirteen double bonds, dissolved in 2-MeTHF. As the oligomers have a terminal phenyl ring conjugated to the rest of the polymer chain, the effective number of double bonds is $N_{eff} = 4.5 - 14.5$. The (0-0) transition energy is plotted as a function of $1/N_{eff}$ together with a linear fit in figure 4.3. The upper x axis in this figure shows the effective length of the conjugation. The fit gives

$$E_{0-0} = (8.6 \pm 0.1)/N + (1.76 \pm 0.02) \text{ eV} \tag{4.5}$$

If the oscillator strength and Franck Condon factors were independent of N, the absorption of any conjugated segment containing N double bonds at an energy E could be expressed as

$$\mathcal{A}_N(E) \propto A_{olig}[E - (E_n - E_{olig})] \tag{4.6}$$

Where A_{olig} is the absorption of the oligomer template, $E_N = A + B/N$, the 0-0 transition energy predicted by equation 4.5 and $E_{olig} = A + B/N_{olig}$ where N_{olig} is the number of conjugated double bonds in the template used for the vibronic line-shapes. $N_{olig} = 11$ for β-carotene and lycopene, for **D** $N_{olig} = 10.5$ as there are nine double bonds in the repeat units conjugated to the terminal phenyl ring.

In order to estimate the change in the intensity of absorption with the number of conjugated double bonds (N), the squares of the transition dipole moments given by the Hückel Spectrum Simulator (HSS) model of Kohler [20] are used. In the HSS model the transition dipole moment increases with N, approaching a constant asymptote for large N [11]. The full expression for the absorption of a conjugated segment with N double bonds at energy E is given by:

$$\mathcal{A}_N(E) = \mu_N^2 A_{olig}[E - (E_n - E_{olig})] \tag{4.7}$$

Where μ_N is the transition dipole moment and all other symbols have the same meaning as in equation 4.6.

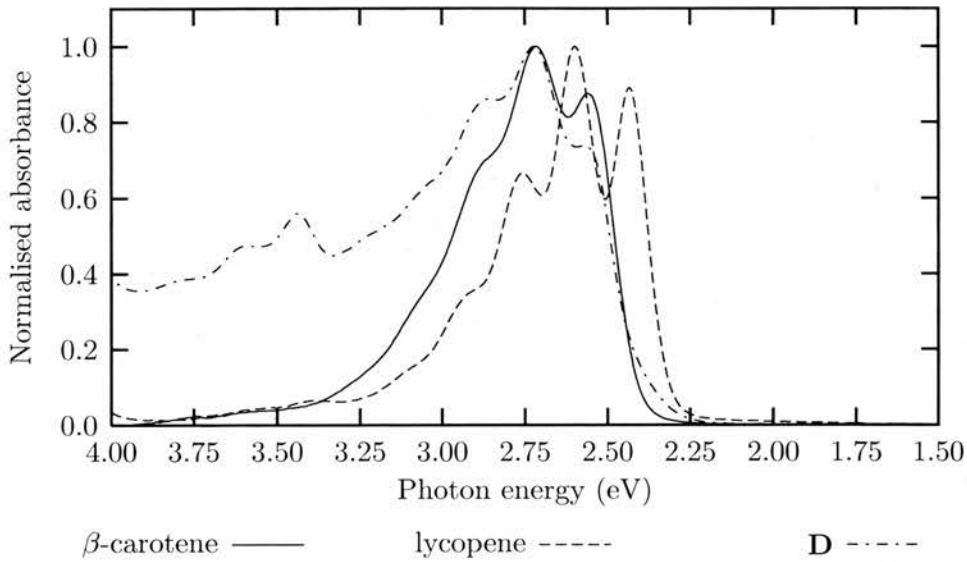

Figure 4.4: *The absorption profiles of the oligomers used as line-shape templates for the absorption library.*

The simplifying assumption that the line-shape is independent of the length of the molecule makes generating the library of absorption spectra relatively simple. The absorption of a fully conjugated oligomer can be used. Several oligomers have been used as line-shape templates for the oligomer library. The absorption of these templates in 2-MeTHF is plotted in figure 4.4. Lycopene and β-carotene have the same number of conjugated double bonds, however there are some differences between their spectra. Lycopene has more vibronic structure than β-carotene and absorbs at lower energies. This is likely to be due to subtle conformational differences between the two molecules due to the terminal rings in β-carotene [21]. **D** has much more high photon energy absorption than either lycopene or β-carotene; this is due to the presence of both cis and trans isomers in **D** and only trans isomers in the lycopene and β-carotene samples.

A library of absorptions of conjugated segments containing between 5 and 100 double bonds is plotted in figure 4.5. The library was generated using the

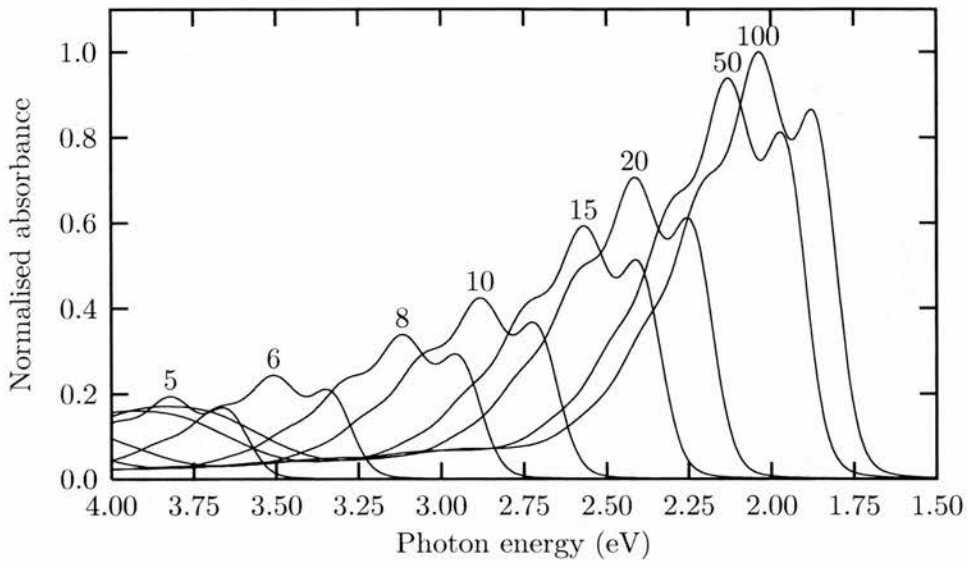

Figure 4.5: *Library of absorptions of conjugated segments. The length of conjugation is indicated.*

absorption of β-carotene as a template, the position of the absorption was calculated from the data of Knoll and Schrock [5] and the transition dipole moments were taken from Kohlers HSS model [20]. The absorption spectra of short segments (small N) in the high-energy end of the plotted photon energy range do not overlap very much. (Note that there is some overlap between the absorption of the long segments and the absorption of the short segments in the high-energy range.) As the length of the conjugated segment increases, the spectra move towards lower energies (longer wavelengths) and their $1/N$ dependence gives rise to considerable overlap in the spectra of segments with comparable lengths. In addition, the Kohler HSS model predicts an approximately six-fold increase in the absorption in changing from $N = 5$ to $N = 100$.

4.3.2 Uniqueness of NNLS fits

Using equations 4.2 and 4.7 it is possible to calculate a distribution of segment lengths for an arbitrary polymer absorption spectrum. However it is important to ensure that the fits obtained are unique. Minimising χ^2 in equation 4.2 is equivalent to minimising

$$||\boldsymbol{\mathcal{A}}\boldsymbol{a} - \boldsymbol{A}|| \tag{4.8}$$

where $\boldsymbol{\mathcal{A}}$ is a matrix containing the absorption of conjugated segments of lengths 1 to P at energies E_1 to E_Q

$$\boldsymbol{\mathcal{A}} = \begin{bmatrix} \mathcal{A}_1(E_1) & \mathcal{A}_2(E_1) & \dots & \mathcal{A}_P(E_1) \\ \mathcal{A}_1(E_2) & \mathcal{A}_2(E_2) & \dots & \mathcal{A}_P(E_2) \\ \vdots & \vdots & \ddots & \vdots \\ \mathcal{A}_1(E_Q) & \mathcal{A}_2(E_Q) & \dots & \mathcal{A}_P(E_Q) \end{bmatrix} \tag{4.9}$$

$\boldsymbol{a}$ is a vector of the unknown abundances a_1 to a_P

$$\boldsymbol{a} = \begin{bmatrix} a_1 \\ a_2 \\ \vdots \\ a_P \end{bmatrix} \tag{4.10}$$

and $\boldsymbol{A}$ is a vector of the absorption spectrum at energies E_1 to E_Q

$$\boldsymbol{A} = \begin{bmatrix} A(E_1) \\ A(E_2) \\ \vdots \\ A(E_Q) \end{bmatrix} \tag{4.11}$$

For the fit to be unique the rank of the matrix $\boldsymbol{\mathcal{A}}$ must be equal to the number of columns [19]. In practice this means that the number of steps in energy must be greater than or equal to the number of segment lengths used in the fit and every column and at least P rows in the matrix must be

linearly independent. Substituting equation 4.7 into equation 4.9

$$\mathcal{A}=\begin{bmatrix} \mu^2(1)A_o[E_1-(E_N(1)-E_o)] & \mu^2(2)A_o[E_1-(E_N(2)-E_o)] & \dots & \mu^2(P)A_o[E_1-(E_N(P)-E_o)] \\ \mu^2(1)A_o[E_2-(E_N(1)-E_o)] & \mu^2(2)A_o[E_2-(E_N(2)-E_o)] & \dots & \mu^2(P)A_o[E_2-(E_N(P)-E_o)] \\ \vdots & \vdots & \ddots & \vdots \\ \mu^2(1)A_o[E_Q-(E_N(1)-E_o)] & \mu^2(2)A_o[E_Q-(E_N(2)-E_o)] & \dots & \mu^2(P)A_o[E_Q-(E_N(P)-E_o)] \end{bmatrix} \tag{4.12}$$

In general the rows and columns are linearly independent, so the fits will be unique as long as the number of steps in energy is greater than the number of segment lengths used in the fits.

4.4 Room temperature behaviour of the polymers

The room temperature absorption of the polymers will be discussed, and then NNLS fits to these spectra are presented. The implications of these fits are discussed and then in the next section the temperature dependent absorption and NNLS fits at low temperature are investigated.

4.4.1 Room temperature absorption

Most of the basic issues involved in interpreting the solution absorption spectra of conjugated polymers in terms of conformational disorder are illustrated in figure 4.6. All three polymers exhibit a broad, room-temperature absorption typical of many other conjugated polyenes, and their absorption maxima lie only slightly to the red of the β-carotene template. The upper x axis in this figure shows the $S_0 \rightarrow S_2$ transition energies (E_{0-0}) for selected conjugation lengths, predicted from the results of Knoll and Schrock [5]. While the peak of the absorption profile of the polymers is somewhat lower in energy than that of β-carotene ($N = 11$), it is clear that (E_{0-0}) for **A**, **B** and **C** lie at significantly higher energies than the $\sim 1.82\,\text{eV}$, $\sim 1.77\,\text{eV}$, $\sim 1.76\,\text{eV}$ predicted by application of $E_{0-0} = A + B/N$ to $N = 137$, $N = 880$, $N = 3300$

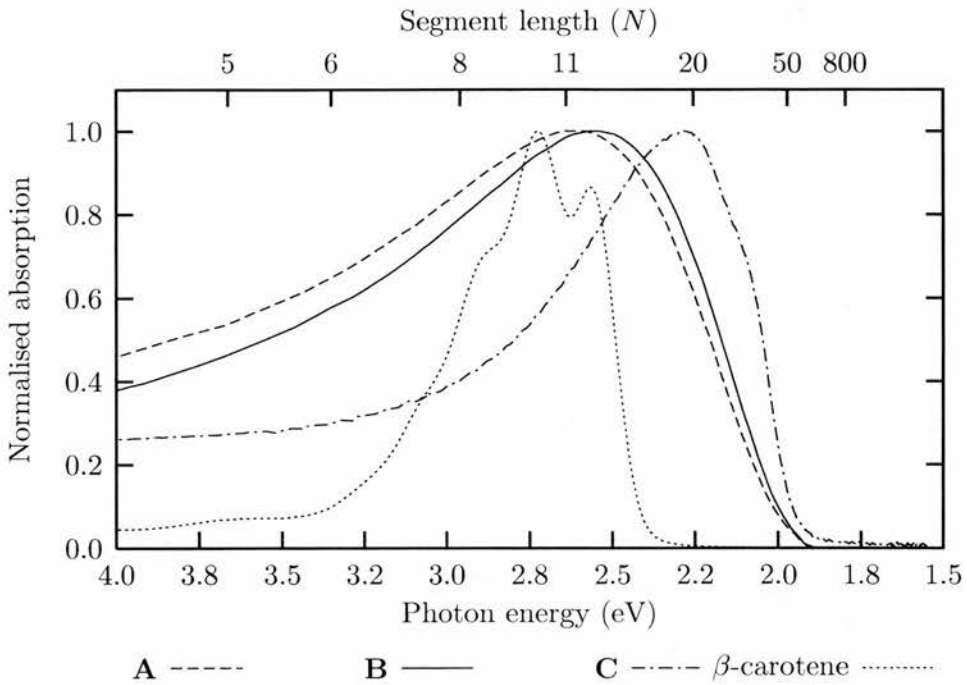

Figure 4.6: *Room temperature absorption of polymers* ***A***, ***B***, ***C***, *and oligomer β-carotene ($N = 11$) for comparison.*

respectively. The room temperature absorption spectrum thus requires that the majority of the absorption of the polymers must be ascribed to conjugated segments with $N < 20$. The mean segment length clearly is much shorter than the chain length of these polymers.

4.4.2 NNLS fits to room temperature spectra

To investigate conformational disorder in samples **A**, **B** and **C**, NNLS fits were performed to their absorption spectra. As a number of possible oligomer line-shapes have been identified, fits to sample **B** were performed using 500 linearly spaced steps in energy between 4.133 eV and 1.550 eV (300 nm and 800 nm), integer segment lengths between 4 and 100 double bonds [$f(i) = i + 4$ and $P = 96$ in equation 4.4] and the three different line-shapes in figure 4.4 to see how sensitive the fits are to this parameter. Figure 4.7 shows

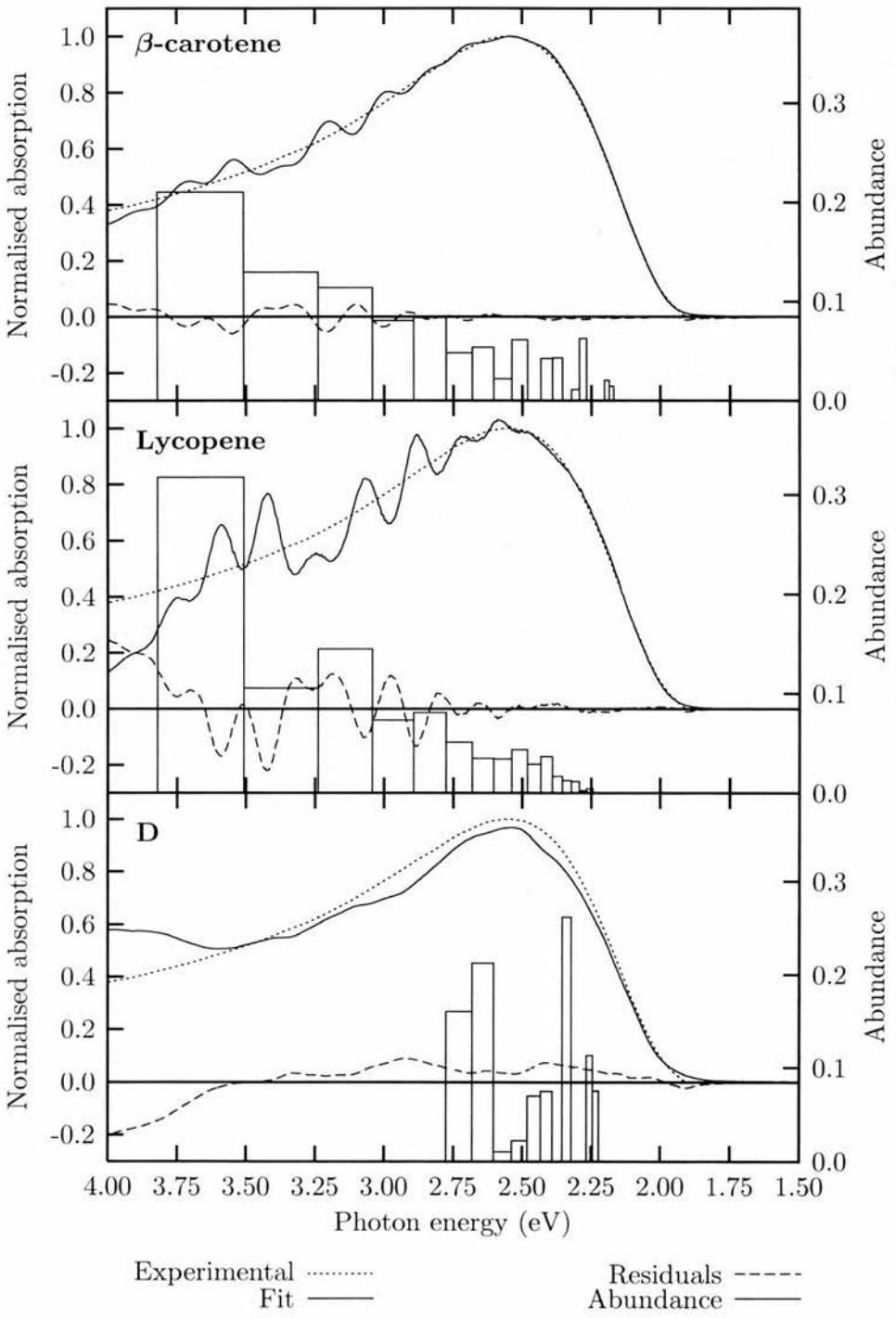

Figure 4.7: *The absorption of* ***B*** *at 300 K (dotted line). NNLS fits to the absorption spectrum of* ***B*** *using different oligomer templates and constant steps in segment length (solid line). The difference between the fit and the experimental spectrum (dashed line) and the positions of the segment lengths used in the fit (bars).*

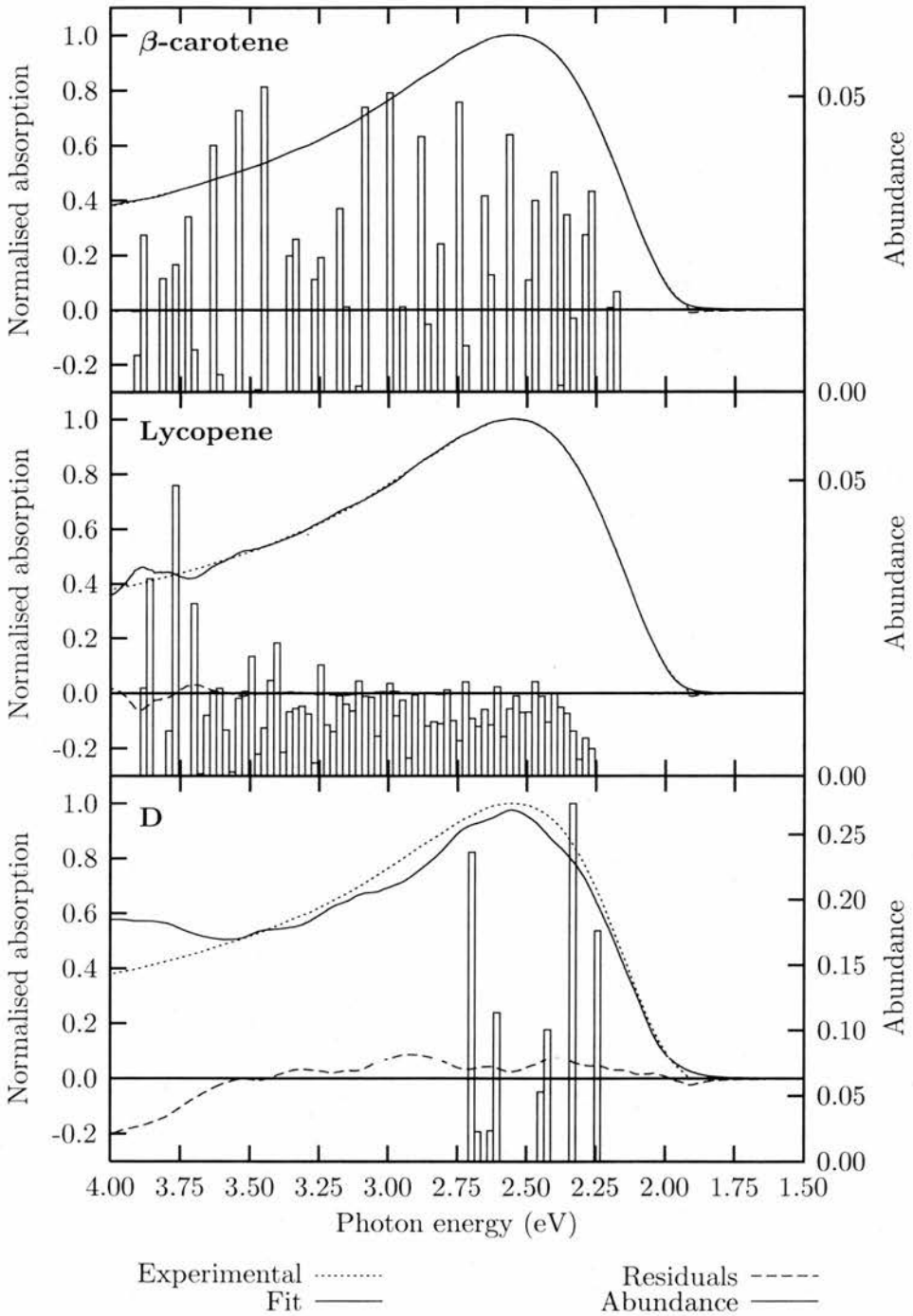

Figure 4.8: *The absorption of* ***B*** *at 300 K (dotted line). NNLS fits to the absorption spectrum of* ***B*** *using different oligomer templates and constant steps in energy (solid line). The difference between the fit and the experimental spectrum (dashed line) and the positions of the segment lengths used in the fit (bars).*

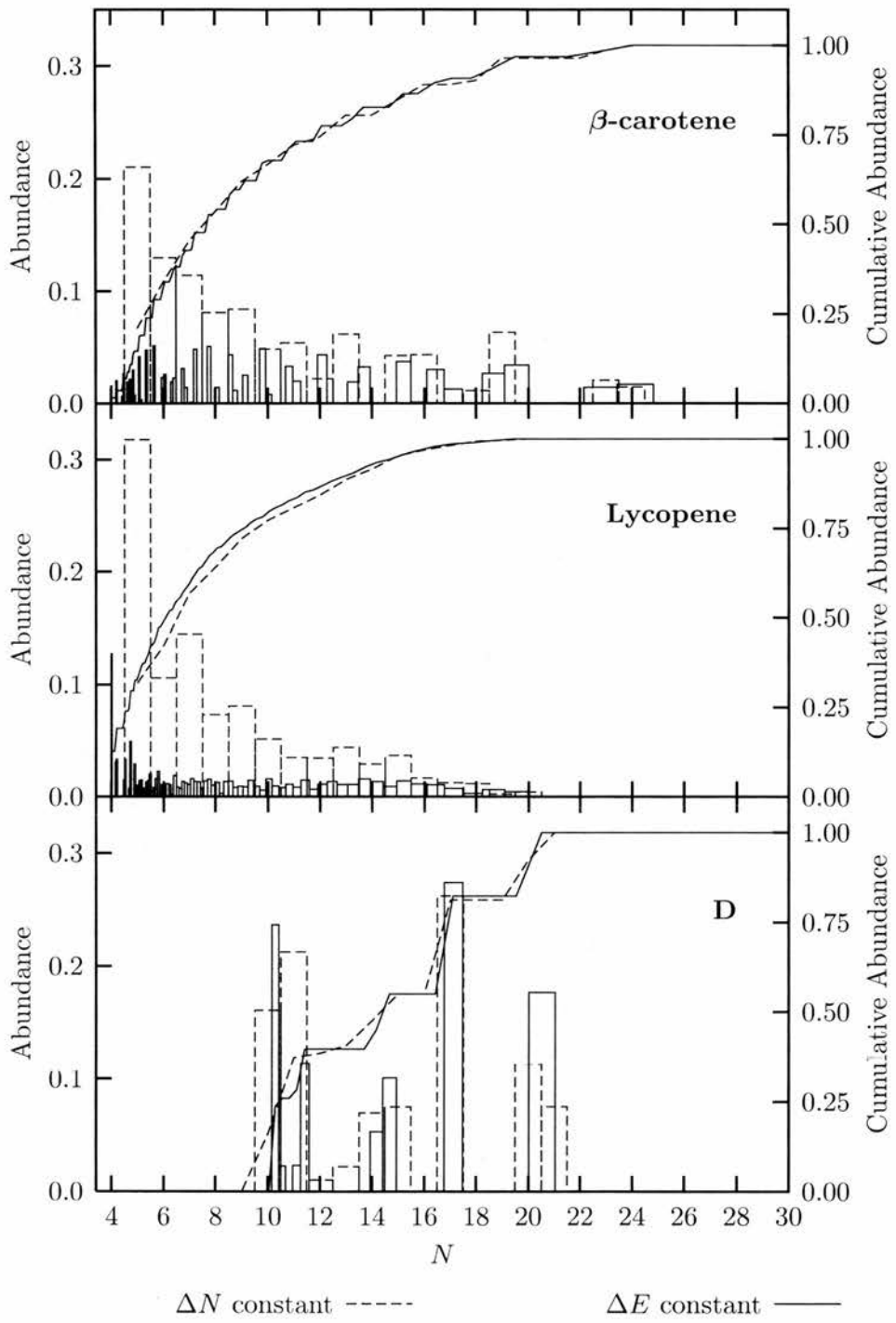

Figure 4.9: *Conjugated segment length distributions for the fits shown in figures 4.7 (dotted line) and 4.8 (solid line). The bars show the abundance of each segment length. The lines show the cumulative abundances.*

NNLS fits to the absorption of **B** at 300 K using different absorption library templates in figure 4.2. It is clear that the choice of the absorption profile of the library has an effect on the quality of the fit. The bars in figure 4.7 show the positions of E_{0-0} of the absorptions of the conjugated segments which are used in the fit. The width of the bars indicates the spacing of E_{0-0} of the segments. With the library of conjugated segments evenly spaced in chain length there are many more library members at low photon energies than high photon energies (see figure 4.5). The fit with a library based on β-carotene gives the best fit. The fit with lycopene is not as good, there is more oscillation in the fit and the residuals are much larger. This is due to the more pronounced vibronic structure in the lycopene spectrum and the relatively large spacing of the library members at high energies. As there are relatively few library members absorbing at higher energies due to the $A + B/N$ relationship of the position of the absorption and the fact that the fits were performed using integral steps in segment length, it is hard to fit the smooth absorption with the structured absorption of lycopene. The library members used for these two fits are quite similar, so the choice of line-shape has not significantly affected the distribution of segment lengths. This is important as it is the distribution of segment lengths which gives information on the disorder within the sample.

The fit using oligomer **D** is not as good, especially at high energies. This is because the absorption of this oligomer in figure 4.4 is much broader than that of β-carotene or lycopene. β-carotene and lycopene have very little absorption in the $3.2 - 4.0$ eV region as they are all-trans isomers. In contrast oligomer **D** contains a mixture of cis and trans isomers and has a large absorption in this region from cis isomers. The broad absorption means that when the main peak of the polymer absorption is fitted, a large absorption at higher energies is also present in the fit, preventing a good representation of the experimental spectrum. This explains why the fit using a library based on this oligomer does not fit as well at high photon energies. There are no short (high photon energy) library members used in this fit for the same

reason. The absorption of the longer (low photon energy) members of the library extends to the higher photon energies and so a fit is obtained without shorter segments. There is clearly a difficulty in fitting with the spectrum of this oligomer, as it is consists of a mixture of cis and trans isomers and so is disordered itself.

To improve the quality of the fits, a library of 100 conjugated segments whose absorption maxima were evenly spaced in energy between E_5 and E_{100} [$f(i) = 1/((1/5-1/100)(x-1.0)/99.0+1/100)$ and $P = 100$ in equation 4.4], rather than evenly in segment length, were performed. It was expected that the results from these fits would be smoother, as the library members would be evenly distributed throughout the polymer absorption spectrum, rather than clustered towards the low photon energies when the library was evenly spaced in segment length. The resulting fits are plotted in figure 4.8. The fits using β-carotene and lycopene are much better than the fits using a library with members spaced evenly in segment length. This is because the vibronic structure of the oligomers can be better smoothed out with an even spacing of the absorbing segments in energy. The fit using oligomer **D** is not appreciably different from the fit using an even spacing in segment length and is not as good as the fits using β-carotene or lycopene. This is because the fit does not use any shorter segments, as the absorption of the oligomer is so broad. As the main difference in the two libraries is at short segment lengths, there is little difference in a fit which does not use short members.

The object of performing the NNLS fits is to extract a distribution of conjugated segment lengths from the polymer absorption spectrum. These distributions for the fits in figures 4.7 and 4.8 are shown in figure 4.9. The lines in this figure indicate the cumulative abundances, the bars indicate the abundance as a function of segment length. The most striking feature of the distribution obtained from the fits with β-carotene and lycopene templates is that they peak at the shortest segment length. This was also observed by Kohler and Samuel [11], and can be rationalised using a simple model in which the probability of a single bond twisting out of the plane of conjugation

is independent of its position on the chain [14]. The more sophisticated treatment of Yaliraki and Silbey [15] also predicts that the shortest segments should dominate the distribution of segment lengths within a polymer.

When the library is equally spaced in energy many more members are used in the fit. This results in a smoother fit than when the members are evenly spaced in segment length. The cumulative abundance of segment lengths is insensitive to the spacing of the segments in the fitting library. The fitting algorithm uses a little of many closely spaced segment lengths when the library is evenly spaced in energy rather than a bigger proportion of one length when the library is evenly spaced in segment length. The distributions are quite similar when either β-carotene or lycopene is used as the oligomer. This is important as it shows that the fitting routine is relatively insensitive to the absorption profile of the library members. This means that the distributions obtained are representative of the distribution of segment lengths within the polymer. When **D** is used for the line-shape of the library members the distributions are quite different, with fewer members used and no short members feature in the distributions. As explained previously, this is due to the broad absorption of **D** and the significant contribution of the absorption of cis isomers within it.

At room temperature the samples have smooth, broad absorption spectra which peak significantly to the blue of the positions predicted by a simple extrapolation of the peak positions of oligomers. NNLS fits to these spectra give distributions which indicate that the shortest segments lengths are the most abundant. The distribution of segments lengths is largely insensitive to the details of the fitting parameters.

4.5 Temperature dependence of the absorption and segment length distributions

By exploring the effect of temperature on polymer and carotenoid absorptions it is possible to probe models of conformational disorder and better

understand the torsional motions that disrupt conjugation. These measurements take advantage of the high solubilities of the polymers even in low temperature glasses. The temperature dependence of the absorption of a polymer provides information on the relative strength of steric forces trying to keep the chain straight and attractive forces trying to fold the chain back on itself [22]. It is interesting to compare the temperature dependent behaviour of the oligomers to that of the polymers. If, as is widely believed, the oligomers are free from conformational disorder at room temperature then their spectra should change less than the polymers as they are cooled because the polymers are believed to be disordered at room temperature. For oligomer **D** this is less clear as the solution contains a mixture of several isomers, however β-carotene and lycopene should exhibit less change in their spectra as the temperature is lowered than the polymers.

4.5.1 Temperature dependent absorption of polymers and oligomers

Figure 4.10 shows the temperature dependent absorption of β-carotene, lycopene and **D**. As they are cooled, all three show an increase in their vibronic structure and a modest red-shift of the absorption. There is also an increase in the intensity of the absorption. β-carotene and lycopene have a larger increase in the strength of their absorption as they are cooled than **D**. Figure 4.11 shows the temperature dependent absorption of polymers **A**, **B** and **C** at 300 K and 80 K. **A** and **B** show no vibronic structure even at low temperatures, **C** shows some vibronic structure at 77 K. All three polymers show both a significant red-shift in the peak of the absorption and increase in their integrated absorption strength $[\int (A(E)/E)\, dE]$. The shift of E_{0-0} and the increase in the integrated absorption strength (which is proportional to the transition dipole squared) for the oligomers and polymers in figures 4.10 and 4.11 are given in table 4.2. All samples exhibit a smooth shift of the maxima of their absorption as the temperature is reduced, there are no discontinuities around the glass transition temperature (135 K). The

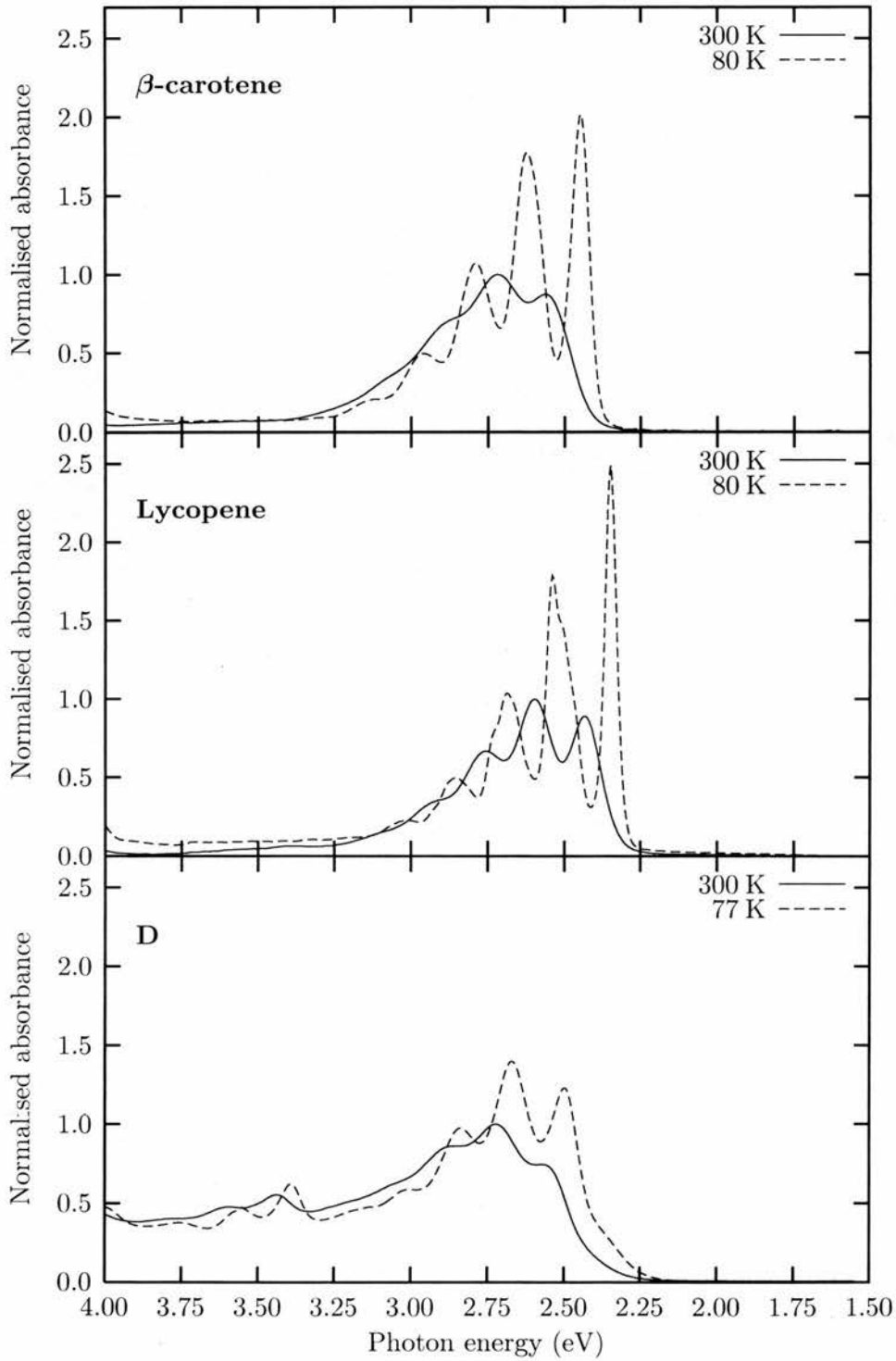

Figure 4.10: *Temperature dependent absorption of the oligomers used in this study.*

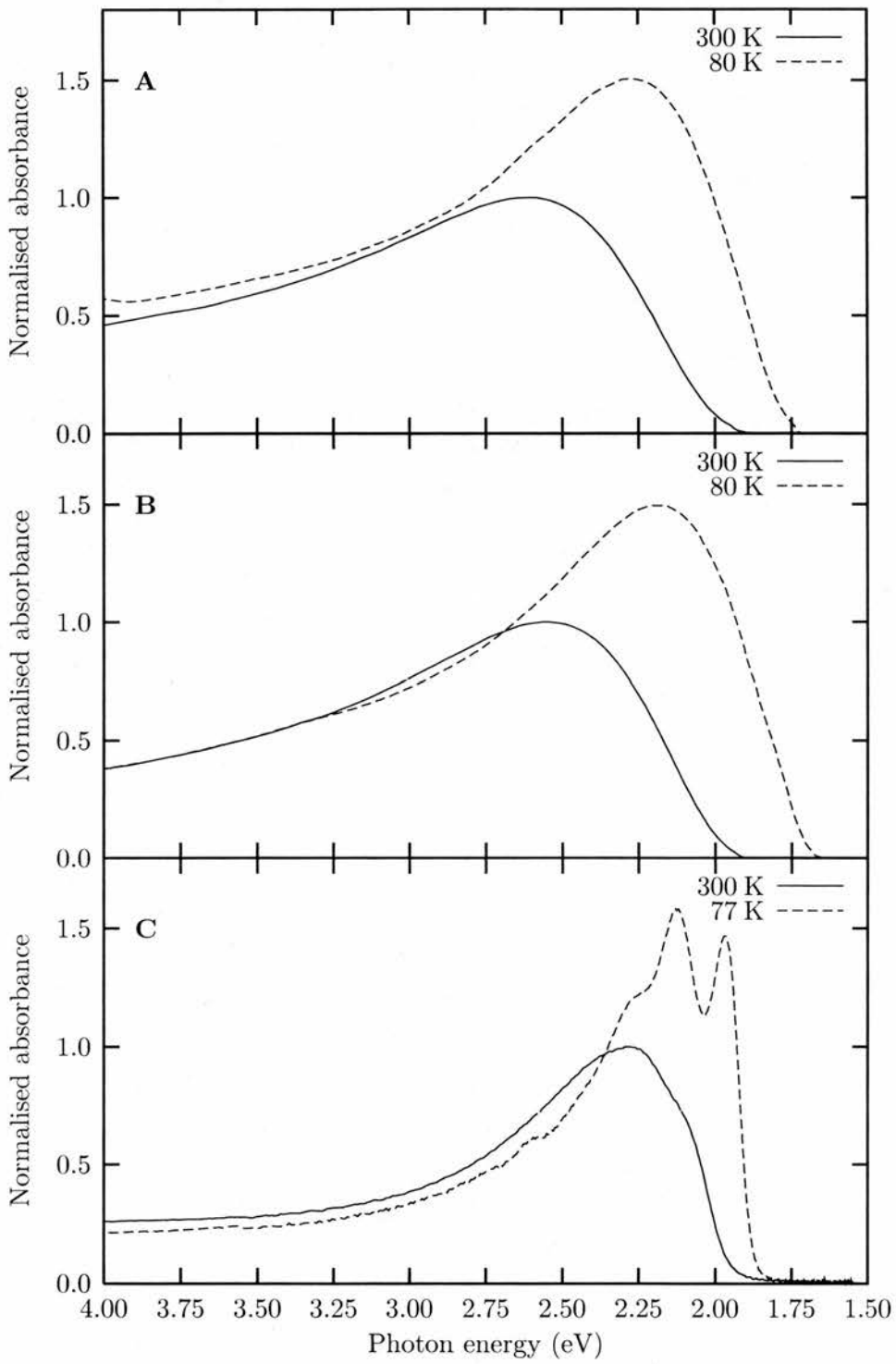

Figure 4.11: *Temperature dependent absorption of the polymers used in this study.*

polymers exhibit a larger (by a factor of three) shift in the peak of the absorption than the oligomers do. The relatively small red-shift of the oligomers can be attributed to the increase in polarisability of the solvent as it is cooled and subtle conformational effects such as the double bonds becoming more planar [23]. The increase in the absorption of the oligomers is due to solvent shrinkage and the increased polarisability of the solvent. The vibronic structure in the room temperature spectra of the oligomers indicates that they all contain a narrow set of conformations at room temperature. The larger shifts in the peaks of the absorption of the polymers suggest that they are undergoing more significant conformational changes as they are cooled. The smooth spectra of **A** and **B** at low temperature imply that there are still conformational breaks present, even when the thermal energy is greatly reduced. The absence of discontinuities in the shift of the spectra as the samples are cooled means that the red-shifted spectra cannot be assigned to solvent phase changes or the effects of folding or aggregation. The differences between the three polymers are more pronounced at low temperatures. The vibronic structure in the absorption spectrum of **C** indicates that there is a narrow range of conjugated segment lengths present. This could be due to the very low polydispersity of the sample.

4.5.2 Temperature dependent NNLS fits

To investigate the change in conformation as the polymer is cooled NNLS fits to the absorption spectrum were performed at room temperature and liquid nitrogen temperature using β-carotene as a template. The fits are shown in figure 4.12 and the corresponding conjugated segment length distributions are shown in figure 4.13. The fits to polymers **A** and **B** are quite good at high and low temperatures. The oscillations at higher energies are due to the fact that a library with conjugated segments evenly spaced in length was used in these fits. The fit to polymer **C** is much better at high temperature than low temperature. This is because of the increase in the vibronic structure as it is cooled which is hard to fit with the line-shape of β-carotene.

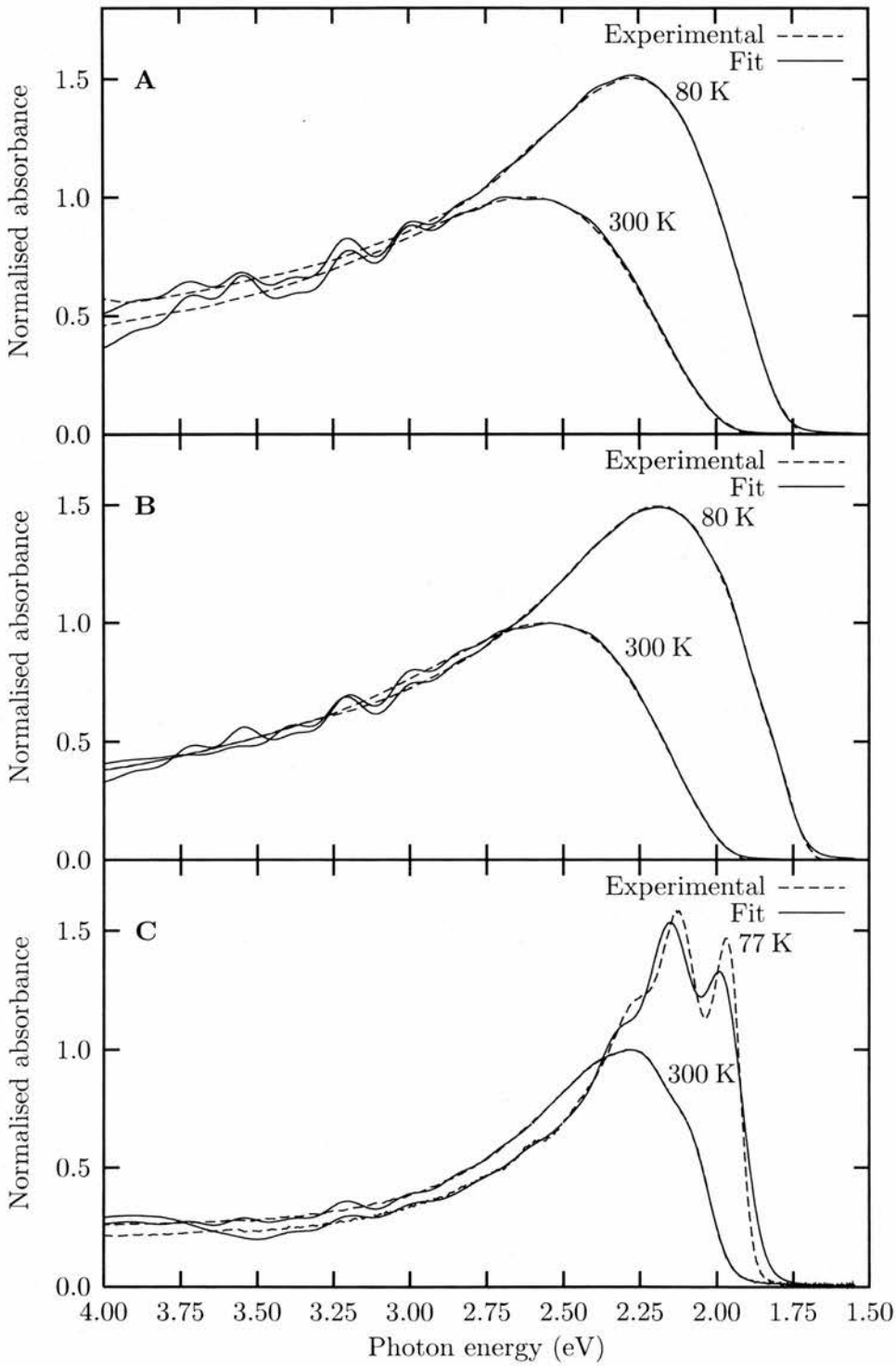

Figure 4.12: *NNLS fits to the absorption of polymers* ***A***, ***B*** *and* ***C*** *at* 300 K *and* 77 K.

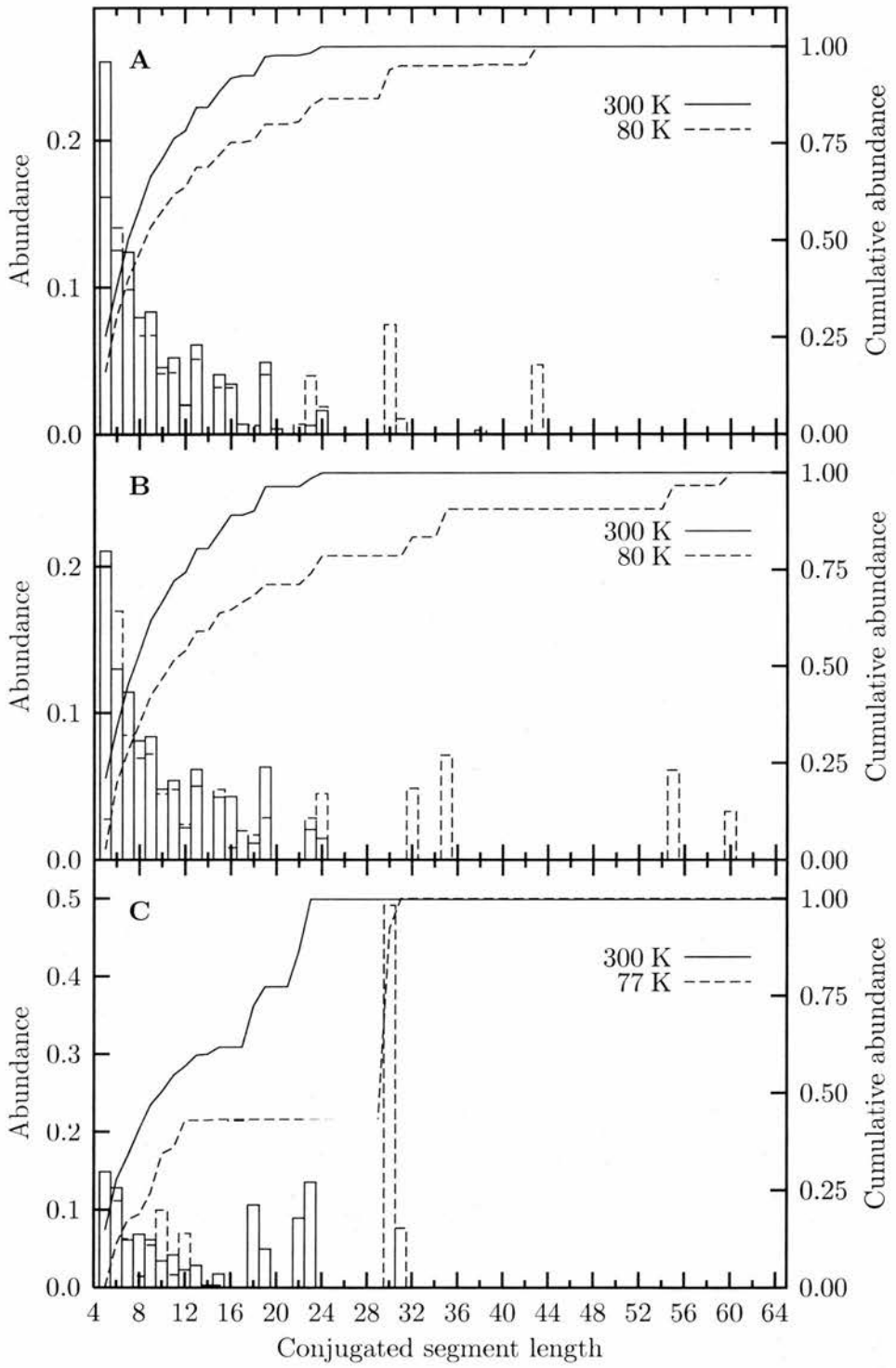

Figure 4.13: *Conjugated segment length distributions for the fits in figure 4.11.*

Compound	ΔE_{0-0} **(meV)**	$\frac{\int A_{80\,\mathrm{K}}(E)/E\,dE}{\int A_{300\,\mathrm{K}}(E)/E\,dE}$
β-carotene	115	1.3
Lycopene	80	1.4
D	70	1.1
A	310	1.7
B	375	1.6
C	310	1.3

Table 4.2: *The red-shift and increase in absorption intensity for the polymers and oligomers when they are cooled from* 300 K *to* 80 K. *Note for polymers* ***A***, ***B*** *and* ***C*** *the shift in the peak of the absorption is given as it is not possible to determine* E_{0-0}.

As the polymers are cooled the distribution of conjugated segments within them shown in figure 4.13 moves to longer lengths. The large peak at a length of 30 double bonds in the distribution for polymer **C** at low temperature comes from trying to fit the vibronic structure of the low temperature absorption spectrum of this polymer. The mean segment length, $\langle N \rangle$, calculated from

$$\langle N \rangle = \frac{\sum_{i=1}^{P} i a_i}{\sum_{i=1}^{P} a_i} \tag{4.13}$$

for the three polymers as a function of temperature is shown in table 4.3. **C** has a much longer mean length at room temperature and low temperature than **A** or **B**. At room temperature this is reflected in the red-shifted absorption of **C** relative to **A** and **B**. At low temperature the longer length comes about from the large abundance of $N = 30$ in the distribution. **B** has longer conjugated segments in the fit than **C** but the abundances of these segments are sufficiently low for **C** to have the longer mean length. The shift of the segment length distributions to longer lengths is consistent with estimate of a few $k_B T_{room}$ for the torsional barriers for breaking the planes of conjugation in these systems [10, 15].

Polymer	300 K	250 K	200 K	150 K	100 K	80 K
A	8.5	8.8	9.2	10.1	11.5	11.7
B	9.0	9.3	10.7	12.7	13.8	13.8
C	12.9	-	-	-	-	20.9

Table 4.3: *Mean conjugated segment length $\langle N \rangle$ calculated from equation 4.13 for polymers* ***A***, ***B*** *and* ***C*** *as a function of temperature.*

4.6 Yaliraki and Silbey fits

The model of Yaliraki and Silbey is one of the more sophisticated conformational disorder models and deserves further attention. The model predicts a distribution of conjugated segment lengths within the polymer. This is an important step forward from other models [8, 10, 24] which predict a mean conjugation length as it represents a more realistic situation since there will be a distribution of lengths present within the polymer. In order to fully explain the scaling of the third order non linearity [13] with chain length and the width as well as the position of the absorption spectrum, it is necessary to use a distribution of conjugated segments. Models of conformational disorder broadly fall into two categories (*i*) "wormlike" chains and (*ii*) "platelet" chains. In wormlike models the polymer chain is viewed as distorting in a continuous manner, slowly twisting and bending along its length with no large rotational defects [25]. In platelet models the chain is considered to be made up of almost planar segments separated by rotational defects which break the conjugation [10, 14, 15, 24]. Yaliraki and Silbey use a platelet model where adjacent platelets lie at an angle ϕ to each other. Yaliraki and Silbey derive

$$H = \sum_{i=1}^{N} -E_c \cos 2\phi_i - E_s \cos \phi_i \tag{4.14}$$

which is the Hamiltonian used phenomenologically by Rossi et al. [10]. E_s represents an effective steric hinderance energy and E_c is a conjugation energy, the conjugation term has periodicity π with a minimum when the

platelets are aligned and a maximum when their relative angle (ϕ) is $\pi/2$. Using statistical mechanics Yaliraki and Silbey show that the most probable number of flips (m^*) on a polymer chain with N double bonds is given by

$$m^* \approx Ne^{-(E_s+E_c)/k_BT} \tag{4.15}$$

and the abundance, a_n,of a segment length, n, is given by

$$a_n = p^{n-1}(1-p) \tag{4.16}$$

where

$$p = \frac{N-1-m^*}{N-1} \tag{4.17}$$

Equation 4.16 makes it possible to calculate the distribution of segment lengths in a polymer chain based on an energy parameter (note m^* depends on $E_c + E_s$ and so the distribution is dependent on their sum, not the individual values). As the length of the chain increases the distribution becomes less sensitive to chain length. This model has successfully described the third order nonlinearity in a series of polyenes of well defined length [13, 18]. There is a clear temperature dependence in the model.

To test the model a fit was made to polymer **B** at room temperature. Then the spectrum predicted by the model at 80 K was compared to the experimental spectrum. This is a powerful test of the temperature dependence of the model. As the model predicts a distribution of segment lengths based on an energy parameter $E_s + E_c$, it was necessary to construct an absorption spectrum from the segment length distribution predicted by the model. To do this the library of absorptions of conjugated segments used in the NNLS fits was used and $E_s + E_c$ was varied to get the best fit to the measured spectrum at 300 K. The fit was obtained by minimising χ^2 in

$$\chi^2 = \sum_{i=1}^{Q} (A(E_i) - \mathcal{A}(E_i))^2 \tag{4.18}$$

where $A(E_i)$ is the measured absorption spectrum at photon energy E_i and $\mathcal{A}(E_i)$ is the absorption spectrum calculated from the model at the same

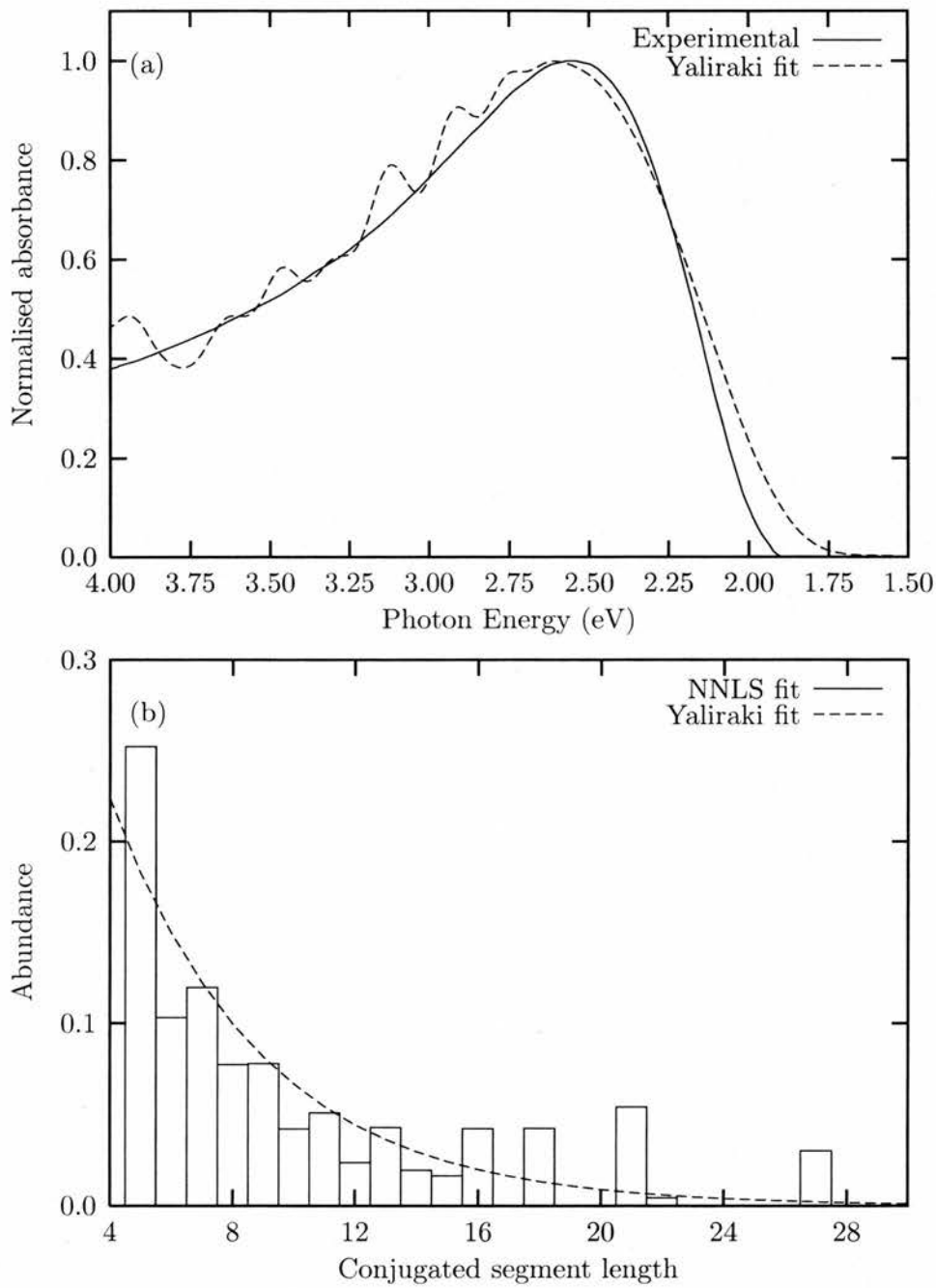

Figure 4.14: *(a) Fit to the absorption of* **B** *at* 300 K *using the model of Yaliraki and Silbey [15]. (b) Conjugated segment length distributions predicted by NNLS and Yaliraki and Silbey fits to the absorption of* **B** *at* 300 K.

energy. The fit to the 300 K absorption spectrum is shown in figure 4.14. The model parameters are $E_s = 0.024\,\text{eV}$ $(0.92k_BT)$ and $E_c = 0.015\,\text{eV}$ $(0.58k_BT)$ at $T = 300\,\text{K}$. The fit is not as good as the NNLS fits in figure 4.7 but follows the absorption of the polymer reasonably well. The oscillations at higher photon energies are due to the fact that a library of absorptions of segments evenly spaced length was used in the fit. This leads to a relatively large spacing of library members in the high photon energy region which gives a "bumpy" fit in this region. The segment length distribution for this fit is shown in the lower panel of figure 4.14, together with the distribution from an NNLS fit in figure 4.7. The segment length distribution from the Yaliraki and Silbey model is a smooth function, whereas the NNLS fits gives discrete data points. Both have been normalised such that the area under the distribution between $N = 5$ and $N = 100$ is one. They both peak at the shortest segment length. The distribution predicted by the Yaliraki and Silbey model matches fairly well with the NNLS distribution although the Yaliraki and Silbey distribution slightly overestimates the importance of long conjugated segments.

From the fit in figure 4.14 it is possible to construct the absorption spectrum at 80 K predicted by the model of Yaliraki and Silbey. This is shown with the experimental spectrum in the top of figure 4.15. It is clear that spectrum predicted by the model does not match up with the experimental spectrum. The inset in this figure shows how the peak position of the absorption spectrum changes experimentally and in the model. The model has a stronger temperature dependence than the real polymer. The segment length distribution predicted by Yaliraki and Silbey and from an NNLS fit to the 80 K absorption spectrum of **B** are shown in the lower half of figure 4.15. The two distributions are quite different. The NNLS distribution peaks at short segment lengths and generally decreases with increasing segment length. The distribution predicted by the model of Yaliraki and Silbey is very flat, with little segment length dependence. The flat segment length distribution predicted by the model of Yaliraki and Silbey leads to the large

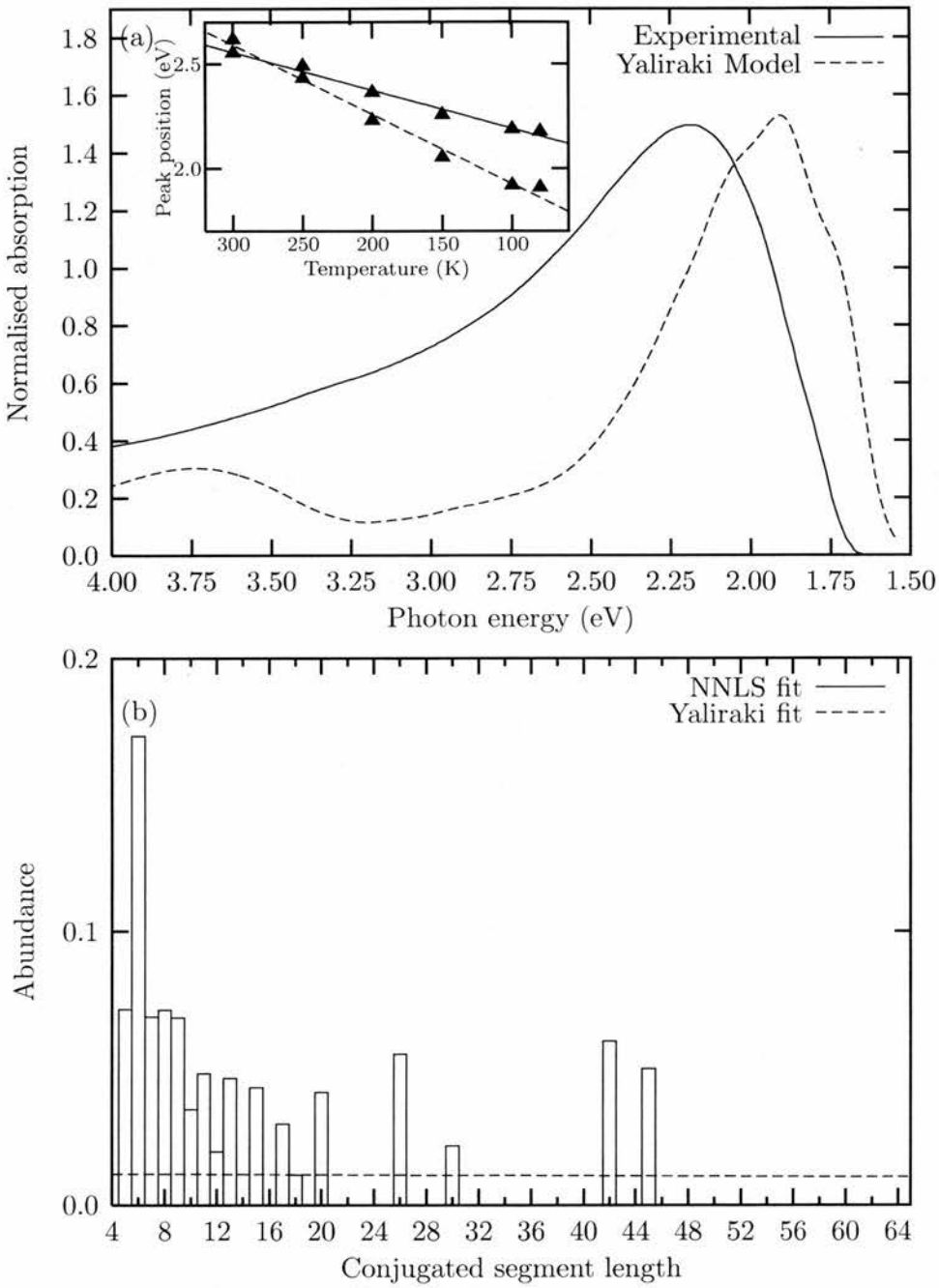

Figure 4.15: *(a) Absorption spectrum of* ***B*** *at* 80 K *and the spectrum predicted by the model of Yaliraki and Silbey [15] from the fit in figure 4.14. The inset shows the peak position as function of temperature for the experimental spectrum and the spectrum calculated using the model. (b) Conjugated segment length distributions predicted by NNLS and Yaliraki and Silbey fits for* ***B*** *at* 80 K.

red-shift in the absorption spectrum; as the transition dipole is greater for longer segment lengths and the energy of absorption converges for long segment lengths there is a large low energy absorption from these longer lengths. The short lengths which contribute to the higher energy absorptions have a weaker absorption and do not overlap as much and hence a lower absorption in this region is obtained. The second peak in the absorption at 3.75 eV is due to the second absorption band of longer segments.

The Yaliraki and Silbey model shows qualitative agreement with the temperature dependence observed experimentally but it overestimates the red-shift of the spectrum. There are several possible reasons for the failure of the model to predict the low temperature absorption spectrum accurately. Firstly the assumptions of the model may be simply unrealistic, leading to an overestimate of the importance of long conjugated segments in the distribution. It is also possible that the increased viscosity of cooled solutions increases the barriers to torsional motion, partially locking the samples into their high temperature conformations. In addition to conformational breaks in conjugation, sample **B** may also contain irreversible breaks in conjugation due to defects in the original synthesis or subsequent chemical degradation. The lengths of the conjugated segments then would be limited by both chemical and conformational disruptions. It is important to note that the spectra reported by Schattenmann [16] originally exhibited absorption maxima (in room temperature THF) at 480 nm for **A** and 507 nm for **B**. the spectra of solutions of **A** and **B** used in this study were significantly blue shifted with absorption maxima at 474 nm and 486 nm, indicating that samples **A** and **B** have additional chemical breaks. This is the most likely reason for the apparent overestimate of the red-shift of the absorption upon cooling by the Yaliraki and Silbey model. In principle it should be possible to incorporate chemical breaks into the model. Sample **C** was synthesised much more recently and does not show any signs of degradation, the low temperature absorption spectrum contains vibronic structure and the room temperature spectrum is at significantly lower energies than **A** and **B** (note that some of

this difference is due to the different structures, the samples used by Kohler and Samuel had the same structure as **C** and for a similar length absorbed to the red of fresh samples with the same structure as **A** and **B**), however it was not possible to get a good fit of the Yaliraki and Silbey model to the absorption of this sample. This is because the absorption of this sample is narrower than **A** and **B** (this is further evidence of the sample has not degraded) and the spectra predicted by the Yaliraki and Silbey model are too wide. The vibronic structure visible in the low temperature spectrum of **C** shows that there is a relatively narrow range of segment lengths present at this temperature. In comparison the 80 K spectra of **A** and **B** are quite broad and featureless, indicating that they contain a wider range of segments. This is reflected in the results of the NNLS fits presented in the previous section.

4.7 Discussion

The results presented in this chapter support the original hypothesis of Exharos et al. [8], Shand et al. [9] and others concerning absorption maxima and vibrational frequencies that fall well short of those expected for extremely long conjugated systems. The simple theoretical models proposed by Kohler and Woehl [14] and Yaliraki and Silbey [15] predict distributions of conjugated segment lengths that are similar at least qualitatively to those extracted from the empirical NNLS fits presented in sections 4.5.1 and 4.5.2. Nevertheless, these models and the fits deserve careful scrutiny. Most problematic is the predication that solutions of even relatively short conjugated systems also should have length distributions that are dominated by the shortest conjugated segments. However, the vibronically resolved absorption spectra of molecules such as β-carotene and lycopene in figure 4.4 point to the absence of appreciable concentrations of conjugated segments with $N < 11$ (the chain length), and neither the Kohler/Woehl nor the Yaliraki/Silbey models account for the observation that conjugation lengths are equal to chain lengths in simple polyenes and carotenoids. More work will be needed

to develop models that establish a smooth connection between the optical properties of short and long polyene systems.

It is also important to acknowledge the inherent simplifications of a linear superposition model (equation 4.1), which assumes a collection of essentially orthogonal, noninteracting segments. Coupling between these segments could result in the transfer of electronic energy to neighbouring sequences on very short time scales. This would lead to homogeneous broadening due to the extremely rapid dephasing of the S_2 excited state. One might then question whether the vibronic profiles and line-widths of molecules such as β-carotene are appropriate for describing the line-widths observed for polymers. Recent time resolved studies by Scholes et al. [26] indicate that inhomogeneous broadening plays an important role in the optical properties of substituted polypheneylenevinylenes (PPVs) which are the subject of the next chapter of this thesis. If the spectra are broadened beyond $\sim 60 - 120\,\mathrm{meV}$ of homogeneous and inhomogeneous broadening experienced by β-carotene and lycopene [27, 28] equation 4.1 will then overestimate the importance of long polyene segments in accounting for the absorption of the long wavelength end of the polymer solution spectra. However, given that the shortest polyene segments already dominate the distribution of conjugated segment lengths, corrections for coupling effects would not significantly alter the conclusions presented here.

In addition to making realistic choices for vibronic band shapes and intensities, any model that purports to extract population distributions from polymer absorption spectra also must accurately portray the dependence of the $S_0 \rightarrow S_2$ oscillator strengths on conjugation length. The spectra used in the library of absorption of conjugated segments conform to the experimental observation of an apparent levelling off of oscillator strengths for polyenes with 2-12 double bonds [29, 30]. However there is very little experimental or theoretical guidance on the behaviour of oscillator strengths in the long polyene limit.

4.8 Conclusions

Previous research on polyacetylenes, polydiacetylenes and other conjugated polymers indicates that conformational disorder has a profound effect on the photophysics of these systems. Conformational disorder explains the typically broad blue-shifted optical spectra of these polymers and the dispersion of their C=C vibrational frequencies in resonance Raman excitation experiments. This chapter has shown that the absorption spectra may be expressed as the linear superposition of absorptions of shorter conjugated segments. The fits presented yield distributions of conjugated segments that are dominated by short polyene segments. The average conjugation length increases when the polymers are cooled from room temperature to 80 K, providing additional evidence for conformational disorder.

The temperature dependence of the polymer spectra allows a demanding test of the conformational disorder model of Yaliraki and Silbey, and there is qualitative agreement between experiment and theory. However for the polymers used in this work the Yaliraki and Silbey model overestimates both the importance of long conjugated segments in the distributions and the red-shift of the absorption profile upon cooling. Further refinement of the conjugated segment length distribution awaits a more accurate picture of how the transition energies, oscillator strengths, and vibronic intensities of polyene absorptions change with the length of conjugation. Current models of conformational disorder assume that the probability for twisting about a given single bond is independent of the geometry of adjacent bonds. The models also neglect the possibility of chemical breaks in conjugation and the interactions between polyene segments. It is important to note that these simple models predict that short segments should also dominate the conformational distributions of short polyenes and carotenoids. However, these molecules show no evidence for species with conjugation lengths significantly shorter than the full chain length. A major challenge for theory is thus to account for polyene absorption spectra in both the short and long chain length limits. Understanding the origins of the absorption spectra of conjugated

polymers is a challenging problem with many factors to take into account. However, even with the simplified approach presented here it is possible to gain considerable insight into the importance of conformational disorder in these systems.

References

[1] H. Petek, A. J. Bell, Y. S. Choi, B. A. Tounge K. Yoshihara, and R. L. Christensen. *Journal of Chemical Physics*, **98**, 3777, (1993).

[2] Y. S. Choi, T-S. Kim, H. Petek, K. Yoshihara, and R. L. Christensen. *Journal of Chemical Physics*, **100**, 9269, (1994).

[3] H. Petek, A. J. Bell, Y. S. Choi, K. Yoshihara, B. A. Tounge, and R. L. Christensen. *Journal of Chemical Physics*, **102**, 4726, (1995).

[4] J. F. Pfanstiel, D. W. Pratt, B. A. Tounge, and R. L. Christensen. *Journal of Physical Chemistry A*, **103**, 2337, (1999).

[5] K Knoll and R. R. Schrock. *Journal of the American Chemical Society*, **111**, 7989, (1989).

[6] R. L. Christensen, M. Goyette, L. Gallagher, J. Duncan, B. DeCoster, J. Lugtenburg, F. J. Jansen, and I. van der Hoef. *Journal of Physical Chemistry A*, **103**, 2399, (1999).

[7] R. H. Baughman and R. R. Chance. *Journal of Polymer Science, Polymer Physics Edition*, **14**, 2037, (1976).

[8] G. J. Exharos, W. M. Risen, and R. H. Baughman. *Journal of the American Chemical Society*, **98**, 396, (1976).

[9] M. L. Shand, R. R. Chance, M. Postollec, and M. Schott. *Physical Review B*, **25**, 4431, (1982).

[10] G. Rossi, R. R. Chance, and R. J. Silbey. *Journal of Chemical Physics*, **90**, 7594, (1989).

[11] B. E. Kohler and I. D. W. Samuel. *Journal of Chemical Physics*, **103**, 6248, (1995).

[12] H. H. Fox, M. O. Wolf, R. Odell, B. L. Lin, R. R. Schrock, and M. S. Wrighton. *Journal of the American Chemical Society*, **116**, 2827, (1994).

[13] I. D. W. Samuel, I. Ledoux, V. Dhenaut, J. Zyss, H. H. Fox, R. R. Schrock, and R. J. Silbey. *Science*, **265**, 1070, (1994).

[14] B. E. Kohler and J. C. Woehl. *Journal of Chemical Physics*, **103**, 6253, (1995).

[15] S. N. Yaliraki and R. J. Silbey. *Joural of Chemical Physics*, **104**, 1245, (1996).

[16] F. J. Schattenmann, R. R. Schrock, and W. M. Davis. *Journal of the American Chemical Society*, **118**, 3295, (1996).

[17] F. J. Schattenmann and R. R. Schrock. *Macromolecules*, **29**, 8990, (1996).

[18] I. Ledoux, I. D. W. Samuel, J. Zyss, S. N. Yaliraki, F. J. Schattenmann, R. R. Schrock, and R. J. Silbey. *Chemical Physics*, **245**, 1, (1999).

[19] C. L. Lawson and R. J. Hanson. *Solving least sqaures problems*, Chapter 23. SIAM, (1995).

[20] B. E. Kohler. *Journal of Chemical Physics*, **93**, 5838, (1990).

[21] R. Hemley and B. E. Kohler. *Biophyiscal Journal*, **20**, 377, (1977).

[22] G. Dufresne, J. Bouchard, M. Belletête, G. Durocher, and M. Leclerc. *Macromolecules*, **33**, 8253, (2000).

[23] P. Wood, I. D. W. Samuel, R. R. Schrock, and R. L. Christensen. *Journal of Chemical Physics*, **115**, 10955, (2001).

[24] K. S. Schweizer. *Journal of Chemical Physics*, **85**, 4181, (1986).

[25] Z. G. Soos and K. S. Schweizer. *Chemical Physics Letters*, **139**, 196, (1987).

[26] G. D. Scholes, D. S. Larsen, G. R. Fleming, G. Rumbles, and P. L. Burn. *Physical Review B*, **61**, 13670, (2000).

[27] J.E. Cotting, L.C. Hoskins, and M.E. Levan. *Journal of Chemical Physics*, , 1081, (1982).

[28] G.P. Harhay and B.S. Hudson. *Journal of Physical Chemistry*, **97**, 8158, (1993).

[29] H. Kuhn. *Journal of Chemical Physics*, **29**, 958, (1958).

[30] H. Kuhn. *Forschrift Chemie Organischer Naturstoffe*, **17**, 404, (1959).

Chapter 5

The Effect of Conjugation on the Photophysics of MEH-PPV

5.1 Introduction

The extent of conjugation in conjugated polymers has a dramatic effect on their photophysical properties. In the previous chapter the shift of the absorption of conjugated oligomers to lower energies as the length of the oligomer is increased was shown. This has been observed for simple polyenes, polyacetylene oligomers [1], and oligomers similar to MEH-PPV [2]. In this chapter the effect of the degree of conjugation on the photophysical properties of poly[2-methoxy,5-(2'-ethyl-hexyloxy)-1,4-phenylenevinylene] (MEH-PPV) is investigated. The motivation behind this work is to see how the extent of conjugation affects the nature of the excited state and to see how the introduction of tetrahedral defects into a conjugated polymer affects its conformation.

Since the discovery of electroluminescence in PPV [3] there have been numerous studies of the photophysics of PPV and its derivatives [4–11]. Harrison et al. [4], Heun at al. [6] and Bässler at al. [7] have used site selective spectroscopy to investigate the degree of inhomogeneous broadening in PPV and MEH-PPV. Bässler at al. [7] have also investigated the vibrational structure

of unbroadened individual chromophore and estimate that the Huang-Rhys factor is approximately unity. Leng at al. [5] have used electroabsorption and photoinduced absorption spectroscopy to investigate the energy levels of states with both odd and even parity. They found that the energy of the lowest lying even parity state is above the lowest lying odd parity state. Yan et al. [10] have investigated the effect of dispersing MEH-PPV in a solid matrix. They found that the photophysics of MEH-PPV in a solid matrix closely resembles the photophysics of MEH-PPV in solution as interchain interactions are greatly reduced.

MEH-PPV has received particular attention in the literature and has been studied by many spectroscopic techniques. However, there has been considerable debate on the nature of the excited state with different investigators obtaining different results and drawing different conclusions from similar experiments. Recently it has been realised that sample preparation is of paramount importance to ensure a consistent set of experimental conditions and also to avoid sample degradation during the experiment. The solvent that is used also has an import role in determining the photophysics [12, 13]. Nguyen at al. [12] studied solutions of MEH-PPV in chlorobenzene and tetrahydrofuran (THF) using steady state and time resolved spectroscopy. They found that the chlorobenzene solutions contained more aggregates than THF solutions. Recent single molecule studies [14–20] have highlighted the dependence of the conformation on the solvent used. These studies have also given some insight into the conformation of the molecules. Huser et al. [17, 18] found that films spun from a non-polar solvent such as toluene gave a tightly coiled chain conformation which exhibited luminescence from a few distinct segments on the chain. In contrast films spun from a polar solvent such as chloroform gave an extended chain conformation which exhibited luminescence from multiple segments on the chain. Hu et al. [16] and White et al. [19, 20] found that defects in the polymer have a significant effect on its conformation. Hu et al. [16] compared the results of polarised spectroscopic measurements to simulations of polymer chains of different conformations

and found that MEH-PPV adopts an ordered collapsed conformation. Later Wong et al. [21] confirmed that folds around tetrahedral defects in the chain are energetically favourable.

Near field scanning microscopy investigations [22, 23] have given more direct information on the conformation due to the spatial resolution available. Near field microscopy also has the advantage that it can be performed on the thin films that are used in devices rather than isolated molecules. Nguyen at al. [22] linked the topographic features of the film to its local luminescence characteristics. They found a rough surface where the "bumps" corresponded to areas of aggregation with luminescence to the red of the flatter areas. They also found that annealing the film produced a more uniform surface topography and luminescence characteristics. Wei et al. [23] found that there are domains of partially ordered chain on a length scale of approximately 0.3 μm.

There is one report of partially conjugated MEH-PPV in the literature [24, 25]. In their work Pandmanaban and Ramakrishnan explain the steady state spectra that they observe in terms of energy transfer between separate segments of the chain. However, as they perform only steady state photoluminescence measurements there is not direct evidence for energy transfer. The work presented in this chapter explores the temperature dependence of the photophysics of partially conjugated MEH-PPV for the first time. Using time resolved luminescence combined with transient absorption and steady state anisotropies provides compelling evidence for the presence of static disorder in the partially conjugated samples and energy transfer within them. There have been numerous ultrafast studies of MEH-PPV [10, 26–31] but none have looked at the effect of conjugation on the excited state. Vacar et al. [26] investigated the effect of the excitation photon energy on the ultrafast dynamics of the photo-induced absorption and stimulated emission. They found that for the limited range of photon energies they used there was not effect on the dynamics as the pump photon energy was changed. Hayes et al. [27] have used femtosecond up-conversion to study the time re-

solved luminescence of PPV and MEH-PPV. They find MEH-PPV exhibits a greater red shift of the luminescence spectrum with time than PPV. Nguyen et al. [29] have used transient absorption spectroscopy to investigate energy transfer in MEH-PPV that has been oriented in a microporous solid. They interpret their results to show that energy transfer between adjacent polymer chains is faster than energy transfer along the polymer chain.

In early transient absorption experiments different investigations have produced different results from similar experiments (e.g. [32] and [33]). It is now clear that these difference come from sample preparation with the results of some investigations (e.g. [32]) being dominated by the effects of photo-oxidation of their samples [12]. There are a couple of reports [34, 35] of time resolved luminescence on partially conjugated PPV but the degree of conjugation was not well characterised in these studies. Samuel et al. [34, 35] found that the lifetime of the luminescence increased as the degree of conjugation was reduced. There is also some evidence that the behaviour of MEH-PPV deviates significantly from PPV [36, 37] particularly where time resolved and nonlinear processes are involved. Whitelegg et al. [38] have investigated excimer formation in films of partially conjugated MEH-PPV but they have not investigated how the reduction of conjugation affects energy transfer within, or the conformation of, the polymer. Therefore the samples presented here provide an unprecedented opportunity to study the effect of the degree of conjugation on the photophysics of a conjugated polymer.

The work in this chapter was carried out in dilute solutions to minimise the effects of interchain interactions. This reduces the number of possible physical processes and allows a more precise interpretation of the results. Much of the work in the literature reports studies on films. This is motivated by the fact that practical devices are made from films, so it is important to understand their photophysics. This is true, but the number of contradictory conclusions and possible interpretations of results illustrates the need for controlled experiments in solution. There is some evidence [12, 13] that polymers in thin films formed from spin casting from a solution retain a

memory of the solvent they were spun from. Nguyen at al. [12] investigated the luminescence of films spun from solutions of MEH-PPV in chlorobenzene and tetrahydrofuran (THF). They found that the films spun from the two different solvents had a memory of the solution chain conformation. This further supports the value of working in solution, as understanding the solution photophysics is relevant to understanding the thin film photophysics.

A number of techniques have been combined to gain an understanding of the processes present in the samples studied. The temperature dependence of the steady state photoluminescence, photoluminescence excitation and absorption spectra has been investigated. The room temperature dynamics of the excited state have been investigated with ultrafast measurements of luminescence using a streak camera and by measuring the ultrafast anisotropy of the transient absorption. The room temperature steady state photoluminescence and photoluminescence excitation anisotropies have also been investigated. The results are rationalised in terms of excitations migrating along the chain to sites with a lower energy. The partially conjugated samples behave as a collection of individual segments. The fully conjugated polymer exhibits stronger electronic coupling along the whole chain.

5.2 Sample preparation

The polymers used in this study were prepared in the group of Dr. Paul Burn at the University of Oxford. The structures of the polymers are shown in figure 5.1. The three samples have 0%, 20% and 34% of the vinylene linkages replaced by single bonds and hydrogens respectively. The mass and polydispersity measured in the group of Dr Burn, together with the approximate number of repeat units per chain for each polymer are given in table 5.1. The number of repeat units was estimated using half the mass obtained from GPC, as it is known that GPC calibrated using polystyrene standards overestimates the mass of conjugated polymers by a factor of approximately two [39]. The samples were prepared by a base catalysed elimination of a

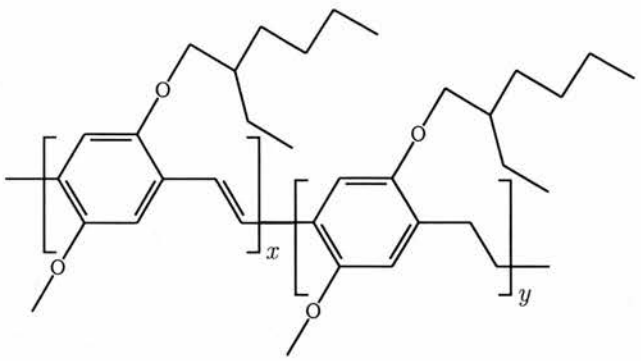

Figure 5.1: *The structure of polymers used in this study, the polymer consists of a random mixture of the two repeat units. The values of x and y are given in table 5.1.*

Conjugation	x	y	M_n	M_w	γ	$\bar{n}$
100%	1.00	0.00	274000	72500	3.8	530
80%	0.80	0.20	123000	50600	2.4	240
66%	0.66	0.34	311000	155000	2.0	600

Table 5.1: *The ratio of double to single bonds (x/y), number average (M_n) and weight average (M_w) molecular masses, polydispersity (γ), and approximate average number of repeat units per chain ($\bar{n}$) of the polymers used in this study.*

precursor polymer which had the desired fraction of leaving groups replaced with hydrogen [40].

5.3 Room temperature steady state spectra

The results of room temperature steady state photoluminescence, photoluminescence excitation and absorption measurements are presented in this section. These results are then discussed in section 5.3.4. The arguments developed in section 5.3.4 will be used in the subsequent sections of this chapter

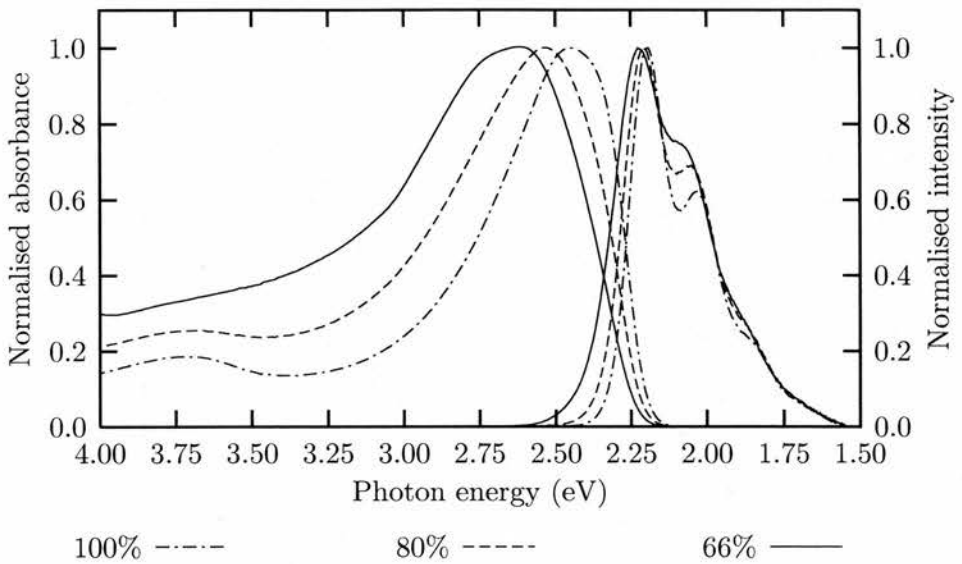

Figure 5.2: *Steady state photoluminescence and absorption of MEH-PPV as a function of conjugation.*

Conjugation	Abs Max (nm)	Abs Max (eV)	PL Max (nm)	PL Max (eV)
100%	505	2.455	563	2.202
80%	489	2.536	559	2.218
66%	474	2.616	554	2.238

Table 5.2: *The position of the peak in the absorption and photoluminescence spectra of MEH-PPV as a function of conjugation.*

in the discussion of temperature dependent spectra, anisotropies and ultrafast measurements.

Conjugation	Abs width (meV)	PL width (meV)
100%	484	280
80%	618	307
66%	792	335

Table 5.3: *The full width at half maximum of the absorption and photoluminescence of MEH-PPV as a function of conjugation.*

5.3.1 Absorption and photoluminescence

Figure 5.2 shows the room temperature steady state photoluminescence and absorption spectra of the three polymers in chlorobenzene. There is a clear shift of the peak of the absorption to higher photon energies and a small shift in the photoluminescence as the extent of conjugation is reduced. Table 5.2 shows the position of the maximum of the absorption and photoluminescence. There is a shift of 36 meV in the photoluminescence and a shift of 161 meV in the absorption as the degree of conjugation is reduced from 100% to 66%. The shift in the absorption is much more pronounced than the shift in the photoluminescence. The half widths of the absorption and photoluminescence spectra are given in table 5.3. The widths of the absorptions are roughly twice that of the photoluminescence. As the degree of conjugation is reduced the widths of the spectra increase.

5.3.2 Excitation energy dependence of the photoluminescence

If a conjugated polymer has strong electronic coupling along the chain, then the photoluminescence spectrum should be independent of the excitation photon energy [8]. The fully conjugated and 80% conjugated polymers do not exhibit a dependence of their photoluminescence on the energy of the excitation photon. However, the photoluminescence of the 66% conjugated sample is dependent on the energy of the excitation photon. The normalised

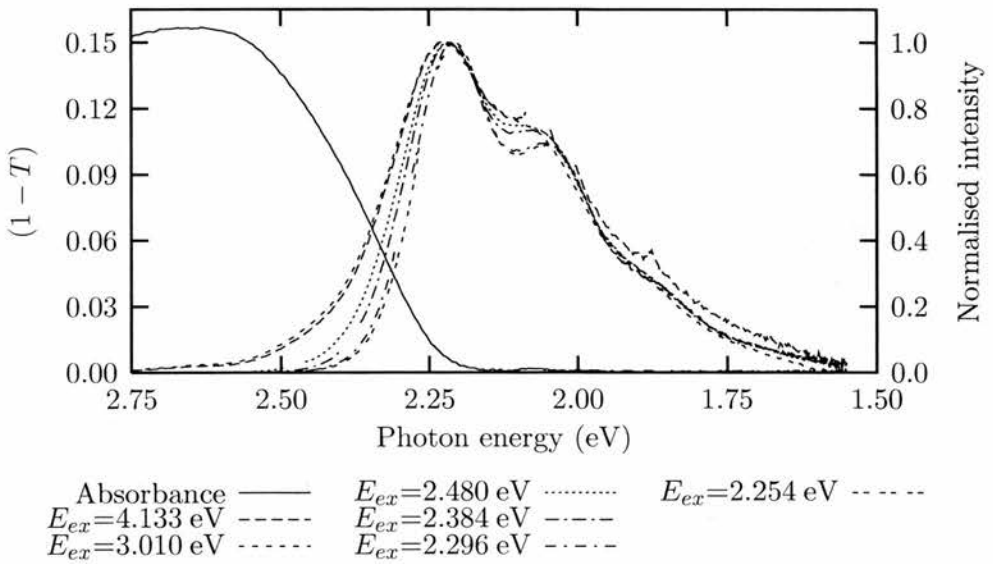

Figure 5.3: *Photoluminescence of 66% conjugated MEH-PPV excited with different photon energies, normalised to the maximum.*

photoluminescence with different excitation photon energies, together with $1 - T$ which (neglecting reflections and scattering) is proportional to the number of absorbed photons, are shown in figure 5.3. There is a significant overlap between the absorption and photoluminescence between 2.2 eV and 2.7 eV. With a higher photon energy excitation, the emission spectrum is broader with much more fluorescence between 2.2 eV and 2.7 eV. The peak position of the 0-0 and 0-1 transitions show a small dependence on excitation photon energy. The vibronic structure is better resolved as the excitation photon energy is reduced.

5.3.3 Detection energy dependence of photoluminescence excitation spectra

The absorbance plotted as number of photons absorbed $(1 - T)$ and photoluminescence excitation spectra for different detected photon energies of the 66% conjugated polymer sample are plotted in figure 5.4. For photon

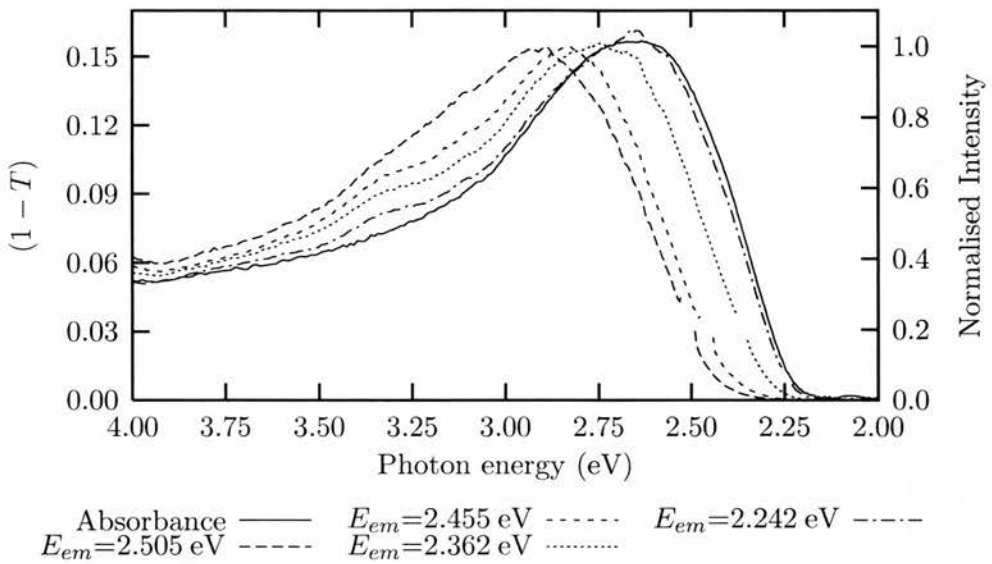

Figure 5.4: *Photoluminescence excitation spectra of 66% conjugated MEH-PPV as a function of detected photon energy.*

energies less than the position of the maximum of the photoluminescence there is no dependence of the photoluminescence excitation spectrum on the energy of the detected photon. In this regime the photoluminescence excitation spectrum closely resembles the absorption spectrum plotted as the number of absorbed photons, indicating that all absorbing species contribute to the photoluminescence at these energies. For detected photon energies greater than the position of the maximum of the photoluminescence, there is a systematic dependence of the position of the peak of the photoluminescence excitation spectrum on the energy of the detected photon. The peak of the photoluminescence excitation spectrum shifts linearly with the detection energy. The shape of the spectra are all fairly similar, they are just displaced from each other.

Figure 5.5 shows the position of the peak of the photoluminescence excitation spectrum as a function of the energy of the detected photon for all three polymers. For emission energies greater than the position of the

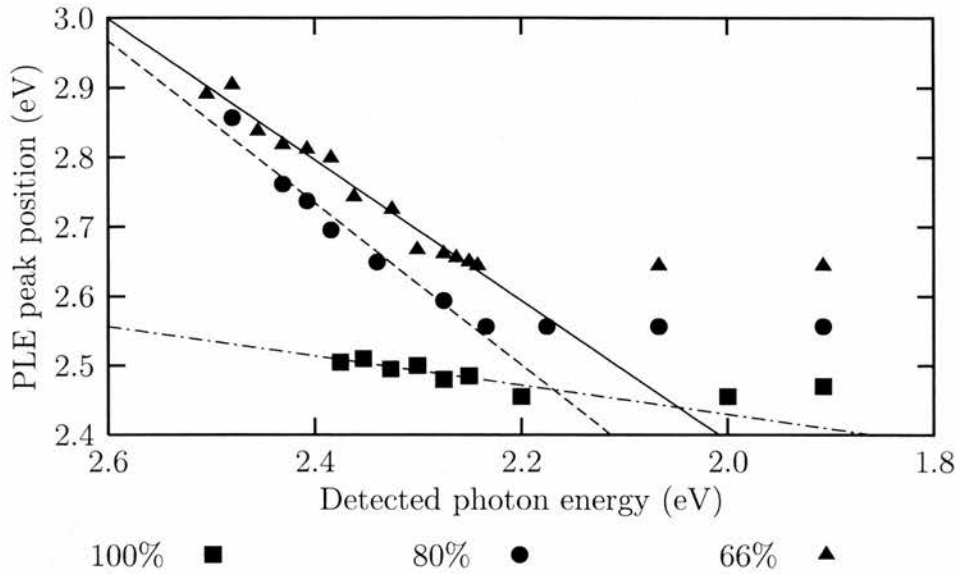

Figure 5.5: *The shift in the peak of photoluminescence excitation spectrum with detected photon energy of MEH-PPV as a function of conjugation.*

maximum of the photoluminescence spectrum the two partially conjugated polymers have a clear dependence of the peak position on the energy of the emitted photon. For the fully conjugated sample there is a very weak dependence of the peak position in this regime. The dashed lines in this figure show linear fits to the peak positions as a function of emitted photon energy. $E_{peak} = (1.0 \pm 0.1)E_{em} + (0.36 \pm 0.36)\,\text{eV}$ for the 66% conjugated sample and $E_{peak} = (1.2 \pm 0.1)E_{em} - (0.1 \pm 0.2)\,\text{eV}$ for the 80% conjugated sample. Within the uncertainties the gradients are equal. The difference in the intercepts of the lines is a consequence of the different limiting values of the peak position for the two samples.

5.3.4 Discussion

The steady state spectra of the partially conjugated samples differ from the fully conjugated sample in a number of ways. Their absorption and photoluminescence is blue shifted and broader and the peak of the photoluminescence

excitation spectrum has a strong dependence on the energy of the emitted photon, for photon energies greater than the peak of the photoluminescence spectrum. The photoluminescence spectrum of the 66% conjugated polymer depends on the energy of the excitation photon. The key physical difference between the partially conjugated and fully conjugated polymers is that the partially conjugated polymers contain a large number of randomly placed single bonds to break the conjugation. On average the 80% conjugated polymer will have a break of conjugation every five repeat units and the 66% conjugated polymer will have a break in conjugation every three repeat units. As the breaks are randomly placed on the chain there will be a distribution of segment lengths within it. In addition to the chemical breaks in conjugation which are static, there will be dynamic breaks due to conformational disorder. These conformational breaks will be present in the fully conjugated polymer as well [41].

The presence of extra chemical breaks in conjugation in the partially conjugated samples explains their broader and blue shifted absorption spectra. As the number of chemical breaks in conjugation is increased the number segments increases and their average length decreases. As explained in chapter 4, as the length of a conjugated segment is reduced the peak of the absorption shift to higher photon energies. This shift is empirically described by $E_{0-0} = A + B/N$ where A and B are constants and N is the number of double bonds [1, 2]. Also the rate of change of the peak position with segment length increases as the length of the segment is reduced. The absorption of the polymer is considered to be the superposition of the absorption of all the segments on the chain. The shift of the peak of the absorption to higher photon energies as the length of a segment is reduced explains the blue shift of the absorption spectra as the degree of conjugation is reduced because the chain contains shorter segments which absorb at higher photon energies. The increase in the width of the absorption is explained by the larger spacing of the absorbance of shorter segments. As the segments on a chain become shorter their absorptions no longer overlap as much so the absorption of the

chain becomes broader.

It is widely believed that the photoluminescence of conjugated polymers is predominately from the longest segments on the polymer chain [27, 28]. This would explain the relatively small shift in the position of the photoluminescence as the conjugation is reduced. As there is a distribution of segments present in the polymer there are likely to be long segments present on the chain even on the 66% conjugated polymer and the small shift in the photoluminescence suggests that the majority of excitations are migrating to these segments before they decay. The increase in the width of the photoluminescence indicates that there are some shorter segments emitting, this could be from excitations which decay whilst they are migrating but before they reach the lowest energy segment, or excitations that are trapped on an isolated segment.

The dependence of the photoluminescence of the 66% conjugated polymer on the energy of the excitation photon suggests that there are some very short segments present on the chain which can only be excited with higher energy photons. As the mean conjugated segment length is three repeat units it is reasonable to assume that there will be some conjugated segments consisting of just one or two repeat units. Excitations created on these segments will migrate to segments of lower energy, however some will decay as they are migrating. As excitations created on these segments have a high initial energy then it is possible for them to decay with a relatively high energy when they are migrating to sites with an energy lower than their initial energy. It is also possible that these short segments are isolated from the others on the chain. The increase in the structure of the emission as the energy of the excitation photon is reduced indicates that the emission is coming from a narrower distribution of segment lengths.

The dependence of the photoluminescence excitation spectrum of the partially conjugated polymers on the energy of the emitted photon can also be rationalised using the fact that there are a larger number of single bonds on the chain. The situation in the fully conjugated polymer is very different.

There is little dependence of the photoluminescence excitation spectrum on the energy of the detected photon. This can be understood by considering the strong electronic coupling along in the fully conjugated polymer [8]. The strong dependence of peaks of the photoluminescence excitation spectrum on the energy of the detected photon for the partially conjugated samples implies that the electronic coupling is much weaker along the chain. The large number of single bonds interrupt the conjugation and destroy the strong coupling along the chain. This means that the interaction between segments on the chain is much less in the partially conjugated polymers than the fully conjugated polymer.

5.4 Temperature dependence of the steady state spectra

The temperature dependence of the absorption and luminescence is a powerful tool for studying the effect of conformation on the photophysics of polymers. As a polymer solution is cooled the absorption and photoluminescence shift to different photon energies. The direction and extent of the shift is dependent on the interplay of steric forces trying to keep the chain straight and attractive forces trying to fold the chain back on itself [42, 43]. The majority of conjugated polymers display a red-shift in absorption and photoluminescence as they are cooled [44–46]. However, it is possible for there to be a blue-shift with decreasing temperature [47, 48]. MEH-PPV is known to show a red-shift as the temperature is reduced [49, 50]. The red-shift can be explained by the straightening of the polymer backbone as the thermal energy available to twist the chain is reduced when the sample is cooled. The straightening of the chain with cooling makes it possible to probe new conformations of the polymer. In the partially conjugated polymers this is particularly interesting, as when the polymer chain straightens the majority of the breaks in conjugation due to conformational disorder are removed and the behavior of the polymers will be predominately determined

by the chemical breaks in conjugation.

5.4.1 Temperature dependent absorption

Figure 5.6 shows the temperature dependent absorption of all three polymers in 2-methyl-tetrahydrofuran (2-MeTHF) between 100 K and 300 K. This solvent was chosen as it forms an optical glass at low temperatures (below 135 K). As the temperature is reduced, the spectra become more structured and the absorption shifts to lower photon energies. The intensity of the absorption increases as it is cooled; this is thought to be due to solvent shrinkage. The fully conjugated polymer (top panel) has the greatest red-shift and increase in vibronic structure as it is cooled. There is a large decrease in the absorption in the $2.5 - 3.0$ eV region as the absorption shifts to the red. At 100 K the edge of the absorption is very steep. The partially conjugated polymers (middle and lower panel) also show a red-shift and some increase in the structure of the absorption. The red edge of the absorption becomes less steep as the degree of conjugation is decreased. There is less of a reduction in the absorption of the partially conjugated polymers in the $2.5 - 3.0$ eV region as they are cooled. The absorption increases in width as the peak moves to the red rather than the whole absorption band shifting.

5.4.2 Temperature dependent photoluminescence

Figure 5.7 shows the temperature dependent photoluminescence of all three polymers between 100 K and 300 K. As the solutions are cooled, there is a red-shift of the spectrum and a large increase in vibronic structure. This increase is most pronounced in the fully conjugated polymer. Below 175 K the spectrum of the fully conjugated polymer shows a small blue tail that has the appearance of a photoluminescence spectrum that is distorted by self absorption. The optical density of the solution was kept low to avoid this problem. To rule out self absorption the photoluminescence spectrum at 100 K was corrected for the absorption of the sample at emission photon

by the chemical breaks in conjugation.

5.4.1 Temperature dependent absorption

Figure 5.6 shows the temperature dependent absorption of all three polymers in 2-methyl-tetrahydrofuran (2-MeTHF) between 100 K and 300 K. This solvent was chosen as it forms an optical glass at low temperatures (below 135 K). As the temperature is reduced, the spectra become more structured and the absorption shifts to lower photon energies. The intensity of the absorption increases as it is cooled; this is thought to be due to solvent shrinkage. The fully conjugated polymer (top panel) has the greatest red-shift and increase in vibronic structure as it is cooled. There is a large decrease in the absorption in the $2.5 - 3.0$ eV region as the absorption shifts to the red. At 100 K the edge of the absorption is very steep. The partially conjugated polymers (middle and lower panel) also show a red-shift and some increase in the structure of the absorption. The red edge of the absorption becomes less steep as the degree of conjugation is decreased. There is less of a reduction in the absorption of the partially conjugated polymers in the $2.5 - 3.0$ eV region as they are cooled. The absorption increases in width as the peak moves to the red rather than the whole absorption band shifting.

5.4.2 Temperature dependent photoluminescence

Figure 5.7 shows the temperature dependent photoluminescence of all three polymers between 100 K and 300 K. As the solutions are cooled, there is a red-shift of the spectrum and a large increase in vibronic structure. This increase is most pronounced in the fully conjugated polymer. Below 175 K the spectrum of the fully conjugated polymer shows a small blue tail that has the appearance of a photoluminescence spectrum that is distorted by self absorption. The optical density of the solution was kept low to avoid this problem. To rule out self absorption the photoluminescence spectrum at 100 K was corrected for the absorption of the sample at emission photon

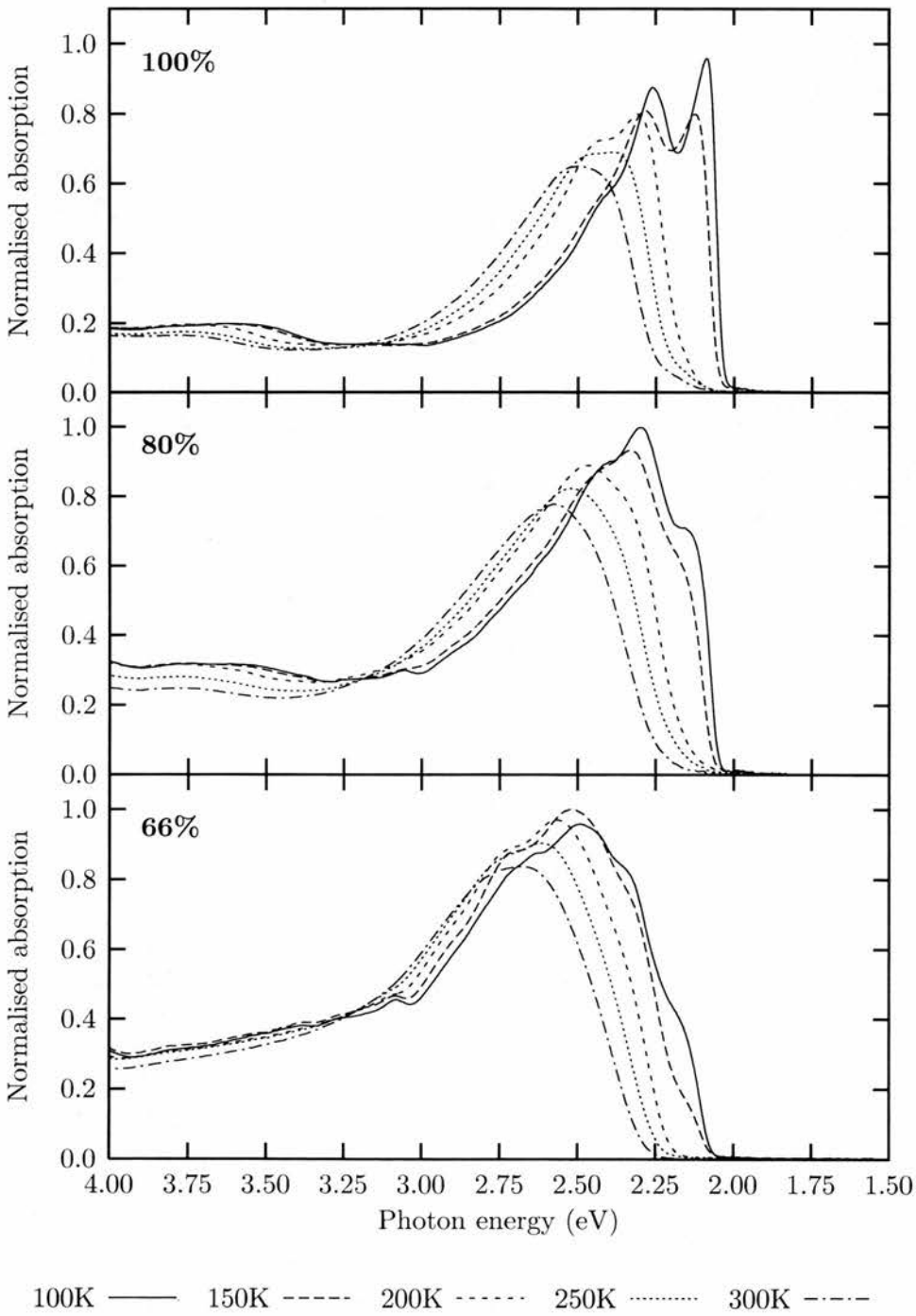

Figure 5.6: *The temperature dependent absorption of MEH-PPV in 2-MeTHF as a function of conjugation.*

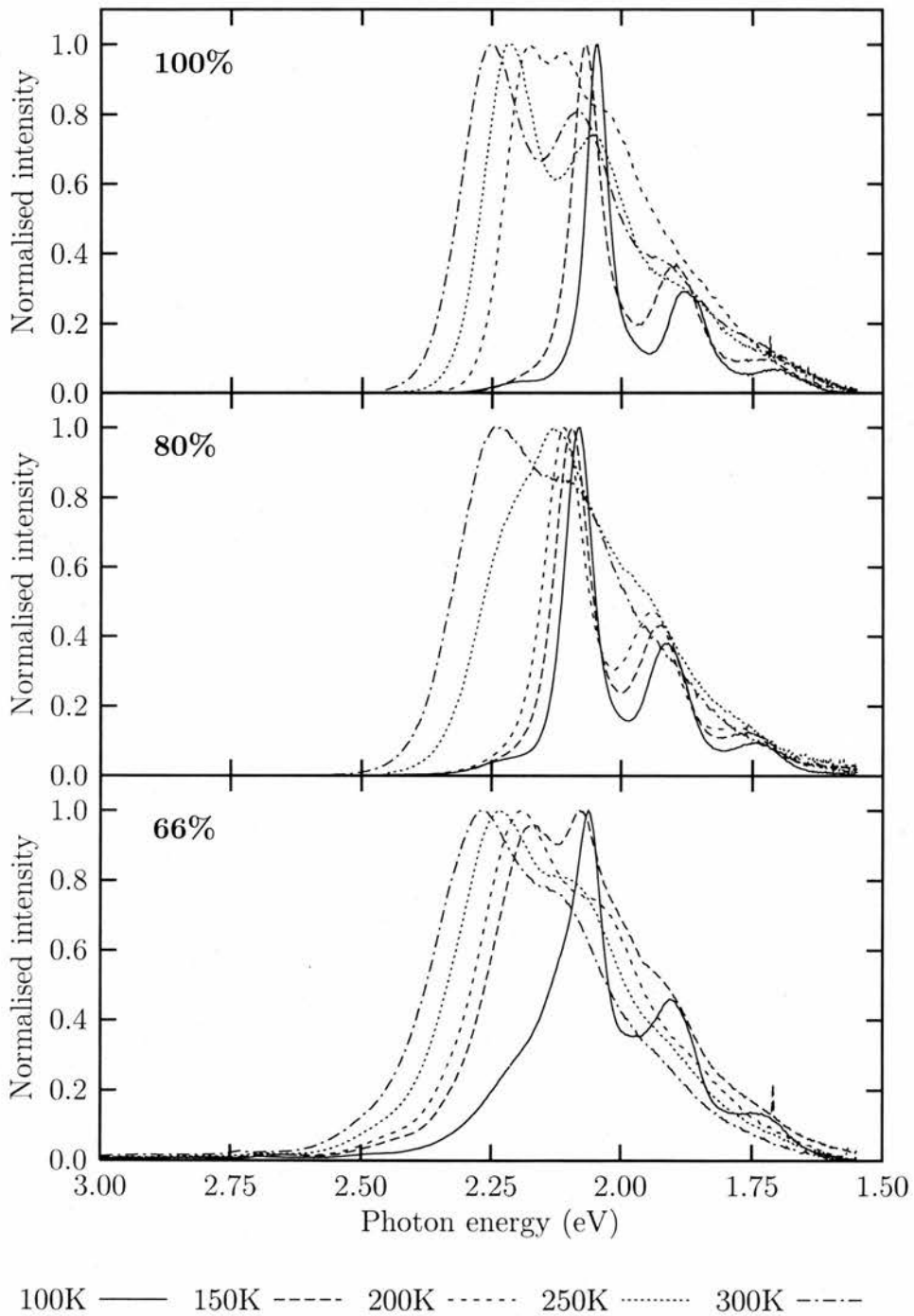

Figure 5.7: *The temperature dependent photoluminescence of MEH-PPV in 2-MeTHF as a function of conjugation.*

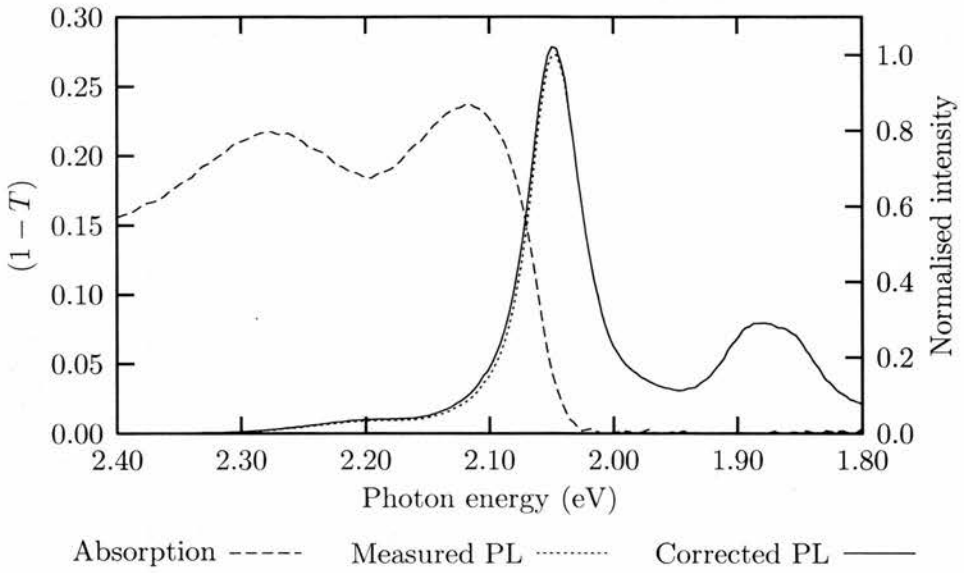

Figure 5.8: *The photoluminescence of fully conjugated MEH-PPV at* 100 K *corrected for self absorption.*

energies. This is shown in figure 5.8 together with the uncorrected photoluminescence spectrum and the absorption spectrum plotted as $1 - T$. The spectrum was corrected by dividing the measured photoluminescence spectrum by the square root of the transmission of the sample, as the measured photoluminescence travelled through approximately half the sample to reach the detector. It is clear from this figure that self absorption has only a very minor effect on the shape of the spectrum. To probe the origin of this small blue shoulder, photoluminescence excitation spectra shown in figure 5.9 were taken, probing the photoluminescence in this region of the spectrum and also at lower photon energies. The photoluminescence excitation spectrum obtained by detecting in the red of the photoluminescence closely resembles the absorption spectrum of the polymer. Detecting at higher photon energies, the edge of the photoluminescence excitation spectrum shifts to higher photon energies.

Figure 5.10 shows PLE spectra for 66% conjugated MEH-PPV at 100K.

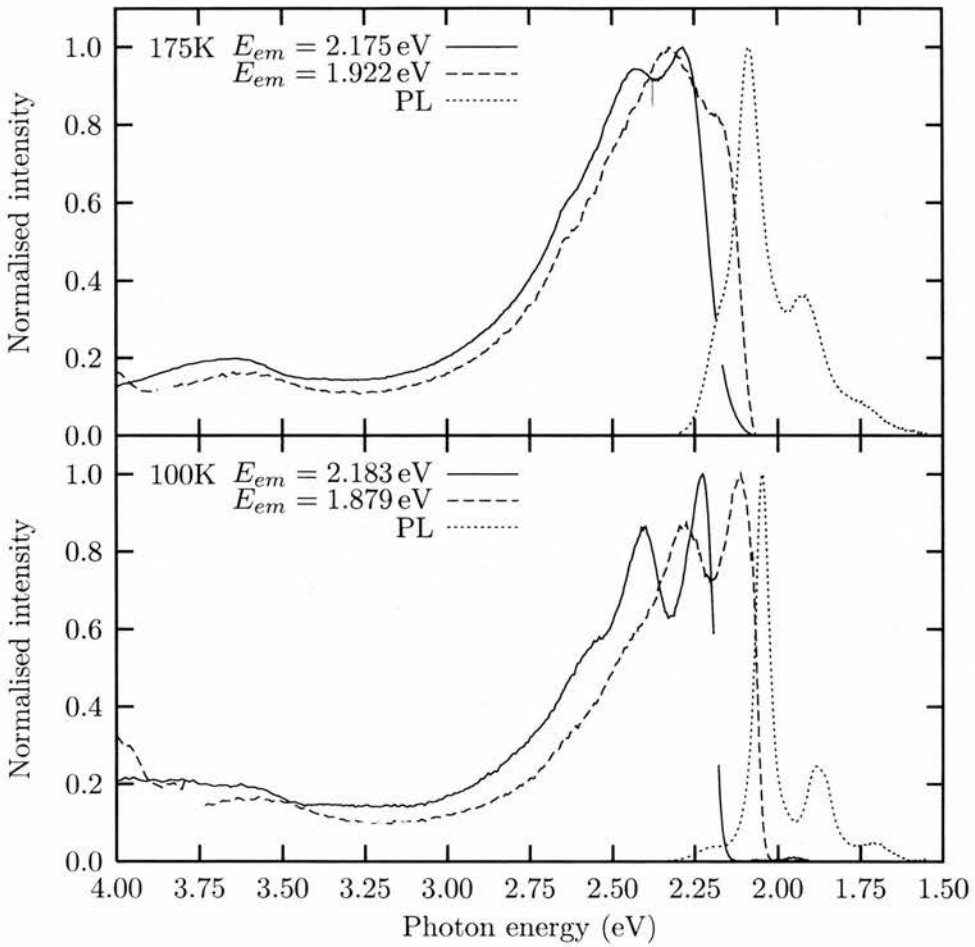

Figure 5.9: *Temperature dependent photoluminescence excitation spectra of fully conjugated MEH-PPV in solution for different detected photon energies.*

Detecting emission in the red tail of the photoluminescence gives a spectrum similar to the absorption spectrum. As the emission energy is moved to higher energies the photoluminescence excitation spectra start to show more structure and an increase in intensity at short wavelengths.

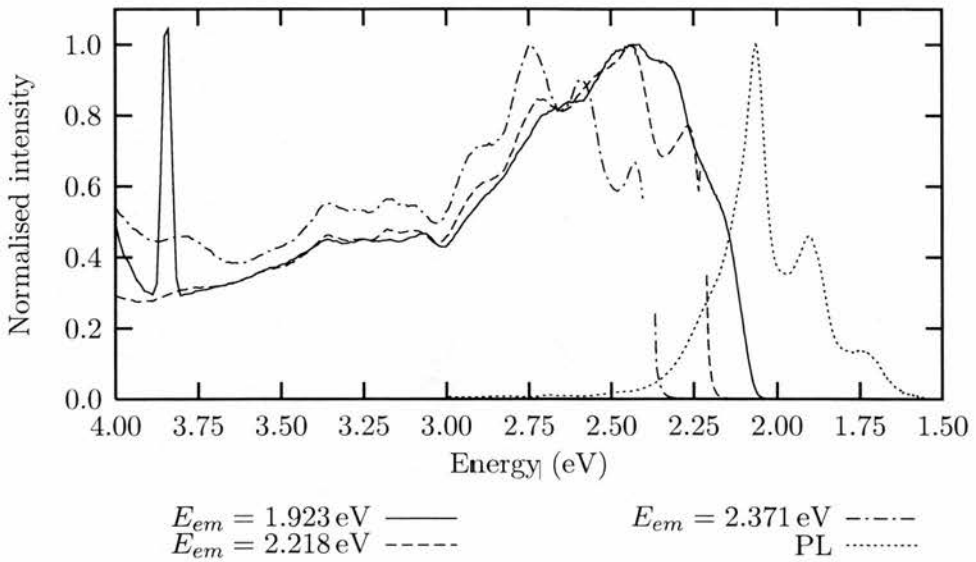

Figure 5.10: *Photoluminescence excitation of 66% conjugated MEH-PPV at* 100 K *for various detection energies.*

5.4.3 Discussion

There are significant differences between the behaviour of the fully conjugated and partially conjugated polymers. The red-shift of the polymers as they are cooled indicates that they are straightening out as the amount of thermal energy available to twist the chain is reduced [42, 43, 48]. The increase in vibronic structure can also be attributed to the reduction of the number of conformational breaks in conjugation. As the fully conjugated polymer is cooled it will become straighter and so the mean conjugated segment length will increase. Longer segments absorb at lower energies so the absorption of the polymer moves to the red. The shift towards long conjugated segments within the chain also explains the increase in vibronic structure in the absorption spectrum. As the absorption of longer segments reaches an asymptotic limit, the segments within the chain will all be absorbing at similar energies and so their vibronic structure will coincide, leading to a structured absorption spectrum of the polymer.

The red-shift of the photoluminescence of the fully conjugated polymer is also linked to the reduction in conformational disorder. It is believed that the longest, lowest energy segments on a chain are predominately responsible for the emission [27, 28]. As the longest segments increase in length, the photoluminescence will red-shift due to the decrease in the energy of the longest segments. The increase in the vibronic structure comes from the increase in length as well. There will be a small distribution of segments emitting but they will all emit at essentially the same energy leading to an enhancement in the structure of the spectrum. The small blue tail on the photoluminescence of the fully conjugated polymer can be attributed to the emission of short conjugated segments. The fact that the photoluminescence excitation spectrum of emission in this region is at higher energies than the photoluminescence excitation of the main emission band suggests the segments are either, short isolated segments present on the polymer chain due to small defects in the synthesis or, shorter molecules in the sample.

The partially conjugated samples do not have as large an increase in the structure of their absorption or photoluminescence spectra as the fully conjugated polymer and the width of the absorption spectra increase as they are cooled. This is due to the chemical breaks in conjugation in these samples. When the solutions are cooled the number of conformational breaks is reduced; however, the number of chemical breaks in conjugation is constant. The maximum length of a conjugated segment is limited by the chemical breaks in conjugation. This explains why the absorption gets wider rather than shifting. The longer segments on the chain will red-shift as the conformational breaks in conjugation are reduced. However, when the solution is cooled there will still be a number of short segments present on the chain due to the chemical breaks in conjugation. These will absorb at higher photon energies, leading to the increase in the width of the absorption and photoluminescence. The more gradual increase in the absorption at low photon energies of the partially conjugated polymers, compared to the fully conjugated polymer, is due to the presence of different segment lengths in the partially

conjugated polymer which do not have overlapping absorptions. The long blue tail of the photoluminescence of the 66% conjugated sample (bottom panel in figure 5.7) is due to the emission of short segments in the sample before the excitations have migrated to longer segments. This is supported by the photoluminescence excitation spectra of the 66% sample in figure 5.10. The increase in the photoluminescence excitation signal at higher photon energies for emission at higher photon energies shows that there are a number of different conjugated segments present on the polymer chain.

5.5 Steady state anisotropies

The anisotropy of the photoluminescence and photoluminescence excitation of a conjugated polymer can give information on the migration of excitations along the chain. If an excitation decays radiatively on the same part of the chain that it was created on, the anisotropy will be relatively high, as the transition dipoles of the absorbing and emitting segments will have a similar orientation. However, if the excitation travels a distance along the chain before it decays radiatively, the emitted and absorbed photons will generally have differing polarisations, as the transition dipole of the chain where the excitation decays is likely to be pointing in a different direction to the dipole where the photon was absorbed. By monitoring how the anisotropy of the photoluminescence and photoluminescence excitation changes with excitation and emission photon energy it is possible to infer if excitations created with different energies travel different distances along the chain. It is interesting to compare the position of the peak of the anisotropy to the peak of the photoluminescence excitation for the same detection energy. If they are appreciably separated then it suggests that the excitation is migrating along the chain as the maximum of the absorption does not coincide with the minimum angular separation of the absorption and emission dipoles. This is potentially an elegant way of studying excitation migration in conjugated polymers and it is surprising that this type of study does not appear to have

been undertaken before.

There are few reports of steady state anisotropies of conjugated polymers in the literature. Wu et al. [51] report a polarisation ratio of between 1.6 and 1.7 for MEH-PPV in chlorobenzene solutions excited at 2.541 eV. Wu et al. [51] and later Nguyen et al. [29, 52] used steady state anisotropy measurements to show alignment of polymers in silica nanocells. These seem to be the only reports of steady state anisotropies of MEH-PPV in the literature. This might be because it is not obvious that an anisotropy signal will be present. If the molecule rotates in a similar or shorter time than its radiative lifetime, then the anisotropy will be reduced by physical motion of the molecule. However Rumbles [53] has shown that the rotational time of a relatively short ($\sim$ 20 repeat units) PPV derivative is 6 ns. As the radiative lifetimes of polymers are generally under 1 ns (the lifetimes of the polymers studied here are discussed in section 5.7.1 and are under 500 ps) the anisotropy is not significantly distorted by molecular rotation. The steady state anisotropies of the photoluminescence and photoluminescence excitation of the fully conjugated polymer and 66% conjugated polymer at room temperature and 100 K have been measured.

5.5.1 Room temperature anisotropies

The anisotropy of the photoluminescence of the fully conjugated polymer in chlorobenzene is shown in figure 5.11. The anisotropy is very flat over the majority of the photoluminescence, with a value of $r = 0.120 \pm 0.005$ for excitation at 2.755 eV. This corresponds to an angle between the absorbing and emitting dipoles of $\varphi = 43.11 \pm 0.05^o$. As the excitation is moved to a lower energy of 2.255 eV, the anisotropy increases to 0.18 ± 0.01 corresponding to an angle between the absorbing and emitting dipoles of 37.29 ± 0.05^o. Figure 5.12 shows the anisotropy of the photoluminescence of the 66% conjugated polymer in chlorobenzene. When this polymer is excited at relatively high photon energies the anisotropy is higher in the blue part of the emission and decays to a constant value [$r = 0.095 \pm 0.005$, ($\varphi = 45.45 \pm 0.01^o$) for an

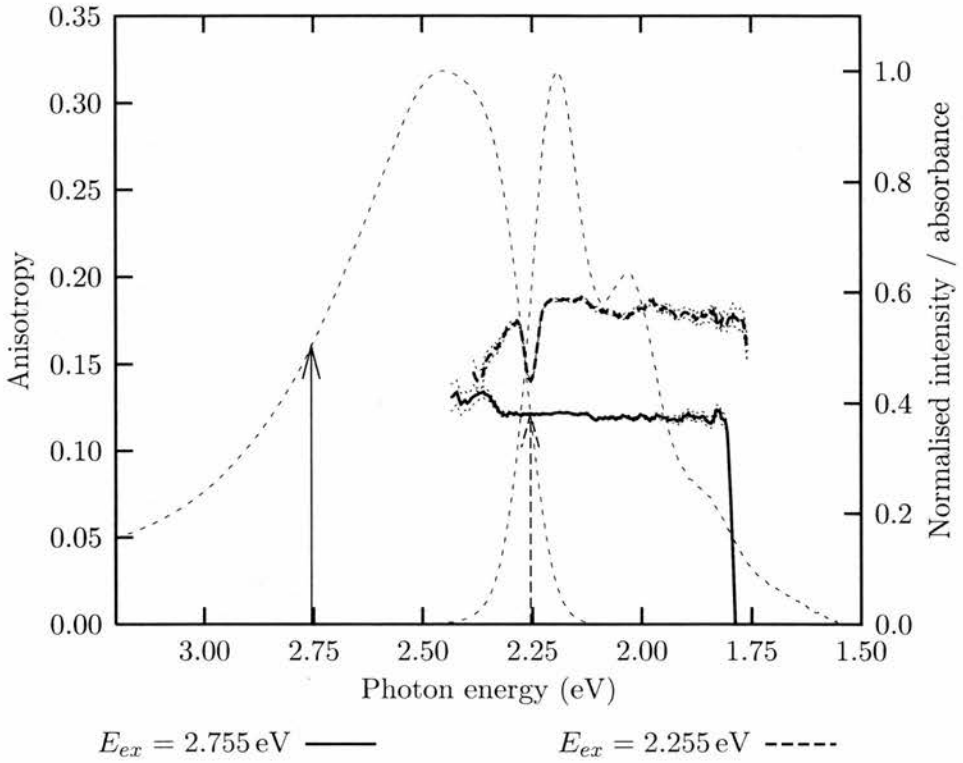

Figure 5.11: *Anisotropy (thick lines) of the photoluminescence (thin dotted line) of fully conjugated MEH-PPV. The arrows indicate the position of the excitation in the absorption spectrum (thin dotted line).*

excitation photon energy of 3.1 eV; $r = 0.141 \pm 0.005$, ($\varphi = 41.04 \pm 0.01^o$) for an excitation photon energy of 2.756 eV] from the peak of the photoluminescence into the red tail of the emission spectrum. When the polymer is excited in the tail of the absorption there is a higher anisotropy [$r = 0.30 \pm 0.01$ ($\varphi = 24.7 \pm 0.4^o$)] which is fairly constant through the emission.

The anisotropies of the photoluminescence excitation spectra of the fully and 66% conjugated polymers are shown in figures 5.13 and 5.14 respectively. The anisotropy for the fully conjugated polymer (figure 5.13) shows little dependence on the energy of the detected photon. Both of the anisotropy curves peak at about 2.2 eV, the absorption edge of the polymer. The anisotropies

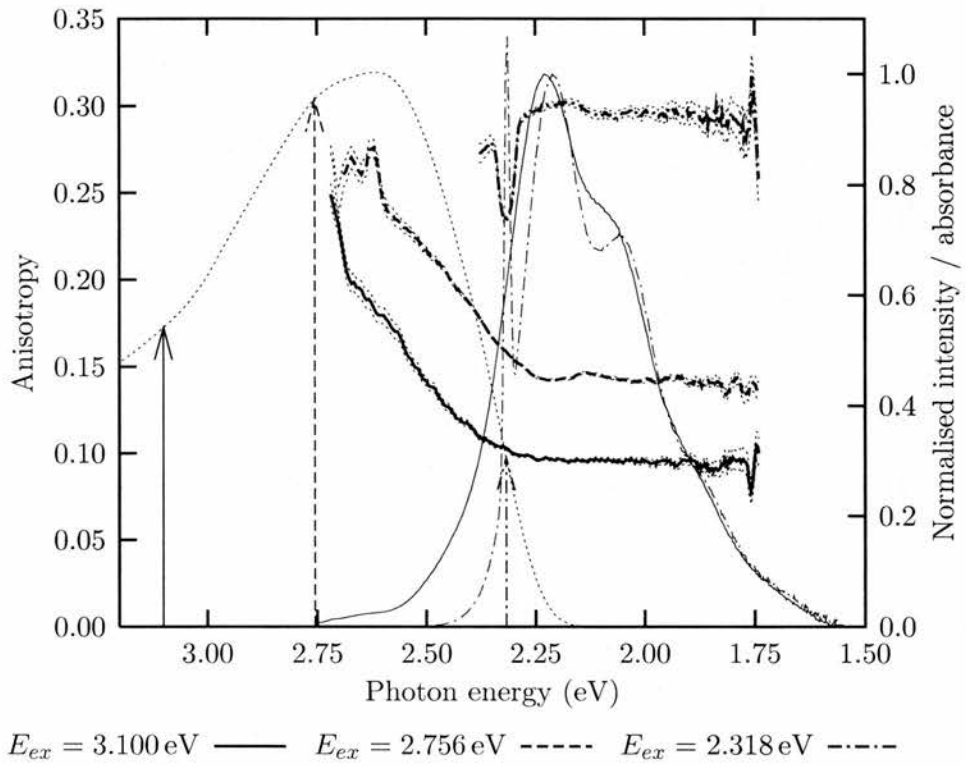

Figure 5.12: *Anisotropy (thick lines) of the photoluminescence (thin lines) of 66% conjugated MEH-PPV. The arrows indicate the position of excitation in the absorption spectrum (thin dotted line). The photoluminescence for excitation at* 2.756 eV *is not shown but is very similar to the photoluminescence spectrum for excitation at* 3.1 eV *(thin solid line).*

of the 66% conjugated polymer in figure 5.14 exhibit a marked dependence on the energy of the detected photon. As the detection is moved to lower photon energies, the anisotropy between 3.25 eV and 2.4 eV is reduced, the peak of the anisotropy moves to a lower energy, and the maximum value of the anisotropy increases. The anisotropy peaks at a significantly higher value than the anisotropy of the fully conjugated polymer (around 0.3 compared to 0.2).

The flat anisotropy of the photoluminescence of the fully conjugated poly-

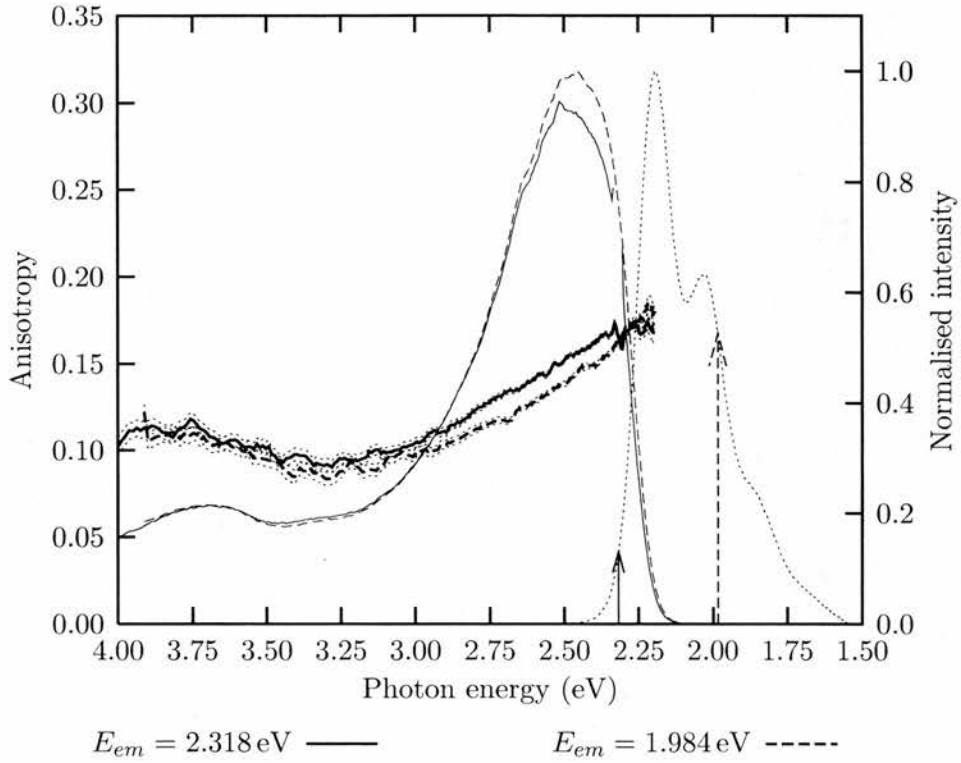

Figure 5.13: *Anisotropy (thick lines) of the photoluminescence excitation (thin lines) of fully conjugated MEH-PPV. The arrows indicate the position of the emission in the photoluminescence spectrum (thin dotted line).*

mer in figure 5.11 indicates that there is a constant angle between the absorption and emission dipole throughout the emission spectrum. The increase in the anisotropy as the energy of the excitation photon is lowered suggests that this lower energy excitation is decaying closer to where it is created as the absorption and emission dipoles are more closely aligned.

The decay of the anisotropy of the photoluminescence of the partially conjugated polymer in figure 5.12 from a high value to a lower constant level indicates that the absorption and emission dipoles are more closely aligned at higher photon energies. This can be explained by proposing that the excitation migrates along the chain from an initial high energy segment to a lower

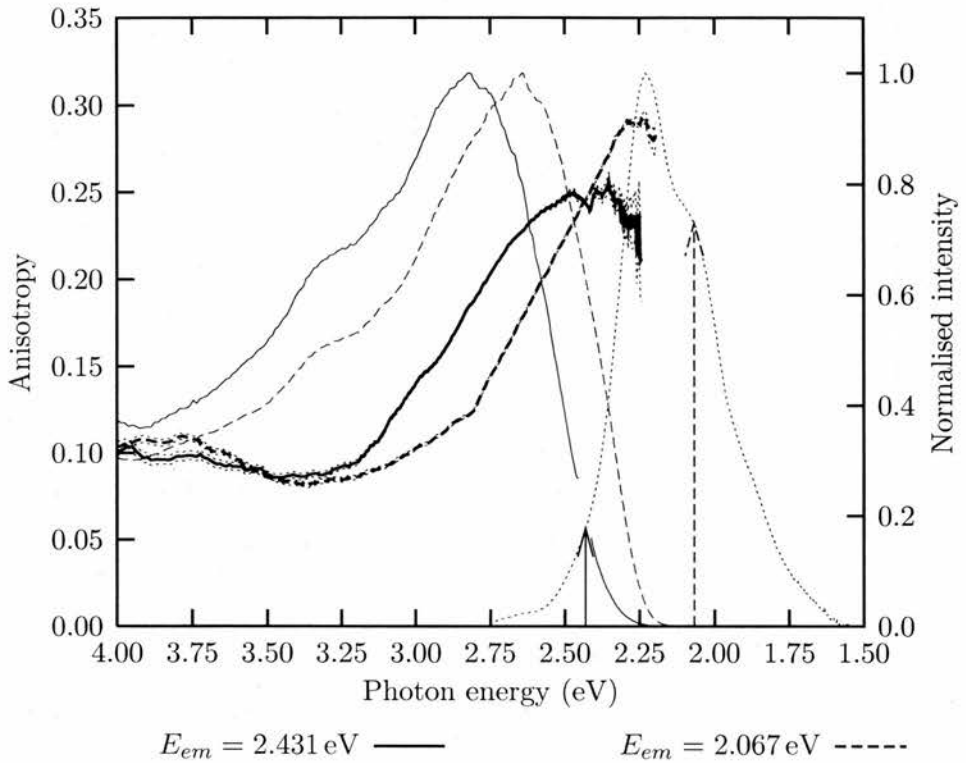

Figure 5.14: *Anisotropy (thick lines) of the photoluminescence excitation (thin lines) of 66% conjugated MEH-PPV. The arrows indicate the position of the emission in the photoluminescence spectrum (thin dotted line).*

energy segment. The higher anisotropy in the blue region of the photoluminescence comes from excitations decaying close to where they are created, or excitations that are trapped on isolated segments. The flat anisotropy over the rest of the spectrum comes from excitations that are trapped on a low energy segment and emitting further away from where they are created. The dependence of the photoluminescence excitation spectrum on the detected photon energy supports the hypothesis that excitations are migrating along the chain in this way. The higher constant anisotropy when the polymer is excited towards the red tail of the absorption can also be rationalised within this framework. As the excitation is created by a relatively low energy pho-

ton, there are not many sites for it to migrate to and so it is likely to be trapped very close to where it was created. This leads to a higher anisotropy value in a similar manner to the fully conjugated polymer excited in the red tail of the absorption.

The anisotropy of the photoluminescence of the partially conjugated polymer is lower than that of the fully conjugated polymer when it is excited with similar energy photons. However, when it is excited in a similar position in the tail of the absorption the anisotropy is over one and a half times higher. The fact that the anisotropy for excitation in the main absorption band is lower suggests that the chain is more folded or coiled up than the fully conjugated polymer, as there is a larger angle between the absorbing and emitting dipoles. As the partially conjugated polymer contains a large number of tetrahedral carbon atoms it is easier for the partially conjugated polymer to fold than the fully conjugated polymer [16]. This is supported by Monte Carlo simulations [54]. The higher anisotropy of the partially conjugated polymer compared to the fully conjugated polymer, when they are excited in the red tail of their absorptions, suggests that in this regime the excitations in the partially conjugated polymer are less mobile than those in the fully conjugated polymer. The strong shift in the peak of the photoluminescence excitation spectrum of the partially conjugated polymer, compared to the fully conjugated polymer, suggests that electronic coupling is stronger in the fully conjugated polymer.

The relative insensitivity of the anisotropy of the photoluminescence excitation of the fully conjugated polymer to the energy of the emitted photon in figure 5.13 is a reflection of the very flat anisotropy of the photoluminescence in figure 5.11. The increase in the anisotropy of the photoluminescence excitation as the energy of the excitation photon is reduced reflects the increase in the anisotropy of the photoluminescence as the excitation is moved to the red. As the energy of the excitation photon is reduced, it is decaying closer to where it was created. The stronger dependence of the anisotropy of the photoluminescence excitation of the partially conjugated polymer, in fig-

ure 5.14, on the energy of the emitted photon reflects the dependence of the anisotropy of the photoluminescence on the energy of the emitted photon, in figure 5.12. The fact that the anisotropies peak at the lowest absorbed photon energy, rather than the maximum of the photoluminescence excitation signal, provides additional evidence for the hypothesis that excitations migrate along the polymer chain and the lower energy parts of the chain are more likely to emit. The fact that between 3.25 eV and 2.4 eV the anisotropy detecting photons from the blue side of the photoluminescence is higher than the anisotropy from the red side of the photoluminescence is further evidence of the weaker electronic coupling along the chain of the partially conjugated polymer.

5.5.2 Low temperature anisotropies

The low temperature anisotropy provides useful information on how the conformation of the polymer changes with temperature. As the solvent for the low temperature measurements was 2-MeTHF, rather than chlorobenzene which was used in the previous section, it is important to compare the room temperature anisotropies of the polymer in the two solvents before drawing any conclusions about the low temperature anisotropy, as the solvent can have a dramatic change on the conformation adopted by the polymer [12]. Figure 5.15 shows the anisotropy of photoluminescence excitation of 66% conjugated MEH-PPV at two emission energies, for chlorobenzene and 2-MeTHF solutions. With a lower detected photon energy, there is clearly little difference between the anisotropies in the two solvents. When detecting photons with a higher energy, there is a small difference, with the 2-MeTHF solution having a slightly higher anisotropy. However, over most of the spectrum they are the same. The anisotropies for 2-MeTHF solutions stop at a photon energy of 3.25 eV because polaroid rather than calcite polarisers were used for these measurements and they do not transmit photons with a higher energy than this. Polaroid polarisers were used because the calcite polarisers are too large to fit into the fluorimeter with the cryostat. Figure 5.16 shows

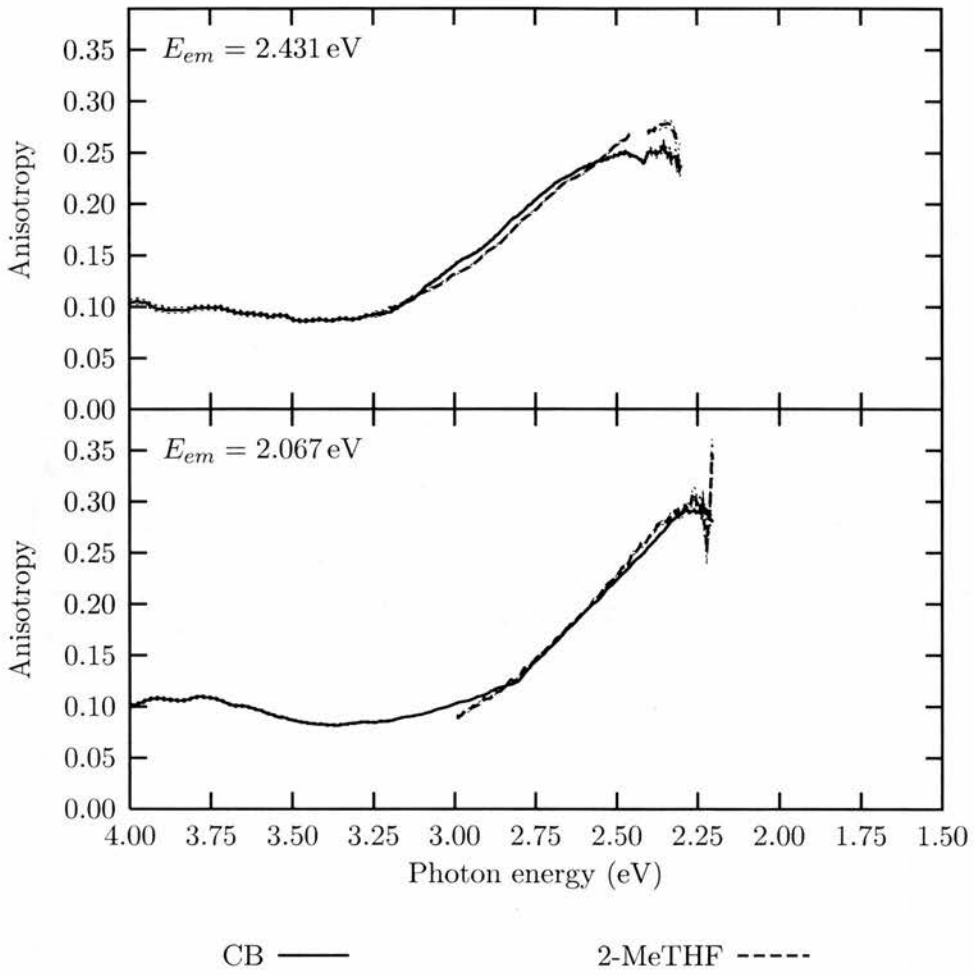

Figure 5.15: *The anisotropy of the photoluminescence excitation of 66% conjugated MEH-PPV in chlorobenzene and 2-MeTHF solutions.*

the anisotropy of the emission at high and low temperatures, for excitation with two different photon energies. At both temperatures, when the polymer is excited with a high energy photon, the anisotropy shows a decay from a higher value in the blue part of the photoluminescence spectrum to a constant value. The anisotropy is higher at lower temperatures; $r = 0.10 \pm 0.05$ ($\varphi = 45.00 \pm 0.05^o$) at 300 K and $r \approx 0.21$ ($\varphi \approx 35^o$) at 100 K. The fluctuations in the anisotropy at 100 K in the red of the photoluminescence, in the top panel of figure 5.16, are believed to be due to a poor baseline on the

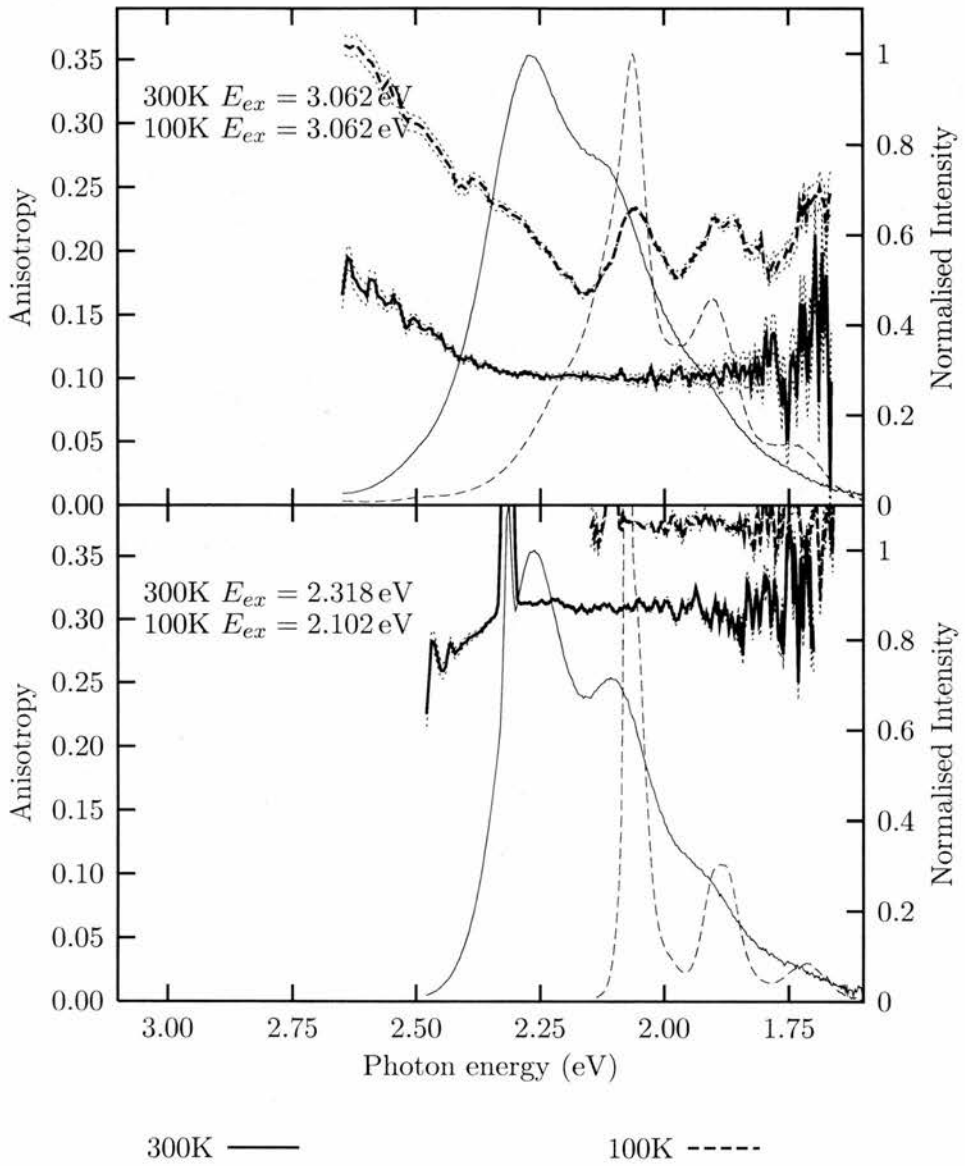

Figure 5.16: *The anisotropy (thick lines) of the photoluminescence (thin lines) of 66% conjugated MEH-PPV at 300K at 100K for different excitation energies.*

photoluminescence spectra. At low temperature and high temperature the anisotropy increases as the energy of the excitation photon is reduced. At 300 K $r = 0.31 \pm 0.05$ ($\varphi = 22.8 \pm 0.1^0$) and $r = 0.38 \pm 0.05$ ($\varphi = 10.5 \pm 0.1^0$)

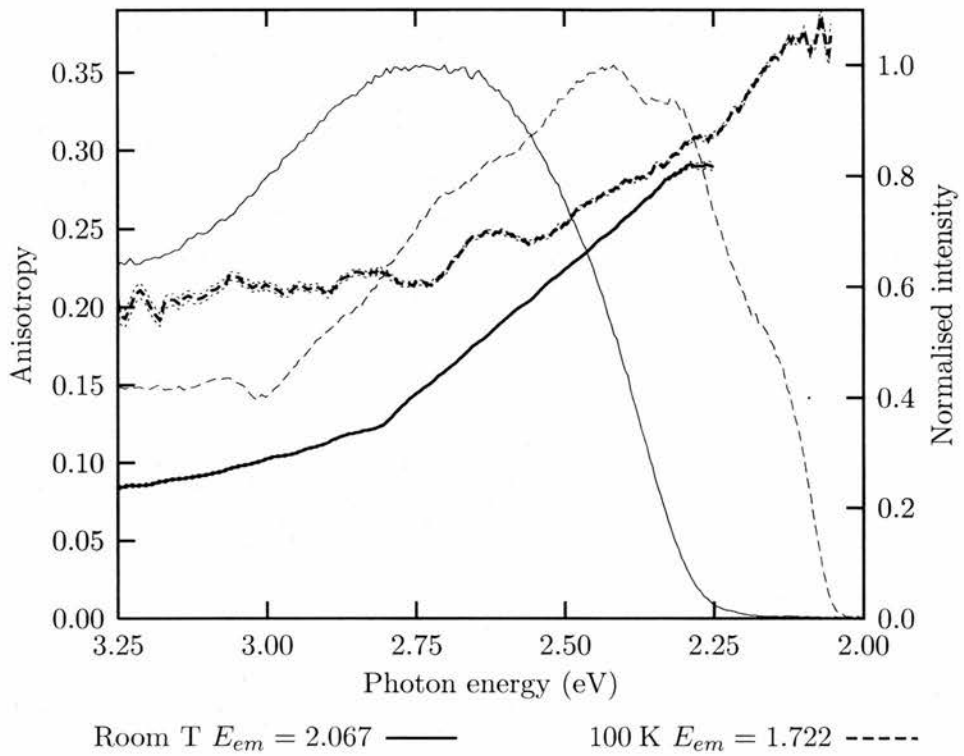

Figure 5.17: *The anisotropy (thick lines) of the photoluminescence excitation (thin lines) of 66% conjugated MEH-PPV at 100K and 300K.*

at 100 K when the polymer is excited in the tail of the absorption spectrum.

The anisotropy of photoluminescence excitation at room temperature and 100 K is presented in figure 5.17. The anisotropy is higher at 100 K than at room temperature, the difference being most pronounced at high photon energies. The anisotropy increases with decreasing photon energy. The relative angle of a segment absorbing a photon with an energy of 3 eV and the segment emitting the detected photon decreases from approximately 48^o at room temperature to 33^o at 100 K.

The increase in anisotropy of the photoluminescence and photoluminescence excitation as the temperature is reduced could be the result of reduced excitation migration at this temperature or a straightening of the chain as

it is cooled. As the spectra move to the red upon cooling it is likely that some of this increase in anisotropy comes from a straightening of the chain as the polymer is cooled. It is also possible that there is reduced excitation migration as the thermal energy is reduced. The large decrease of 15^o in the angle between the absorption and emission dipoles of the photoluminescence excitation at 3 eV suggest that there is a considerable straightening of the polymer chain as it is cooled. The very high anisotropy and the very well resolved vibronic structure at 100 K, in the bottom panel of figure 5.16, when the polymer is excited with a lower photon energy suggest that as the emission is tuned into the tail of the absorption it is possible to select a very small subset of segments or possibly a single segment on each of the polymer chains.

From steady state anisotropy measurements it has been possible to infer that the polymer chain straightens as it is cooled and that the fully conjugated polymer is stiffer than the partially conjugated polymer. The photon energy dependence dependence of the anisotropy of the photoluminescence of the 66% conjugated polymer adds further support to the hypothesis that excitations are migrating along the chain, from shorter higher energy segments, to longer lower energy segments.

5.6 PLQY of partially conjugated MEH-PPV

The PLQY of a material is an important technological and fundamental parameter. It is technologically important for display applications where it is essential to have a high efficiency of light output. Fundamentally, when combined with time resolved luminescence data, the radiative and non-radiative

% Conjugation	100	80	66
Φ(%)	22 ± 2	26 ± 2	25 ± 2

Table 5.4: *PLQY of MEH-PPV as a function of conjugation.*

decay rates can be calculated. These parameters are important for understanding the decay mechanisms within the polymer.

The PLQY of each of the three polymers in dilute chlorobenzene solution has been measured using quinine sulphate as a standard. The experimental method for this is outlined in section 3.6. Care was taken to ensure the absorption of the reference and sample solutions were similar at the excitation wavelengths and that the peak absorption was less than 0.1, to minimise the effects of self-absorption. The absorption and emission spectra of the samples used are plotted in figure 5.18. The noise around 350 nm is due to the instrument changing lamps. The emission spectra have been normalised to the number of photons absorbed. In all cases the samples were excited in the peak of the absorption. The results calculated using equation 3.24 are given in table 5.4. As the degree of conjugation is reduced the PLQY increases. It was been observed that the PLQY of short molecules tends to be higher than longer molecules [55]. This would explain why the partially conjugated samples have a higher PLQY, as they contain shorter segments than the fully conjugated polymer.

The temperature dependence of the steady state photophysics of partially conjugated MEH-PPV has been studied for the first time. Measurements of the anisotropy suggest that the polymer chains straighten as they are cooled. They also suggest that the partially conjugated polymers adopt a more folded conformation than the fully conjugated polymer. A distribution of conjugated segments is clearly visible in the photophysics of the partially conjugated polymers. As the degree of conjugation is reduced there is an increase in the PLQY.

5.7 Ultrafast spectroscopy

The results in the preceding sections of this chapter have been rationalised by the idea of excitations migrating along the polymer chain. This provides a plausible explanation of the steady state photophysics. However it is not

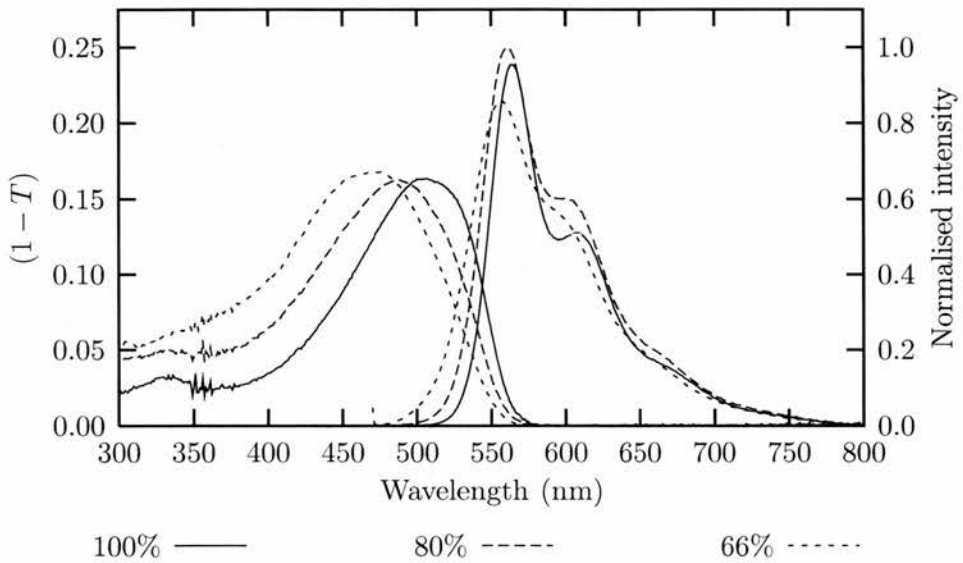

Figure 5.18: *Absorption and photoluminescence spectra for PLQY measurements of fully and partially conjugated MEH-PPV. The emission spectra are normalised to the number of photons absorbed.*

possible to obtain direct evidence of excitation migration from a steady state experiment. To provide compelling evidence it is necessary to look at the time evolution of the photoluminescence, absorption and anisotropy of the absorption and photoluminescence on the time scale of excitation transfer. This requires the use of ultrafast spectroscopy to probe the excitation on a femtosecond time scale. If there is excitation transfer in these polymers then the photoluminescence spectrum should show a red-shift with increasing time as the excitations migrate from high energy segments to lower energy segments. The time scale of this shift will indicate the time scale of excitation transfer. The transient absorption spectrum should also show a red-shift and the time dependence of the anisotropy will show the spatial migration along the chain.

Time resolved luminescence data were recorded using the streak camera set up described in section 3.7. These measurements reveal a red-shift of

the emission in the first few picoseconds after excitation but within the time resolution of this instrument it was not possible to resolve any initial decay of the anisotropy. Transient absorption measurements performed using the apparatus introduced in section 3.8 reveal a depolarisation time of a few picoseconds for the partially conjugated polymers. It was not possible to resolve the decay of the anisotropy of the fully conjugated polymer within the time resolution of this experiment.

5.7.1 Time resolved luminescence

Time resolved luminescence reveals how the photoluminescence spectrum of a material changes with time after excitation. The time resolved luminescence of MEH-PPV in solution has been reported in the literature [10, 27], however, the ultrafast dynamics of partially conjugated MEH-PPV in solution have not been previously reported. It is known that there is a red-shift of the photoluminescence of the fully conjugated polymer in the first few picoseconds after excitation. This has been ascribed to excitation migration along the chain [27] to lower energy sites on the chain and this is reflected in the red-shift of photoluminescence with time. The time resolved measurements presented here were performed using a Hamamatsu streak camera. The experimental layout is described in section 3.7. The anisotropy of the ultrafast time resolved photoluminescence should also reveal information about excitation migration. However within the time resolution of the streak camera no decay of the anisotropy could be detected. This indicates that the anisotropy reaches a long time value within 2 ps. All the samples were degassed prior to experiments and absorption and photoluminescence spectra were taken before and after the experiments to check for sample degradation. The samples were excited with a power of 0.5 mW at 3.123 eV. This corresponds to an excitation energy of 6 pJ per pulse. The excitation spot size was less than 100 μm diameter.

The time resolved photoluminescence spectra of all three samples are shown in figure 5.19. These spectra were obtained by integrating the data

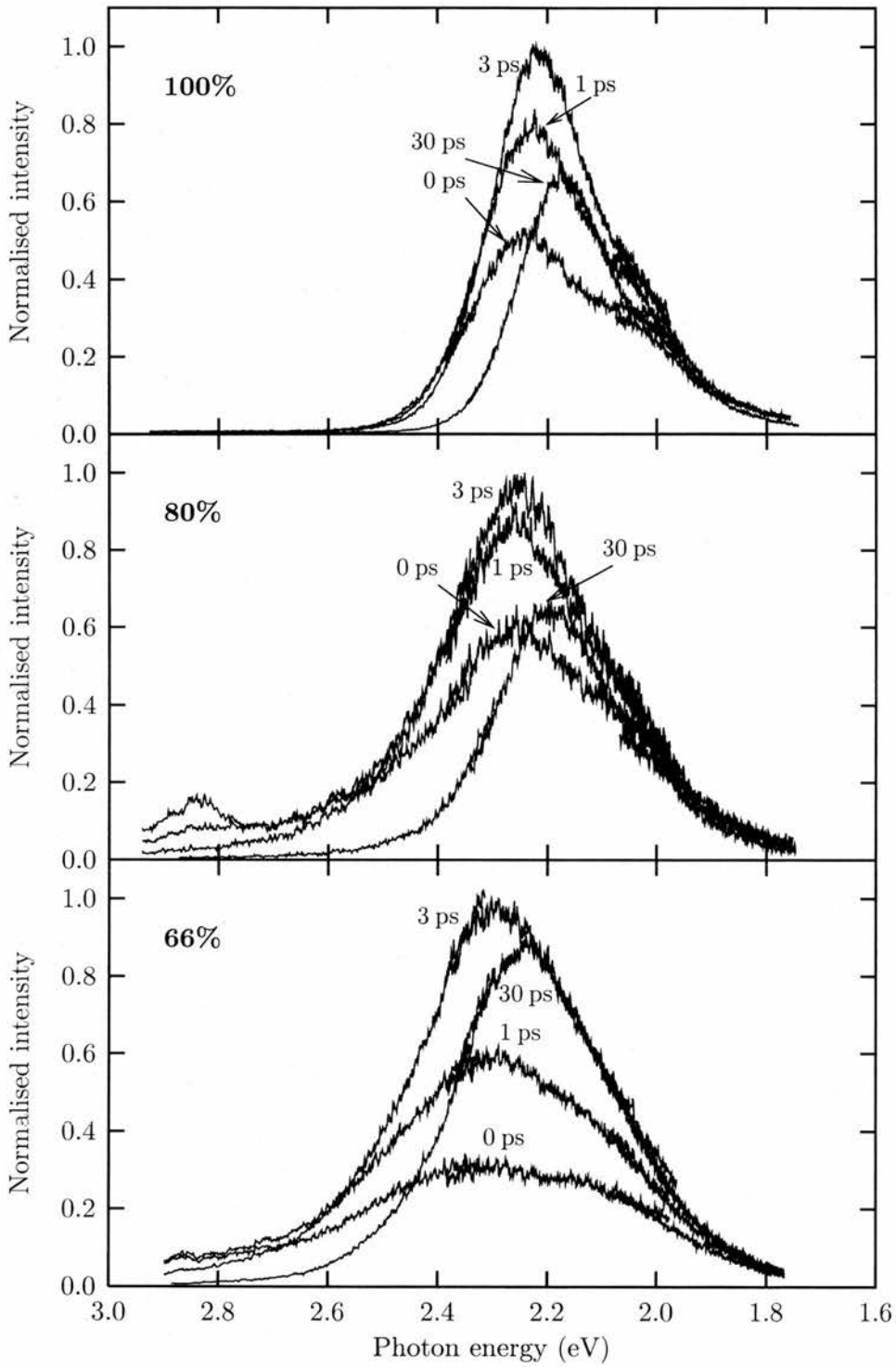

Figure 5.19: *The time resolved photoluminescence of fully and partially conjugated MEH-PPV.*

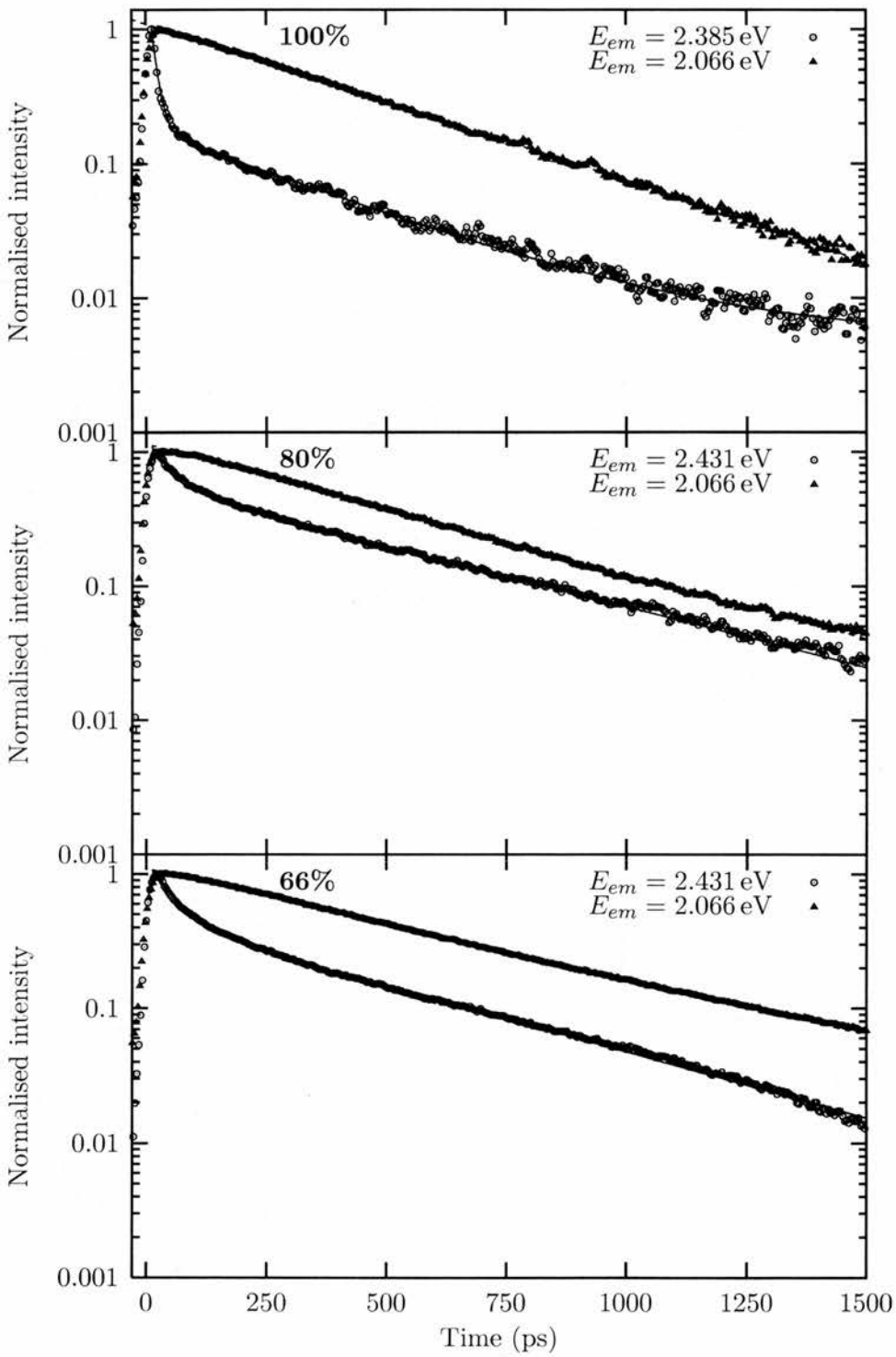

Figure 5.20: *The decay of the photoluminescence of fully and partially conjugated MEH-PPV at high and low photon energies.*

Conjugation	**Photon energy (eV)**	A_1	τ_1 (ps)	A_2	τ_2 (ps)	τ_r (ns)
100%	2.385	0.164	322 ± 1	0.836	12 ± 1	
100%	2.067	1	376 ± 1			1.7 ± 0.2
80%	2.431	0.522	476 ± 4	0.478	47 ± 1	
80%	2.067	1	447 ± 2			1.7 ± 0.1
66%	2.480	0.637	441 ± 8	0.363	51 ± 1	
66%	2.067	1	526 ± 3			2.1 ± 0.2

Table 5.5: *The lifetimes of fully and partially conjugated MEH-PPV.*

from the streak camera over a 2 ps wide area centered on the time indicated in the figure. The zero time point was set as the time halfway up the rise of the signal. It is clear that all the polymers undergo a significant red-shift of their photoluminescence after excitation. The top panel shows the spectra of the fully conjugated polymer. The peak in the photoluminescence shifts by 80 meV in the first 30 ps after excitation. The middle panel shows the spectra for the 80% conjugated polymer and the lower panel shows the 66% conjugated polymer. Both the partially conjugated polymers show a slightly smaller red-shift of 65 meV in the first 30 ps after excitation. The shape of the spectrum changes significantly with time. Immediately after excitation there is a much larger high photon energy component to the spectrum than at later times.

The decay of the intensity of the luminescence at a high and low photon energy for each sample is plotted in figure 5.20. The high photon energies were selected to be in roughly the same place on the blue side of the photoluminescence spectrum for each polymer. The low photon energies are the same for each sample, as the red side of the photoluminescence spectra of all three polymers are very similar. The decays were obtained by integrat-

ing over a 5 nm wide area centered on the photon energy indicated. For all the polymers the decay at low photon energies is mono-exponential and at high photon energies it is bi-exponential. The fully conjugated polymer (top panel) shows the fastest decay. The time constants and amplitudes for the two components for the bi-exponential decays are given in table 5.5. The fully conjugated polymer shows the fastest decay, the luminescence of the partially conjugated polymers is longer lived. The bi-exponential decay at high photon energies show a very fast component. This is consistent with excitation migration to lower energy sites after they are created. The fact that the fast component is longer lived in the partially conjugated polymers is an indication that excitation migration is slowed by the introduction of single bonds in the polymer backbone. In the fully conjugated polymer, this is the dominant component of the decay. In the partially conjugated polymers, this component becomes smaller as the degree of conjugation is reduced. The fact that a slow component of the decay of the luminescence at high photon energies is observed shows that a number of excitations decay before they reach low energy sites. The steady state spectra in figure 5.2 most closely resemble the spectra from the streak camera at 30 ps. This shows that the migration is mostly complete by this time.

The radiative lifetimes in table 5.5 suggest that the lifetime is largely independent of the degree of conjugation. The slightly longer radiative lifetime of the 66% conjugated polymer, compared to the 80% conjugated polymer, is due to the fact that a longer lifetime was measured by the streak camera for the 66% conjugated sample, but they both had the same PLQY. This could be due to the fact that the 66% conjugated polymer was synthesised at a different time to the other two samples, by a different chemist, so may not have been prepared in exactly the same way, or it could be a consequence of the reduced conjugation in this sample. The radiative lifetimes are indicative of a fully allowed transition.

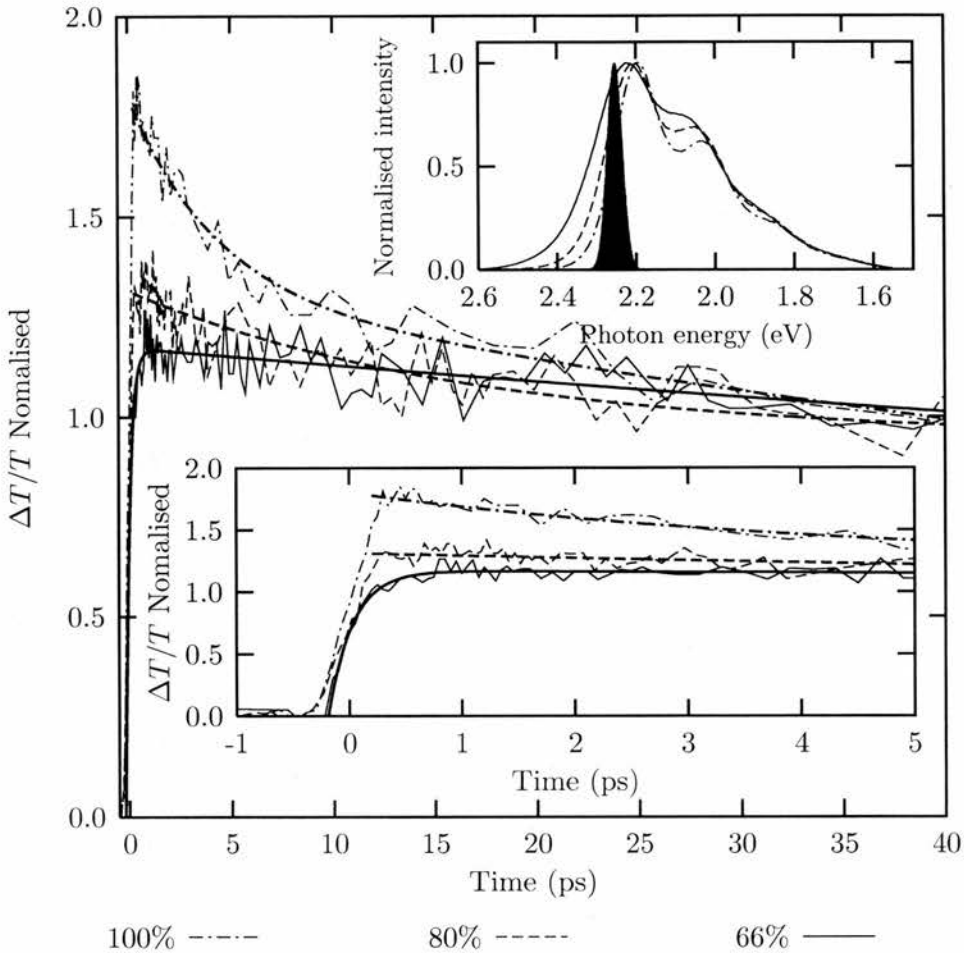

Figure 5.21: *The normalised magic angle decay of the transient absorption of all three polymers probed at 2.255 eV. The top inset shows the position of the probe pulse with respect to the photoluminescence spectra. The lower inset shows the short time behaviour on an expanded scale.*

5.7.2 Transient absorption

Figure 5.21 shows the decay of the transient absorption signal measured at the magic angle for all three polymers. The most deconjugated polymer has a slower rise than the other two polymers which exhibit a more pronounced decay of the signal in the first 40 ps after excitation. This can be explained by

Conjugation	A_1	τ_1/ps	A_2	τ_2/ps
100%	0.26	4.1 ± 0.3	0.74	140 ± 10
80%	1	8 ± 1		
66%	1	170 ± 30		

Table 5.6: *The decay times of the transient absorption at* 2.255 eV *of MEH-PPV as a function of conjugation.*

considering the spectral position of the probe pulse on the photoluminescence spectra in the upper inset in this figure. The probe pulse lies very close to the peak of the photoluminescence spectrum of the 66% conjugated polymer and is on the blue side of the emission spectra of the other two polymers. The decays exhibited by the other two polymers indicate that the absorption of the excitation is decaying. If the excitations are migrating to lower energy sites then this would explain the decay as the probe is on the blue side of the emission. For the 66% conjugated sample, the probe is on the peak of the emission so there is a slower decay as there is less migration to lower energies and a small rise as higher energy excitations migrate to this energy.

The anisotropies of these decays are shown in figure 5.22. Normally, for a two level system, the anisotropy decays from an initial value of 0.4 [56]. This is the case for the partially conjugated polymers. However, within the time resolution of the experiment ($\sim$ 200 fs) the fully conjugated polymer shows no decay, the anisotropy is constant at around 0.1. This value is similar to the steady state measurements presented in section 5.5. The inability to resolve a decay on this time scale indicates that a very fast depolarisation process is taking place. A number of pump and probe energies were tried but none were found to resolved any decay. Heeger et al. [26] note that the magic angle decay is independent of pump photon energy, however they only present data for three pump photon energies none of which are in the tail of the absorption. Bardeen et al. [44] have studied the anisotropy of the transient absorption of PPV and are unable to resolve a decay. They

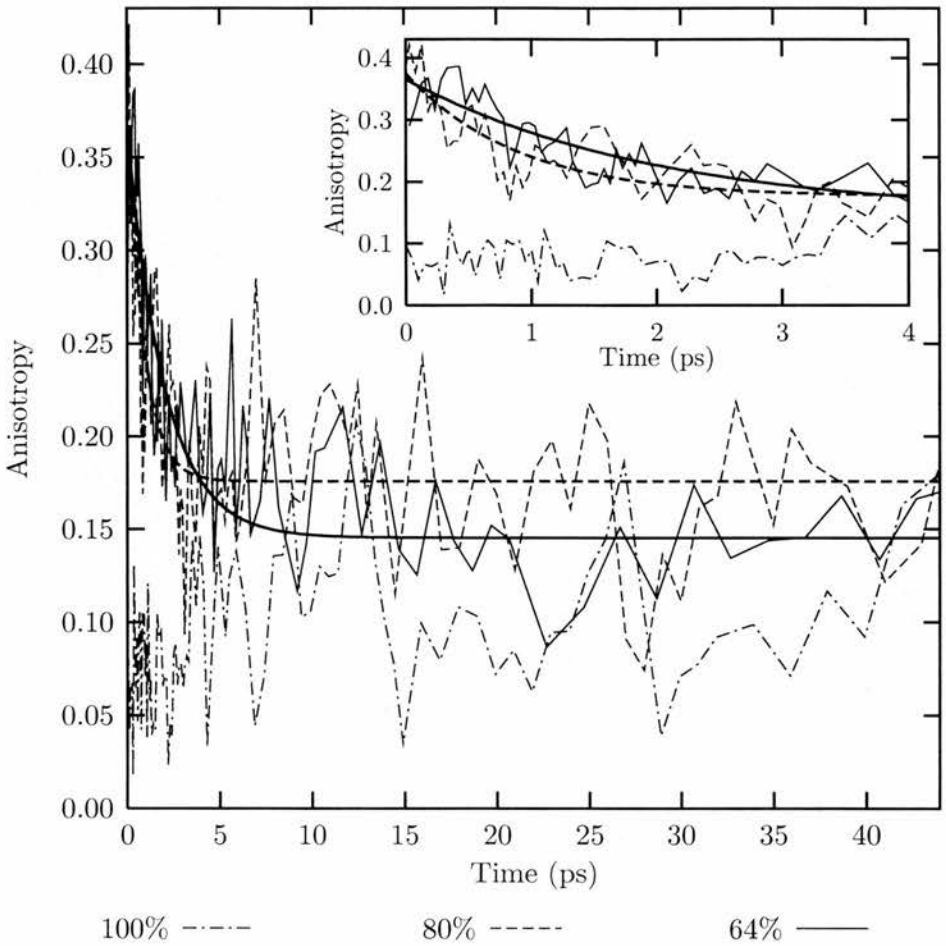

Figure 5.22: *Anisotropy of the transient absorption probed at* 2.255 eV.

suggest that this is due to the overlap of a two photon absorption band with their pump photon energy. It is difficult to see how this would affect the anisotropy as the two photon absorption band is not coupled to the pump as the transition is parity forbidden. Nguyen et al. [12, 29, 52] have reported anisotropies for MEH-PPV that show an initial value of 0.4 (figure 8 in reference [12]) and anisotropies under similar conditions that show an initial value of between 0.2 and 0.3 depending on solvent and sample concentration (figures 2 and 4 in reference [52] and figure 4 in reference [29]). Scholes et al. [8] suggest that there is a very fast depolarisation mechanism in MEH-

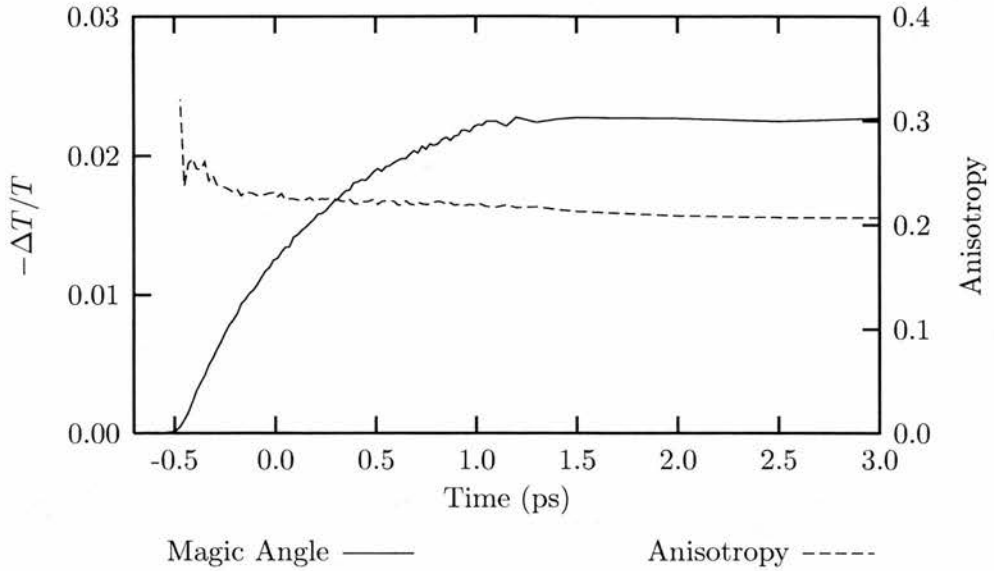

Figure 5.23: *Anisotropy of MEH-PPV with a probe photon energy of* 1.459 eV *using* 20 fs *pulses.*

PPV, where the excitation effectively samples the whole chain in under 200 fs. This is consistent with the results obtained in the present work. It should be noted that the samples for the work presented here and the work of Scholes both came from the same source and so the results should be consistent. The results presented here show that the partially conjugated polymers clearly have a different depolarisation mechanism which is likely to be due to energy transfer along the chain to segments of lower energy. The fully conjugated polymer shows stronger electronic coupling along the entire length of the polymer chain.

Figure 5.23 shows the magic angle signal and anisotropy of the transient absorption at 1.459 eV measured using an amplified femtosecond laser system pumping a non-collinear phase matching optical parametric amplifier. This system had much shorter pulses ($\sim$ 20 fs). However there is a very slow rise of the transient signal. This could be due to a slow rise of the absorption. The pump and probe photon energies were widely spaced in this experiment

so the long rise could be due to a slow instrument response function as the pump and probe pulses would experience different refractive indices and hence have different group velocities in the sample. This would result in the probe probing the absorption at a range of times after excitation rather than one well defined time as the pump and probe were overlapped over a few millimeters. The anisotropy from this data shows a small decay at very short times. This might indicate that it would be possible to study the depolarisation with a shorter instrument response function. Unfortunately, due to the limited time available on this laser system, only the measurement presented in figure 5.23 could be performed.

5.8 Conclusions

In this chapter the effect of the extent of conjugation on the photophysics of MEH-PPV has been investigated using samples with a well defined degree of conjugation. This is the first time that the photophysics of a conjugated polymer have been throughly studied as a function of conjugation. The time resolved anisotropy of the transient absorption and steady state experiments show that the optical properties of the fully conjugated polymer are significantly different from the partially conjugated polymers. The partially conjugated polymers show clear evidence of static disorder on the chain. The dependence of their photoluminescence excitation spectra on detected photon energy is much stronger than the fully conjugated polymer. The steady state anisotropy of the photoluminescence of all three polymers increases as the energy of the excitation photon is reduced suggesting that excitation migration is taking place. In the partially conjugated samples this is accompanied by a narrowing of the photoluminescence spectrum indicating that only a subset of the segments on the chain are being excited. The steady state anisotropy also reveals a straightening of the polymer chain as it is cooled.

The biggest difference between the fully and partially conjugated polymers is in the anisotropy of the transient absorption. Within the time reso-

lution of the transient absorption experiments (~ 200 fs) it was not possible to resolve any decay of the anisotropy for the fully conjugated polymer. In contrast the partially conjugated polymers show a decay from an initial value of $r = 0.4$. This is the first time that this difference has been reported and has important implications for the interpretation of the photophysics of conjugated polymers, suggesting that electronic coupling is stronger in the fully conjugated polymer than the partially conjugated polymers.

Taken as a whole, the experimental results show that the introduction of chemical breaks in the conjugation significantly reduces the strength of the electronic coupling along the polymer chain and increases the degree of inhomogeneous broadening of the spectra.

References

[1] K. Knoll and R. R. Schrock. *Journal of the American Chemical Society*, **111**, 7989, (1989).

[2] H. Meier, U. Stalmach, and H. Kolshorn. *Acta Polymerica*, **48**, 379, (1997).

[3] J. Burroughes, D. D. C. Bradley, A. R. Brown, R. N. Marks, K. Mackay, R. H. Friend, P. L. Burn, and A. B. Holmes. *Nature*, **347**, 539, (1990).

[4] N. T. Harrison, D. R. Baigent, I. D. W. Samuel, and R. H. Friend. *Physical Review B*, **53**, 15815, (1996).

[5] J. M. Leng, S. Jeglinski, X. Wei, R. E. Benner, and Z. V. Vardeny. *Physical Review Letters*, **72**, 156, (1994).

[6] S. Huen, R. F. Mahrt, A. Greiner, U. Lemmer, H. Bassler, D. A. Halliday, D. D. C. Bradley, P. L. Burn, and A. B. Holmes. *Journal of Physics Condensed Matter*, **5**, 247, (1993).

[7] H. Bässler and B. Schweitzer. *Accounts of Chemical Research*, **32**, 173, (1999).

[8] G. D. Scholes, D. S. Larsen, G. R. Fleming, G. Rumbles, and P. L. Burn. *Physical Review B*, **61**, 13670, (2000).

[9] U. Rauscher, H. Bässler, D. D. C. Bradley, and M. Hennecke. *Physical Review B*, **42**, 9830, (1990).

[10] M. Yan, L. J. Rothberg, E. W. Kwock, and T. M. Miller. *Physical Review Letters*, **75**, 1992, (1995).

[11] N. S. Sariciftci, editor. *Primary Photoexcitations in Conjugated Polymers: Molecular Exciton Versus Semiconductor Band Model.* World Scientific Publishing, (1998).

[12] V. Doan T. Q. Nguyen and B. J. Schwartz. *Journal of Chemical Physics*, **110**, 4068, (1999).

[13] C. J. Collison, L. J. Rothberg, V. Treemaneekarn, and Y. Li. *Macromolecules*, **34**, 2346, (2001).

[14] D. Hu, J. Hu, and P. F. Barbara. *Journal of the American Chemical Society*, **121**, 6936, (1999).

[15] J. Yu, D. Hu, and P. F. Barbara. *Science*, **289**, 1327, (2000).

[16] D. Hu, J. Yu, K. Wong, B. Bagchi, P. J. Rossky, and P. F. Barbara. *Nature*, **405**, 1030, (2000).

[17] T. Huser, M. Yan, and L. J. Rothberg. *Proceedings of the National Academy of Sciences of the United States of America*, **97**, 11187, (2000).

[18] T. Huser and M Yan. *Journal of Photochemistry and Photobiology A: Chemistry*, **144**, 43, (2001).

[19] J. D. White, J. H. Hsu, Shu-Chun Yang, W. S. Fann, G. Y. Pern, and S. A. Chen. *Journal of Chemical Physics*, **114**, 3848, (2001).

[20] J. D. White, J. H. Hsu, W. S. Fann, S. C. Yang, G. Y. Pern, and S. A. Chen. *Chemical Physics Letters*, **338**, 263, (2001).

[21] K. F. Wong, M. S. Skaf, C. Y. Yang, P. J. Rossky, B. Bagchi, D. Hu, J. Yu, and P. F. Barbara. *Journal of Chemical Physics B*, **105**, 6103, (2001).

[22] T. Q. Nguyen, B. J. Schwartz, R. D. Schaller, J. C. Johnson, L. F. Lee, L. H. Haber, and R. J. Saykally. *Journal of Physical Chemistry B*, **105**, 5153, (2001).

[23] P. K. Wei, Y. Fen, W. Fann, Y. Z. Lee, and S. A. Chen. *Physical Review B*, **63**, 045417, (2001).

[24] G. Padmanaban and S. Ramakrishnan. *Journal of the American Chemical Society*, **122**, 2244, (2000).

[25] G. Padmanaban and S. Ramakrishnan. *Synthetic Metals*, **119**, 533, (2001).

[26] D. Vacar, A. Dogariu, and A. J. Heeger. *Chemical Physics Letters*, **290**, 58, (1998).

[27] G. R. Hayes, I. D. W. Samuel, and R. T. Phillips. *Physical Review B*, **52**, R11569, (1995).

[28] R. Kersting, U. Lemmer, R. F. Mahrt, K. Leo, H. Kurz, H. Bässler, and E. O. Göbel. *Physical Review Letters*, **70**, 3820, (1993).

[29] T. Q. Nguyen, J. Wu, V. Doan, B. J. Schwartz, and S. H. Tolbert. *Science*, **288**, 652, (2000).

[30] A. Dogariu, D. Vacar, and A. J. Heeger. *Synthetic Metals*, **101**, 202, (1999).

[31] P. B. Miranda, D. Moses, and A. J. Heeger. *Physical Review B*, **64**, 081201(R), (2001).

[32] M. Yan, L. J. Rothberg, F. Papadimitrakopoulos, M. E. Galvin, and T. M. Miller. *Physical Review Letters*, **72**, 1104, (1994).

[33] N. T. Harrison, G. R. Hayes, R. T. Phillips, and R. H. Friend. *Physical Review Letters*, **77**, 1881, (1996).

[34] I. D. W. Samuel, G. Rumbles, C. J. Collison, R. H. Friend, S. C. Moratti, and A. B. Holmes. *Synthetic Metals*, **84**, 497, (1997).

[35] I. D. W. Samuel, B. Crystall, G. Rumbles, P. L. Burn, and A. B. Holmes. *Synthetic Metals*, **54**, 281, (1993).

[36] N. S. Sariciftci, editor. *Primary Photoexcitations in Conjugated Polymers: Molecular Exciton Versus Semiconductor Band Model*, Chapter 7. World Scientific Publishing, (1998).

[37] S. J. Martin, D. D. C. Bradley, P. A. Lane, and H. Mellor. *Physical Review B*, **59**, 15133, (1999).

[38] S. A. Whitelegg, A. Buckley, M. D. Rahn, A. M. Fox, D. D. C. Bradley, L. O. Pålsson, I. D. W. Samuel, G. R. Webster, and P. L. Burn. *Synthetic Metals*, **119**, 575, (2001).

[39] I. Ledoux, I. D. W. Samuel, J. Zyss, S. N. Yaliraki, F. J. Schattenmann, R. R. Schrock, and R. J. Silbey. *Chemical Physics*, **245**, 1, (2000).

[40] G. R. Webster. *Advanced polymers for light emitting diodes.* PhD thesis, University of Oxford, (2000).

[41] S. N. Yaliraki and R. J. Silbey. *Journal of Chemical Physics*, **104**, 1245, (1995).

[42] G. Dufresne, J. Bouchard, M. Belletête, G. Durocher, and M. Leclerc. *Macromolecules*, **33**, 8253, (2000).

[43] C. Singh and D. Hone. *Synthetic Metals*, **62**, 61, (1994).

[44] S. H. Lim, T. G. Bjorklund, and C. J. Bardeen. *Chemical Physics Letters*, **342**, 555, (2001).

[45] J. Yu, M. Hayashi, S. H. Lin, K. K. Liang, W. S. Fann, C. I. Chao, K. R. Chuang, and S. A. Chen. *Synthetic Metals*, **82**, 159, (1996).

[46] O. Inganäs, W. R. Salaneck, J. E. Österholm, and J. Laakso. *Synthetic Metals*, **22**, 395, (1988).

[47] J. R. Linton and C. W. Frank. *Synthetic Metals*, **28**, C393, (1989).

[48] M. Severin and O. Inganäs. *Journal of Chemical Physics*, **105**, 8446, (1996).

[49] M. Zheng, F. Bai, and D. Zhu. *Journal of Photochemistry and Photobiology A: Chemistry*, **116**, 143, (1998).

[50] A. K. Sheridan, J. M. Lupton, I. D. W. Samuel, and D. D. C. Bradley. *Chemical Physics Letters*, **111**, 531, (2000).

[51] J. Wu, A. F. Gross, and S. H. Tolbert. *Journal of Physical Chemistry B*, **103**, 2374, (1999).

[52] B. J. Schwartz, T. Q. Nguyen, J. Wu, and S. H. Tolbert. *Synthetic Metals*, **116**, 35, (2001).

[53] G. Rumbles, C. J. Collison, D. L. Russell, L. A. Magnani, S. C. Moratti, and I. D. W. Samuel. *Synthetic Metals*, **111**, 501, (2000).

[54] M. L. Grage, P. Wood, A. Ruseckas, W. L. Mitchell, P. L. Burn, I. D. W. Samuel, and V. Sundström. *In preparation*, , (2001).

[55] B. Hudson and B. Kohler. *Annual Reviews of Physical Chemistry*, **25**, 437, (1974).

[56] J. R. Lakowicz. *Principles of Fluorescence Spectroscopy*, Chapter 10, Page 291. Kluwer Academic, Second edition, (1999).

Chapter 6

Conclusions

Conformational disorder and chemical breaks in conjugation both disrupt the delocalisation of electrons in conjugated polymers. This leads to a distribution of conjugated segments within the polymer chain and impacts on the photophysics of the polymer. Using a novel method of fitting the absorption spectrum to the absorption of a set of shorter conjugated segments, the distribution of conjugated segments within several polymers has been obtained [1]. The change in the absorption spectrum and distribution of conjugated segments for these samples as a function of temperature has also been investigated. As the temperature is reduced the absorption of the polymers moves to lower photon energies and the distribution of conjugated segments moves to longer segments. At all temperatures the distribution peaks at the shortest segment. This agrees with the earlier work of Kohler and Samuel [2] who used a simpler fitting method to extract the distribution of conjugated segment lengths from a polymer absorption spectrum, and also the theoretical predictions of Kohler and Woehl [3] and Yaliraki and Silbey [4]. The distributions of conjugated segment lengths have been compared to those predicted by the model of Yaliraki and Silbey. Qualitative agreement was found between the model and the distributions obtain from NNLS fits. However, for the samples studied, the Yaliraki/Silbey model overestimates the importance of long conjugated segments and the red-shift of the absorption

with decreasing temperature. It is also noted that the current models of conformational disorder do not account for the fact that short conjugated molecules show no evidence of conformational disorder and the length of conjugation is equal to the chain length of the molecule.

The effect of the extent of conjugation on the steady state and time resolved photophysics of MEH-PPV has been investigated. It is found that as the extent of conjugation is decreased the quantum yield for fluorescence increases with the radiative lifetime. The fully conjugated polymer shows a different behaviour to the partially conjugated polymers. This can be explained by considering two different migration mechanisms for the fully and partially conjugated samples. Scholes et al. [5] have suggested that in the fully conjugated polymer the excitation samples the whole chain in under 200 fs. This is consistent with the observation in this thesis that the anisotropy does not show an initial decay within a 200 fs time scale. The partially conjugated polymers do show a decay of the anisotropy from an initial value of $r = 0.4$ suggesting a different migration mechanism. Given the presence of a large number of single bonds in the partially conjugated samples disrupting the conjugation, it is likely that the excitation is hopping between different conjugated segments and this would account for the slower depolarisation. In steady state photoluminescence and photoluminescence excitation experiments the partially conjugated samples exhibit evidence of static disorder. Steady state anisotropy measurements as a function of temperature reveal that the chain straightens as the solution is cooled. The excitation photon energy dependence of the anisotropy provides further evidence for static disorder in the partially conjugated samples, as the anisotropy increases as the excitation is tuned into the tail of the absorption.

The results presented in this thesis have an important place in the wider context of technological applications based on conjugated polymers. In order to optimise light emitting and light harvesting devices based on these materials it is necessary to have a thorough understanding of both their photophysics and their electronic properties. The conformation of the polymer

chain and degree of conjugation within it have a dramatic effect on both of these properties. With a better understanding of these properties it should be possible in the future to design materials with the properties desired for a specific application. For commercial applications of these materials to reach their full potential it is imperative that the understanding of their basic physics is improved. The work presented here is a stepping stone to this goal.

In the future, work could focus on developing better expressions for the basic electronic properties (the transition dipole, the energy of the absorption band and its shape) of conjugated molecules as a function of chain length with a view to improving the NNLS fitting. Current disorder models could also be improved to take account of chemical defects on the polymer chain and to account for the different behaviour of short and long conjugated molecules. Future studies could also focus on the time resolved anisotropy of fully conjugated MEH-PPV, further experiments on a shorter pulse laser system might reveal the time scale of decay. Also investigating the effect of the degree of conjugation on the photophysics of films, where three dimensional energy transfer is possible, would provide further insight into the operation of devices based on thin films.

References

[1] P. Wood, I. D. W. Samuel, R. Schrock, and R. L. Christensen. *Journal of Chemical Physics*, **115**, 10955, (2001).

[2] B. E. Kohler and I. D. W. Samuel. *Journal of Chemical Physics*, **103**, 6248, (1995).

[3] B. E. Kohler and J. C. Woehl. *Journal of Chemical Physics*, **103**, 6253, (1995).

[4] S. N. Yaliraki and R. J. Silbey. *Joural of Chemical Physics*, **104**, 1245, (1996).

[5] G. D. Scholes, D. S. Larsen, G. R. Flemming, G. Rumbles, and P. L. Burn. *Physical Review B*, **61**, 13670, (2000).

Appendix A

Papers published as a result of this thesis

- Investigating the effect of conjugation in MEH-PPV, P. Wood, I. D. W. Samuel, G. R. Webster, P. L. Burn. *Synthetic Metals*, **119**, 571, (2001).
- Conformational disorder in long polyenes, P. Wood, I. D. W. Samuel, R. Schrock, R. L. Christensen. *Journal of Chemical Physics*, **115**, 10955, (2001).
- Conformational disorder and energy migration in partially conjugated MEH-PPV, M. M-L. Grage, P. Wood, A. Ruseckas, T. Pullerits, G. R. Webster, W. Mitchell, P. L. Burn, I. D. W. Samuel, V. Sundström. *In preparation for submission to Chemical Physics*